Evaluation of endothelial cell response to drug for intraocular lens delivery

by

Laura Doody

A thesis
presented to the University of Waterloo
in fulfillment of the
thesis requirement for the degree of
Master of Applied Science
in
Systems Design Engineering

Waterloo, Ontario, Canada, 2011

AUTHOR'S DECLARATION

I hereby declare that I am the sole author of this thesis. This is a true copy of the thesis, including any required final revisions, as accepted by my examiners.

I understand that my thesis may be made electronically available to the public.

Abstract

Cataract is one of the leading causes of vision loss worldwide. The rate of cataract surgery has been steadily increasing. Toxic Anterior Segment Syndrome (TASS) is a sterile inflammatory response in the anterior segment of the eye that may occur following cataract surgery. When left untreated, it can lead to permanent vision loss. Corneal endothelial cells are the cells most affected by TASS. These cells are unable to reproduce *in vivo* and consequently once the density of these cells drops below a certain level, vision is reduced and cannot be reversed. The damage is thought to be mediated by cytokines and endotoxins, primarily through the NF-κB pathway. It is hypothesized that anti-inflammatory drug delivery intraocular lenses may help reduce the occurrence of TASS and consequent vision loss. In this research thesis project, an *in vitro* model was developed as a tool to select drug and delivery material to be used in an anti-TASS ophthalmic biomaterial. In an attempt to find a novel and more effective approach to TASS prevention, dexamethasone, a potent anti-inflammatory steroid drug, was compared to triptolide, a cytokine inhibitor; aprotinin, a general protease inhibitor; and PPM-18, a NF-κB inhibitor. To assess the efficacy of these drugs, an *in vitro* assay using human umbilical vein endothelial cells (HUVEC) and lipopolysaccharide as a stimulant was developed. Cell response to dexamethasone (10 nM), triptolide (3 nM), aprotinin (20 μM) and PPM-18 (10 μM) with or without LPS was characterized by cell viability and flow cytometry analysis of cell activation. Activation was characterized using markers for cell adhesion and activation ICAM-1, PECAM-1, VCAM-1, β_1-integrin, CD44 and E-selectin. Following preliminarily testing, the efficacy of dexamethasone (10 nM) and PPM-18 (10 μM) loaded polymer (PDMS) and copolymer (PDMS/pNIPAAm) interpenetrating polymer networks were evaluated over a 4 day release period. The results from soluble drug and LPS (100 ng/mL) testing indicated no decrease in cell viability after 24 h. Dexamethasone, triptolide, aprotinin, and PPM-18 did not reduce the significant ICAM-1 upregulation seen in HUVECs after exposure to LPS for 4 days. PPM-18 in combination with LPS significantly upregulated E-selectin

and CD44 from unstimulated HUVEC cells. The polymer materials without drug loading did not influence the cell phenotype. However, PPM-18 delivering polymer and copolymer materials significantly upregulated VCAM-1, CD44 when compared to all other treatments. Propidium iodide uptake in HUVEC exposed to PPM-18 drug delivering polymer and copolymer treatments indicated that these treatments caused cell necrosis. None of the drugs, or the drug delivering materials were shown to counteract the upregulation seen from LPS stimulation of HUVEC cells. Future work should focus on validating the *in vitro* model to more closely replicate the *in vivo* environment of the anterior segment with the use of primary bovine corneal endothelial cells.

Acknowledgements

The past two years have been a challenging and fulfilling experience at the University of Waterloo. There are many people I owe to my success over my time here to whom I owe many thanks.

I would like to thank Dr. Maud Gorbet for providing me with the opportunity to pursue a Master's degree in Systems Design Engineering at the University of Waterloo. Her support and encouragement throughout my time at UW has provided me with the confidence needed to successfully complete my degree. I have been provided with the opportunity to travel to conferences and present data introducing me to a new world of biomaterials research both academic and industrial.

I would like to thank all the members of the MIBS lab for their moral support through all the challenges faced while completing my degree. Especially Dr. Dave McCanna, who was always willing to share his invaluable knowledge. I must include my fellow graduate students in my thanks: Sara Molladavoodi, Saman Mohammadi, Tidimogo Gaamangwe, Xiaojian Chang, and Dan Cira who all helped make the lab a welcome and enjoyable environment. Sara Luck for understanding when I forgot to order a reagent until too late. Aurore Barthod and Jeff Lu who assisted in my data collection.

Thanks to Lina Liu and Heather Sheardown at McMaster University for synthesizing the materials used in this study.

For technical assistance with FACSVantage in the early stages of my research, thanks to Mihaela Savulescu.

Finally, I would like to thank all my friends and family for supporting me through my Master's degree. Special thanks to my parents, Diana and Brian Doody, who have supported and encouraged me throughout my academic career.

Funding for this research was provided by NSERC and 20/20 NSERC Ophthalmic Materials Network.

Dedication

To Shawn Ranieri, for always listening.

Table of Contents

AUTHOR'S DECLARATION ii
Abstract iii
Acknowledgements v
Dedication vi
Table of Contents vii
List of Figures x
List of Tables xii
List of Abbreviations xiii
Chapter 1 Introduction 1
1.1 Introduction 1
1.2 Corneal Endothelial Cells 3
1.2.1 Cornea pump-leak mechanism for controlling corneal hydration 10
Chapter 2 IOL Complications and Treatments 12
2.1 Toxic Anterior Segment Syndrome (TASS) 12
2.1.1 TASS diagnosis 13
2.1.2 TASS causes 13
2.1.3 Traditional TASS treatment 16
2.2 Endophthalmitis 16
2.2.1 Endophthalmitis symptoms 17
2.3 Intraocular Lenses (IOLs) 18
2.4 Inflammatory inhibitors 19
2.4.1 Corticosteroids 19
2.4.2 NF-κB pathway activation inhibitors 20
2.4.3 Protease Inhibitor 20
2.5 Drug Delivering Methods 21
2.5.1 Topical and intracameral injections 21
2.5.2 Drug delivering devices 21
2.5.3 Current drug delivering devices – non IOLs 22

2.5.4 Drug delivering devices - IOLs 23
2.6 Role of *in vitro* models 24
2.6.1 Interspecies variation in the corneal endothelium 26
2.7 Thesis research questions 27
Chapter 3 Methodology 29
3.1 Cell Culture 29
3.2 Interpenetrating Network (IPN) Preparation 29
3.3 *In vitro* HUVECs activation and drug toxicity 30
3.4 HUVECs interaction with biomaterials 31
3.5 Viability assay 32
3.6 Flow Cytometry 32
3.6.1 Flow Cytometry Protocol 35
3.6.2 Flow cytometry acquisition/analysis 37
3.7 Statistical analysis 37
Chapter 4 Results 38
4.1 HUVECs response to soluble drug 38
4.1.1 Cell Viability following exposure to soluble drug 38
4.1.2 Change in cellular phenotype in response to soluble drug 41
4.2 HUVECs response to LPS 42
4.2.1 Cell Viability following exposure to LPS 42
4.2.2 Change in cellular phenotype in response to LPS 43
4.3 HUVECs response to LPS and soluble drugs 45
4.4 Biocompatibility of polymer and copolymer with and without drug loading 53
4.4.1 HUVECs viability response to materials 60
4.4.2 HUVECs' response to DMSO 67
Chapter 5 Discussion 70
5.1 Response to soluble drug and LPS 70
5.1.1 Viability response 70
5.1.2 Endothelial cell phenotype changes following LPS stimulation 71

5.1.3 Phenotype changes following exposure to drug 73
5.1.4 Soluble drug with LPS phenotype changes 74
5.2 Biocompatibility of polymer and copolymer materials 75
5.2.1 Drug delivering materials 76
5.2.2 DMSO and drug loading response on materials 77
Chapter 6 Conclusions and Future Work 79
6.1 Conclusions 79
6.2 Future work 79
References 81
Appendix A Copyright Permissions 106
Glossary 116

List of Figures

Figure 1: Light micrograph of human cornea and diagram indicating the various layers of the cornea. 3
Figure 2: Right (OD) and left (OS) eye images of a healthy corneal endothelium. 4
Figure 3: Right (OD) and left (OS) eye one year following cataract surgery that led to TASS infection in the right eye.. 5
Figure 4: NF-kb activation pathway showing three possible activation pathways.. 7
Figure 5: Diagram indicating the location of TASS and endophthalmitis. 12
Figure 6: Drug delivery *in vitro* model in either a 24 or 48 well plate 31
Figure 7: BD FACSCalibur optical path configuration. 33
Figure 8: Flow cytometry plot for forward scatter (FSC) vs. side scatter (SSC). 34
Figure 9: Example of typical fluorescent data plots in flow cytometry. 35
Figure 10: Response of HUVECs after 24 h exposure to triptolide. 40
Figure 11: Response of HUVECs to LPS between 3 h and 48 h. 45
Figure 12: ICAM-1 upregulation in HUVEC after 24 h exposure to LPS and LPS with dexamethasone, triptolide, aprotinin, and PPM-18. 46
Figure 13: ICAM-1 upregulation in HUVECs following exposure to dexamethasone with and without LPS for 24 h. 47
Figure 14: Response of HUVECs to varying concentrations of dexamethasone with and without LPS for ICAM-1 at 4 days.. 48
Figure 15: E-selectin expression on HUVECs after 4 day exposure to PPM-18 stimulated cells with or without LPS. 51
Figure 16: CD44 expression in HUVECs after 4 day exposure to PPM-18 stimulated cells with or without LPS. 52
Figure 17: β_1-integrin expression on HUVECs after 4 day exposure to PPM-18 stimulated cells with or without LPS. 53
Figure 18: Scatter plots showing cell shape response to various polymer and copolymer treatments after 4 days exposure to HUVECs.. 55

Figure 19: VCAM-1 expression on HUVECs after 4 day exposure to polymer and copolymer materials with various treatments and dexamethasone (10 nM) or PPM-18 (10 μM)..... 59
Figure 20: CD44 expression on HUVECs after 4 day exposure to polymer and copolymer materials with various treatments and dexamethasone (10 nM) or PPM-18 (10 μM)..... 60
Figure 21: HUVECs' viability after 24 h exposure to dexamethasone and PPM-18: soluble drug, and loaded polymer or copolymer. 61
Figure 22: Plots illustrating necrosis and apoptosis levels in HUVECs following 4 day treatment for first assay performed with PPM-18 (10 μM and 30 μM) and dexamethasone (10 nM). The plots indicate percentage cellular activity by quadrant. 65
Figure 23: Plots illustrating necrosis and apoptosis levels in HUVECs following second 4 day treatment assays performed with PPM-18 (10 μM and 30 μM). 66
Figure 24: ICAM-1 upregulation on HUVEC after 24 h or 4 day exposure to various concentrations of DMSO. 68
Figure 25: β_1-integrin expression on HUVEC after 24 h or 4 day exposure to various concentrations of DMSO. 69

List of Tables

Table 1: Selected CEC membrane receptors and their functions 9
Table 2: Possible causes of TASS [3,9,15,90] 15
Table 3: Drugs and delivery mechanisms often used in treatment of TASS 16
Table 4: Drugs used in treatment of endophthalmitis 18
Table 5: Selected CEC membrane receptors or intracellular stains and their measured response 37
Table 6: HUVECs' viability after 24 h to dexamethasone.. 38
Table 7: HUVECs' viability after 24 h exposure to PPM-18. 39
Table 8: Phenotype changes to soluble drugs after 24 h. HUVECs were exposed to dexamethasone (10 nM), triptolide (3 nM), aprotinin (20 µM), and PPM-18 (10 µM) for 24 h and analyzed by flow cytometry.. 41
Table 10: Necrosis in HUVECs following 4 day exposure to LPS.. 43
Table 11: Relative response of HUVECs to 48 h exposure to LPS. HUVEC were exposed to LPS (0.2 µg/mL and 2.0 µg/mL) for 48 h and analyzed by flow cytrometry 44
Table 12: Response of HUVECs to varying concentrations of dexamethasone with and without LPS at 24 h and 4 days. 49
Table 13: Response of HUVECs after 4 day exposure to PPM-18 stimulated cells with or without LPS.. 50
Table 14: HUVECs' necrosis following 4 days exposure to polymer and copolymer, unloaded or mock loaded. 56
Table 15: Response of HUVEC after 4 day exposure to polymer and copolymer, unloaded or mock loaded. 57
Table 16: ICAM-1 response in HUVECs after 4 day exposure to polymer and copolymer materials, unloaded, mock loaded or loaded with either dexamethasone or PPM-18. 58

List of Abbreviations

ANOVA	analysis of variance
CD	cluster of differentiation
CD44	cell surface glycoprotein
CEC	corneal endothelial cell
Dex	dexamethasone
DMSO	dimethyl sulfoxide
E-selectin	CD62 antigen like family member E
ECGS	endothelial cell growth supplement
ECM	endothelial cell medium
ECGF	endothelial cell growth factor
FBS	fetal bovine serum
FGF	fibroblast growth factor
HUVEC	human umbilical vein endothelial cells
β_1-integrin	CD29
ICAM-1	inter-cellular adhesion molecule 1 (CD54)
IPN	interpenetrating network
IOL	intraocular Lens
IOP	intraocular pressure
Jam A	junctional adhesion molecule A
LC50	median lethal dose of drug
LPS	lipopolysaccharides
MATO	methacryloxypropyltriethoxysilane
MMP	matrix metalloproteinase
MMPi	matrix metalloproteinase inhibitor
MTT	3-(4,5-dimethylthiazol-2-yl)-2,5-diphenyltetrazolium bromide
NF-κB	Nuclear factor kappa beta
NSAIDs	Non-steroidal anti-inflammatory drugs

PBS	phosphate buffered saline
PDMS-V	Vinyl conjugated poly(dimethylsiloxane)
PDMS-OH	Hydroxyl conjugated poly(dimethylsiloxane)
PI	propidium iodide
pNIPAAm	Poly (N-isopropyl acrylamide)
PECAM-1	Platelet endothelial cell adhesion molecule 1 (CD31)
PPM-18	2-Benzoylamino-1,4-naphtoquinone
SD	standard deviation
TASS	Toxic Anterior Segment Syndrome
THF	tetrahydrofuran
TNF-α	tumour necrosis factor alpha.
Trip	triptolide
VCAM-1	vascular cell adhesion molecule 1 (CD106)
ZO-1	zonula-occludins-1

Chapter 1
Introduction

1.1 Introduction

Cataracts cause around half of all visual disabilities and blindness worldwide [1]. Consequently, cataract surgery is one of the most commonly performed surgeries in the world and is relatively safe [1,2]. Cataract surgery is most commonly performed using a technique known as phacoemulsification. This requires a small incision along the edge of the cornea through which a needle vibrating at ultrasonic levels emulsifies and aspirates the crystalline lens [3–5]. An intraocular lens (IOL) is then inserted through the incision to replace the removed lens [3,4]. The physical trauma from cataract surgery can influence the inflammatory response in the eye even without the presence an infectious agent or irritant [4,6]. For this reason, along with possible infections from surgery, anti-inflammatory agents including steroids, antibiotics, and non-steroidal anti-inflammatory drugs (NSAIDs) are used prophylactically to prevent complications [6].

As with any surgery, complications may arise that if left untreated could worsen the initial conditions of the patient. Two of the most devastating cataract complications are toxic anterior segment syndrome (TASS) and endophthalmitis [3,7–12]. TASS is an acute sterile inflammatory response that typically occurs within 48 h post surgery [3,7–9,13]; whereas, endophthalmitis is an infection of the anterior segment of the eye due to bacterial, parasitic or fungal infection [10–12]. Endophthalmitis is most commonly due to Gram-positive bacteria [11,12,14]. Depending on the study, the incidence rate for TASS varies between 0.04 to 0.68% [2,5,15–20]. To prevent its occurrence, many perioperative, intraoperative, and postoperative measures are taken [16,21]. Both of these diseases, if left untreated may lead to permanent vision loss and possible blindness through damage to the corneal endothelium [5,7–9,11–13,22–24].

The human cornea is composed of three major layers, the epithelium, the stroma, and the endothelium [3,25–28]. During cataract surgery the corneal endothelium has the potential to become damaged, and unlike the stroma and epithelium, the human corneal endothelium is

unable to replicate [28–33]. The primary function of the corneal endothelium is to maintain hydration and clarity in the eye [3,25,28,34,35]. Healthy corneal endothelial cells are hexagonal in appearance and a proper arrangement of these cells allows them to maintain their functionality [3,25,28,34,36–42]. As cell numbers decrease through aging or damage, the cells enlarge to compensate and are less efficient in maintaining the necessary pressure for clarity [3,25,28,34,36–44]. If the number of corneal endothelial cells drops below a certain level, vision loss and blindness occurs [42,43]. Various drugs are thus used to reduce the risk of potential damage to the endothelium during cataract removal and IOL implantation.

In the case of the eye, drug can be administered in various ways. Topical application of drugs, via eye drops or ointments, allows only 5% to 10% of the applied amount to reach the endothelium and anterior segment [14,45–47]. Intraocular injections are common, but invasive and uncomfortable to the patient, while also introducing the further possibility of infection into the anterior segment [14,45,48,49]. Drug delivering devices are increasingly used to deliver drugs immediately to the site of implantation, which allows for smaller amounts of drug needed to provide a therapeutic effect locally [48].

This thesis reports the results of *in vitro* assays that were performed to support our hypothesis that anti-inflammatory drug delivery intraocular lenses (IOLs) may help reduce the occurrence of TASS and consequent vision loss. In this research thesis project, an *in vitro* model was developed as a tool to select drug and delivery material to be used in an anti-TASS ophthalmic biomaterial in an attempt to find a novel and more effective approach to TASS prevention. In chapter 1, a review of the current literature is presented on corneal endothelial cells. Chapter 2 focuses on TASS and endophthalmitis mechanisms, current treatment methods, along with *in vitro* models and the thesis research question. The methods used to test our thesis research question are presented in Chapter 3. Chapter 4 presents our findings related to viability and cellular phenotype expression on cells. Discussion of our findings is given in Chapter 5. Conclusions are presented in Chapter 6 along with presenting recommendations for future work.

1.2 Corneal Endothelial Cells

The cornea is composed of different layers each with its distinct type of cells. The three primary cell types are epithelial, stromal keratocytes, and endothelial, as shown in Figure 1 [3,25–28,50]. Each layer possesses different properties and roles within the cornea.

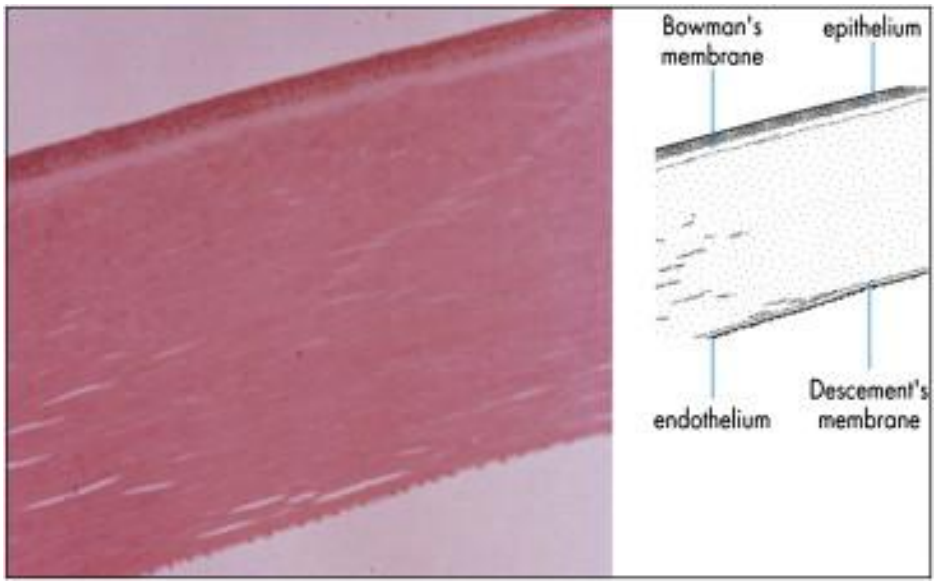

Figure 1: Light micrograph of human cornea and diagram indicating the various layers of the cornea. The stroma is not labelled, but is the area between Bowman's membrane and Descement's membrane.

Corneal endothelial cells (CEC) form a monolayer on the posterior side of the cornea. This layer is clear, transparent, and avascular, and contains many sensory nerves supplied from the corneal stroma [3,25,28,35,38]. Healthy endothelial cells have a hexagonal appearance, shown in Figure 2. As function and health deteriorate, either with age or injury, CEC become increasingly polygonal (pleomorphism) and increase in size (polymegathism) (see Figure 3) [3,25,28,34,36–42]. With aging, the CEC density decreases from around 3000 to

4000 cells/mm^2 at birth to around 2600 cells/mm^2 in adult eyes [3,28,43,44], leading to further risk of CEC damage causing vision loss. Corneal function and transparency is maintained as long as the cell density is greater than 700 cells/mm^2 [42,43].

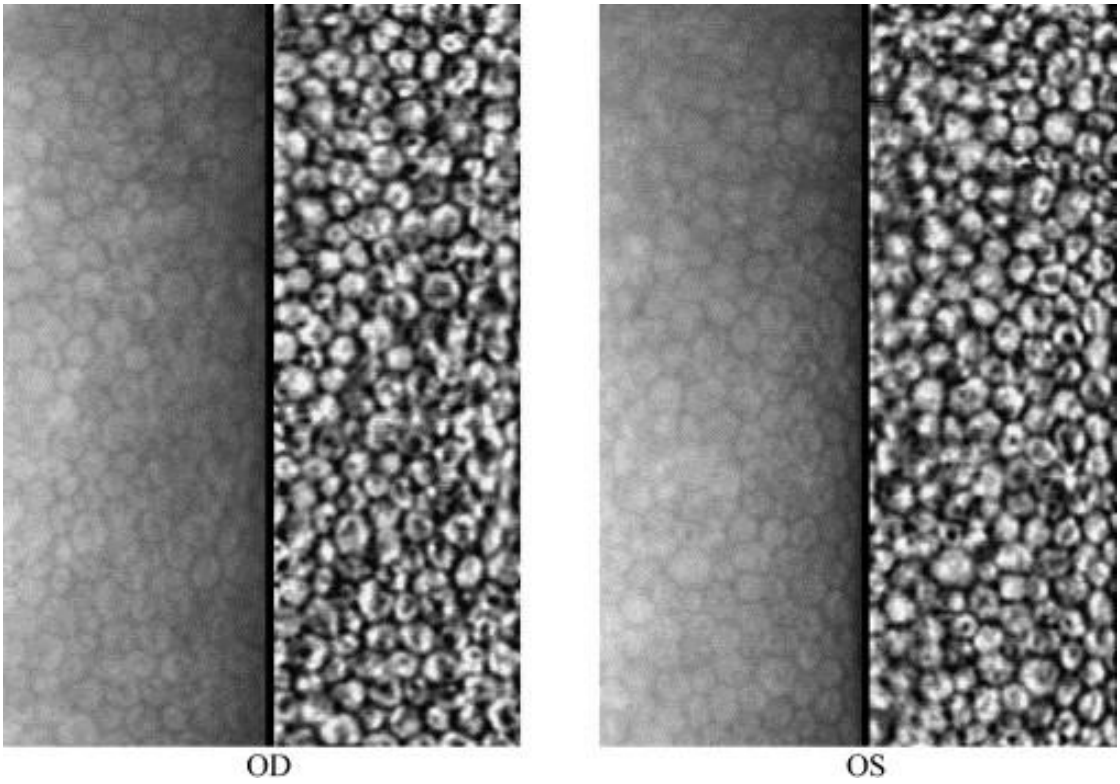

Figure 2: Right (OD) and left (OS) eye images of a healthy corneal endothelium. Their cellular densities are 3081 and 3253 respectively. Both show minimal pleomorphism or polymegathism prior to cataract surgery.

Reprinted from Journal of Cataract & Refractive Surgery, 32, Moshirfar M, Whitehead G, Beutler BC, Mamalis N, Toxic anterior segment syndrome after Verisyse iris-supported phakic intraocular lens implantation, 1233-1237, Copyright (2006), with permission of Elsevier.

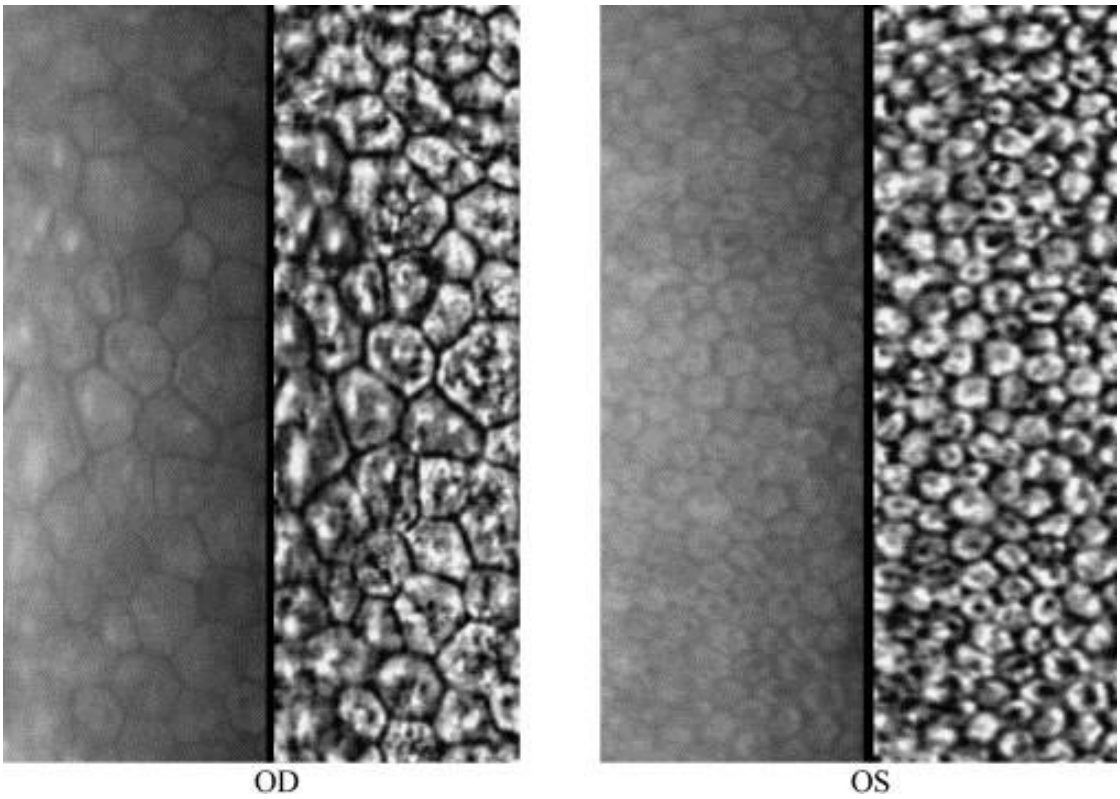

Figure 3: Right (OD) and left (OS) eye one year following cataract surgery that led to TASS infection in the right eye. Final cell densities were 964 and 3136. The right eye also demonstrates an increase in pleomorphism and polymegathism.

Reprinted from Journal of Cataract & Refractive Surgery, 32, Moshirfar M, Whitehead G, Beutler BC, Mamalis N, Toxic anterior segment syndrome after Verisyse iris-supported phakic intraocular lens implantation, 1233-1237, Copyright (2006), with permission of Elsevier.

Cataract surgery causes damage and decreased cell density in the CEC, especially near the incision site [42]. Also, a cornea that is damaged during surgery experiences an accelerated rate of endothelial deterioration [42]. In combination with CEC lost through aging, this may accelerate vision loss in the elderly, so steps should be taken to minimize CEC damage during and following surgery; drug administration can be one of the preventative measures.

Following an injury, an inflammatory stimulus, or as part of the normal aging process, cells may die. Cell death mechanism can be categorized as either apoptosis or necrosis. Apoptotic cell death is a programmed cell death in response to cytokines and stress stimuli [51–53]. Cells undergoing apoptosis shrink, followed by blebbing of the cell membrane, and finally fragmentation of the cell into membrane bound bodies [52,53]. Apoptosis helps to reduce the damage to the surrounding cells [51]. Necrosis typically occurs in response to toxins, physical injury, or restricted blood flow [53]. Necrotic cells swell and their extracellular membrane is disrupted, which allows cellular contents to be lost from the cell. This leads to a severe inflammatory response [53]. In endothelial cells, lipopolysaccharide (LPS) and tissue necrosis factor alpha (TNF-α) induce an inflammatory response and apoptosis, but not necrosis [54].

In CEC, the reasons for apoptotic cell death are not well understood. Metabolic changes, mechanical stress, endotoxins, inflammatory cytokines, and nutrient deprivation are thought to be possible causes for triggering apoptosis [44,55,56]. The responses to cytokines often occur through the nuclear factor – kappa beta (NF-κβ) and nitric oxide pathways [56].

NF-κB is a transcription factor that can induce an inflammatory (activation) response, and/or an apoptotic response, and through its activation can also control cell proliferation, adhesion, invasion and angiogenesis in many cell types [57–59]. It is activated by many different mechanisms and pathways including cytokines, such as TNF-α, and endotoxins, such as LPS [57,58]. NF-κB is bound to an inhibitor (IκB) in the cytoplasm of cells, and activation involves processes that lead to translocation of NF-κB to the nucleus of the cell [57,59–61]. As shown in Figure 4, regardless of the activation pathway there are four primary steps leading to NF-κB activation [58,59]. When activated, NF-κB induces the expression of cell adhesion molecules that are involved in leukocyte recruitment [57,59,62].

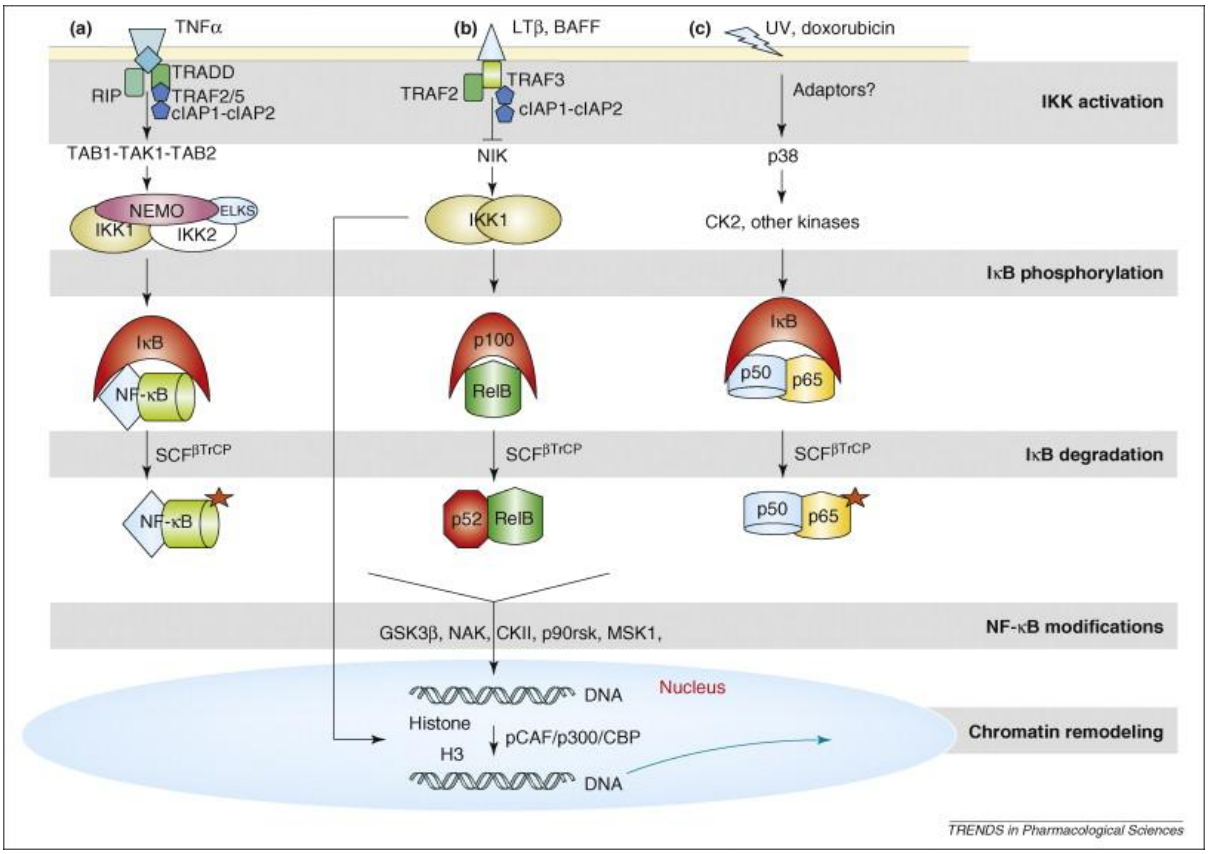

Figure 4: NF-kb activation pathway showing three possible activation pathways. TNFa is the example of an inflammatory cytokine, and the pathway of relevance in this research study.

Reprinted from Trends in Pharmacological Sciences, 30(6), Sethi G, Tergaonkar V, Potential pharmacological control of the NF-κB pathway, 313-321, Copyright (2009), with permission of Elsevier.

The inflammatory response elicits a change in the phenotype of the endothelial cell and the various receptors they express. These membrane receptors (also referred to as activation markers) are either up or down regulated in response to an inflammatory stimulus. In endothelial cells, including CEC, the most common markers are intercellular adhesion molecule-1 (ICAM-1, CD54), platelet endothelial cell adhesion molecule (PECAM-1, CD31), vascular cell adhesion molecule (VCAM-1, CD106), β_1-integrin (CD29), CD44 and

CD62 antigen like family member E (E-selectin, CD62E). Their response to cytokines or inflammatory stimulus is summarized in Table 1. The corneal endothelium is also highly sensitive to toxic agents, so any medicine or device used during surgery needs to be properly chosen for correct pH, osmolarity, and chemical composition to prevent cell activation and severe damage or apoptosis [13,15,56,63].

Table 1: Selected CEC membrane receptors and their functions

Membrane receptor (Cluster determination)	Functions
ICAM-1 (CD54)	▪ endothelial cell adhesion molecule [64–69] ▪ promotes endothelial cell-leukocyte interactions [64,65,68] ▪ increases in response to cytokine stimulation especially LPS and TNF-α [64,67–71]
β_1-integrin (CD29)	▪ cell adhesion molecule present in all human cells [72] ▪ promotes endothelial-leukocyte interactions [72] ▪ upregulated during inflammatory stimulus such LPS [73,74]
PECAM-1 (CD31)	▪ endothelial cell adhesion and signaling receptor [75,76] ▪ increases to maintain membrane permeability in response to stimulation by TNF-α, TCM, IL-1, and LPS [75,77]
CD44	▪ transmembrane endothelium glycoprotein adhesion molecule [78,79] ▪ involved in lymphocyte adhesion to endothelium [79,80] ▪ upregulated by LPS stimulation [78]
E-selectin (CD62E)	▪ endothelial cell adhesion molecule [67,69] ▪ promotes endothelial-neutrophil adherence [64,68] ▪ increases in short term response (<24 h) to TNF-α and LPS [64,67–70] ▪ increased expression in endophthalmitis [81]
VCAM-1 (CD106)	▪ endothelial cell adhesion molecule [64,68] ▪ recruits monocytes, leukocytes, lymphocytes, and T-cells [64,68,82] ▪ upregulated in response to TNF-α and LPS via NF-κB pathway [57,59,62,64,68,70]

1.2.1 Cornea pump-leak mechanism for controlling corneal hydration

The main purpose of the corneal endothelium is to maintain dehydrated levels in the stroma (deturgescence) and clarity of the cornea [3,28,56]. This is achieved through a barrier function and a pump-leak mechanism that was first described by Maurice in 1957, and remains the accepted theory today [83,84]. For the barrier function to work, there must be a sufficient number of CEC to cover the posterior surface of the cornea and maintain integrity of the intercellular tight junctions between CEC [3,44]. This barrier function is somewhat permeable because it permits an ion flux to establish the osmotic gradient [28,85]. The barrier formed prevents the bulk flow of liquid from the anterior segment to the stroma, but still allows diffusion of nutrients and other metabolites through the intracellular spaces [3,28,42,44]. A change in the barrier function of the CEC is characteristic in many corneal diseases or during surgical procedures, such as TASS and cataract surgery respectively [44].

The pump-leak mechanism pumps sodium (Na^+) and bicarbonate (HCO^{3+}) ions across the endothelial barrier from the stroma to the anterior segment [3,28,43]. One of the key proteins required for the "pump" is the sodium/potassium ion-adenosine tri-phosphatase (Na^+/K^+-ATPase) [28,43,44]. This allows for fluid to passively leave the stroma into the anterior segment, which allows for the stroma to remain in its desturged state [28], even if there is a change in the intraocular pressure (IOP) [44]. The Na^+/K^+-ATPase pump increases activity to compensate for increased permeability through the CEC layer as necessary due to disease or age related degeneration [3].

The barrier integrity between CEC must be maintained in order to properly control the CEC's pump-leak mechanism [42,43,86]. This resistance to fluid leak is controlled by the tight junctions of the endothelium [43,86], a supramolecular assembly found close to the apical domains of the endothelial cells in a monolayer [43]. In the CEC, the tight junction only offers weak resistance to the passage of solutes and water, which is believed to be due to an incomplete belt of the molecules present [86,87].

The tight junctions allow cell signalling to control the pump-leak mechanism [86]. They are made up of transmembrane molecules, typically zonula-occludins-1 (ZO-1), claudins,

and the junctional adhesion molecule-A (JAM-A) [33,43,86,88]. The rate of corneal swelling can be linked to their degree of disintegration and consequent increase in permeability of solutes [42]. This leakiness of tight junctions allows the stroma to maintain its state of deturgescence [42,43,86]. Cataract surgery has been shown to significantly impair the barrier function of CEC, leading to increased IOP and reduced vision [42].

Many molecules associated with inflammatory stress, such as TNF-α, break down components of the tight junctions and create intercellular gaps that reduce the barrier integrity of the CEC [43]. The integrity of the barrier is often lost due to selective targeting of only one part of the pump-leak mechanism, such as Na^+/K^+-ATPase of tight junctions [44,86–88]. The sensitivity of tight junctions to various substances shows the importance of carefully selecting wash solutions and drugs used during and after cataract surgery in the anterior segment of the eye [33,43,89].

Chapter 2
IOL Complications and Treatments

2.1 Toxic Anterior Segment Syndrome (TASS)

Toxic anterior segment syndrome (TASS) is a sterile postoperative inflammatory reaction caused by a non-infectious agent in the anterior segment leading to toxic damage of the corneal endothelium [3,9,13,90]. In the past, TASS was often referred to as sterile endophthalmitis, since it is not caused by bacterial, viral, or fungal infection of the eye [13]. Endophthalmitis and TASS also differ due to the location in the eye, as shown in Figure 5, with TASS occurring only in the anterior segment and endophthalmitis occurring anywhere in the ocular cavity [13].

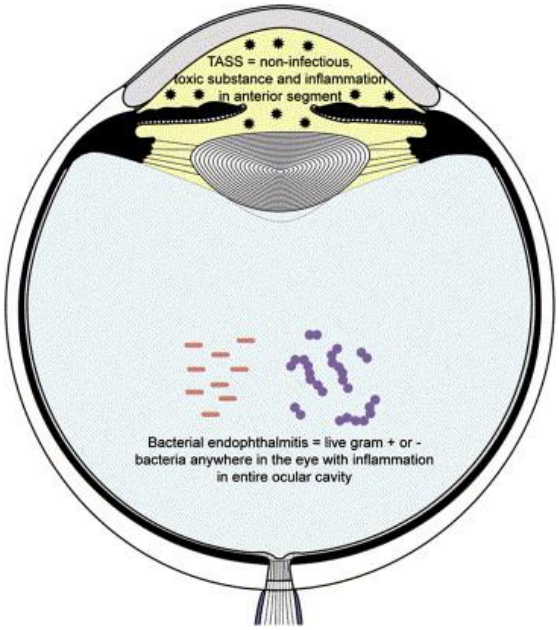

Figure 5: Diagram indicating the location of TASS and endophthalmitis. TASS presents only in the anterior segment of the eye; whereas, infectious endophthalmitis may present itself both in the anterior segment as well as the vitreous of the eye.

Common symptoms of TASS are blurry vision, mild or moderate ocular pain, and eye redness after surgery, with inflammation of the anterior segment within 12-48 hours post surgery [3,9,13,15,90]. TASS usually appears after uneventful cataract surgery; however, there have been a few cases of TASS appearing after penetrating keratoplasty [22]. Permanent edema and vision loss may result from TASS, which is initially related to acute breakdown of the endothelial tight junctions, and consequently the loss of barrier function and vision [3,9,13,15,90,91]. However, with treatment, some, if not complete, vision in patients can be restored and other symptoms significantly improved or eliminated [22,92,93].

2.1.1 TASS diagnosis

Corneal edema from widespread endothelial cell damage is commonly found in TASS patients, resulting in blurred vision, and occasionally, aqueous flare, and an anterior segment reaction with cell flare, and fibrin formation [3,9,15,90,91]. Diagnosis of TASS is based on the timing and severity of the symptoms following surgery. TASS typically occurs within 12-48 h post surgery [3,9,13,15,90]. Eyes expressing a mild to moderate grade of TASS characteristically have low levels of corneal endothelial cell density, high coefficient of variation in the cell area, and a low mean percentage of hexagonal cells [3].

2.1.2 TASS causes

There have been many causes for the development of TASS after cataract surgery, all which show the sensitivity of the CEC to foreign agents in the anterior segment. A complete summary of possible TASS causes is given in Table 2. The CEC show severe sensitivity to preservatives as well as heat stable LPS [3,9,13]. TASS is due to inadequate sterilization, or contamination of the sterilization of the surgical equipment used [3,13,91]. Unfortunately, heat-stable LPS remain enzymatically active following autoclaving. If these are present in

irrigating solutions or medications, they can be injected into the anterior segment and lead to severe inflammation [3,9,13].

Table 2: Possible causes of TASS [3,9,15,90]

Irrigating solutions or ophthalmic viscosurgical devices	• Incomplete chemical composition
	• Incorrect pH
	  ○ <6.5 or >8.5
	• Incorrect osmolality
	  ○ <270 mOsm or >350 mOsm
	• Preservatives or additives

Ophthalmic instrument contaminants	• Detergent residues
	  ○ Ultrasonic
	  ○ Soaps
	  ○ Enzymatic cleaners
	• Bacterial LPS or other endotoxin residues
	• Denatured viscoelastics

Ocular medications	• Incorrect drug concentration
	• Incorrect pH
	  ○ <6.5 or >8.5
	• Incorrect osmolality
	  ○ <270 mOsm or >350 mOsm
	• Vehicle with wrong pH or osmolality
	• Preservatives in drug solution

Intraocular lenses	• Polishing compounds • Cleaning and sterilizing compounds
Contaminated water sources	• Water baths • Autoclave reservoirs • Non-sterile or non-pyrogen-free water

2.1.3 Traditional TASS treatment

Steroids are often used to treat TASS. Topical, systematic, or intravitreal injected steroids are all used in different situations in an attempt to control TASS [9,13,15,22,90–93]. Treatment of mild to moderate cases of TASS with corticosteroids and close patient follow up has been successful [9,13,15,22,90–93]. Care must be taken when treating with steroids due to its known effects to increase IOP or even TASS itself [13,16,94]. Table 3 shows a summary of the various methods of application for the most common drugs used in the treatment of TASS. Most patients begin a topical treatment of steroid four times per day, which is increased if the symptoms do not subside [15,22,90,93]. Also, a systematic oral steroid is administered only if the symptoms do not clear up following a couple of days of topical treatment [15,22,90].

Table 3: Drugs and delivery mechanisms often used in treatment of TASS

Antibiotics	**Treatment**	**Frequency**
Chloramphenicol 0.2%	topical	4x daily [93]
Polymyxin B sulphate 0.25 MU	topical	4x daily [93]
Steroids		
Prednisolone acetate 0.5-1%	topical	4x daily [15,22,90,93]
Prednisolone	oral	60 mg/days, 4 days post op [15,22,90]

2.2 Endophthalmitis

Endophthalmitis is an infection of the eye that involves the vitreous cavity, aqueous humour, and affects surrounding tissues such as the CEC, choroid or retina. Endophthalmitis is one of the most feared complications of cataract surgery because it causes severe and permanent

visual loss when left untreated [16,24,21]. The perceived patient quality of life is lower in cataract surgeries followed by endophthalmitis compared with uncomplicated cataract surgery, even if visual acuity is the same [95].

Due to the severity of endophthalmitis, patients receive topical antibiotics before and after cataract surgery along with povidone-iodine application, both of which are shown to significantly reduce the occurrence of endopthalmitis [2,11,16,23,14]. This is perhaps best shown by the low Swedish rates of only 0.048% where intracameral cefuroxime is standard protocol compared to recent levels in the United States of 0.25% where it is not standard protocol [16]. Routinely administering drugs immediately following cataract surgery appears to diminish the risk of disease.

2.2.1 Endophthalmitis symptoms

Differentiating between an early onset of endophthalmitis and TASS is challenging, since they present many of the same symptoms [11]. Making the proper diagnosis is important, since misdiagnosis may lead to severe and irreversible vision loss. Endophthalmitis usually peaks later than TASS, between three and seven days, although it is possible to occur even many months following surgery. It is accompanied by pain and vitritis, which are typically not present in TASS [11,96,97]. The increase of IOP, due to inflammation secondary to TASS, is rarely seen in endophthalmitis [90]. The success of the treatment is influenced by causative organism, and treatment procedure [2,95]. A variety of drugs may be used based on the bacteria present in the infection [2,24,90,94,98], A summary of the various drugs used is shown below in Table 4. Due to the sensitivity of CEC, some of these drugs may be toxic to the CEC even at low levels and may cause clinical edema [16,99].

Table 4: Drugs used in treatment of endophthalmitis

Drug Family	Drug	Delivery method
4th generation fluoroquinolone	Gatafloxacin	Topical
	Moxifloxacin	Topical, intracameral
2nd generation cephalosporin	Cefuroxime	Intracameral
Glycopeptide	Vancomycin, ancomycin	Intracameral
Aminoglycoside	Gentamicin	Topical
N/A	Povidone-iodine	Topical

2.3 Intraocular Lenses (IOLs)

An IOL is an artificial polymer based lens that is placed during cataract surgery to replace the lens that is removed through phacoemulsion [4]. IOL material has changed little since poly(methyl methacrylate) (PMMA) was first introduced as an IOL in 1949 [1,100]. Despite over 60 years of IOL implantation, complications following cataract surgery still occur, including endophthalmitis and TASS as discussed above [1,101].

IOL material properties have been reported to influence the kind of complication that is more likely to arise following cataract surgery in some studies, yet not in others. According to *in vitro* studies, the attachment of infectious organism to the IOL may depend on both the IOL material and the organism [1], which may lead to endopthalmitis. It has also been reported that organisms are more likely to attach to hydrophobic IOLs than hydrophilic IOLs [1]. The occurrence of endophthalmitis was not different between IOL materials in one study [17], while in two other studies, silicone IOLs or a hydrophobic copolymer appeared to increase the risk for endophthalmitis [14,102]. Thus it is difficult to conclude which material properties affect binding of organisms and complication rates.

2.4 Inflammatory inhibitors

2.4.1 Corticosteroids

Corticosteroids are potent anti-inflammatory agents that have been used to treat many forms of ocular inflammation including endophthalmitis and TASS since the 1950s [6,103,104]. They are able to retard the loss of endothelial tight junction proteins that are essential to endothelial cell function [105]. They also reduce patients' symptoms of eye inflammation, swelling, heat, redness and pain when directly applied to the eye either topically or intracamerally [106].

Corticosteroids have many side effects, such as induction of glaucoma, formation of cataracts, decreased wound healing, and increased intraocular pressure (IOP) [6,45,104]. However, increased IOP that occurs in the week immediately following surgery may be due to the surgical placement of the IOL, and not the steroids themselves [104].

Common corticosteroids used for ocular inflammatory treatment include dexamethasone [106], prednisolone [6], lotepredonol etabonate [6], ciprofloxacin, triamcinolone [103], and recently triptolide [7,107]. Dexamethasone is the most common corticosteroid used to treat inflammation in the anterior segment [47,106–108]. The effects of triptolide with respect to CEC has not yet been investigated, but preliminary investigations suggest its ability to reduce inflammation in the cornea [7].Corticosteroids are commonly applied topically following surgery; however, patient compliance may reduce the effectiveness of topical corticosteroids [103].

A challenge faced with single intracameral injection of corticosteroids is their respective half life in the anterior segment. Dexamethasone has a 3 h half life in vitreous fluid after intracameral injection [104], which is not long enough to effectively combat TASS or endophthalmitis following surgery without multiple injections. Triamcinolone acetate, has a much longer half life of 18.6 days, after a single injection; however, the toxicity and therapeutic efficacy over this time period has not been investigated [109]. In a drug delivery system, the half life of a drug requires attention, as a longer half life of a drug may increase

the likelihood of a toxic accumulation if release from the material is not adequately controlled.

2.4.2 NF-κB pathway activation inhibitors

NF-κB is activated by TNF-α and LPS during the inflammatory response on CEC [57,58,110]. Inhibition of this pathway may reduce CEC damage and the inflammatory response seen in TASS. Two novel drugs, triptolide and PPM-18, have demonstrated inhibition of the NF-κB pathways following their activation with LPS or TNF-α [7,111]. Triptolide, a drug developed from an herbal extract, exhibits anti-inflammatory responses following LPS activation of the NF-κB pathway with immune cells, epithelial cells, and fibroblasts [7]. Although no research exists on its effects on endothelial cells, its current efficacy warrants further exploration. PPM-18 inhibited the increase in NF-κB activity in macrophages caused by LPS stimulation [111]. The anti-inflammatory properties of triptolide and PPM-18 may have beneficial effects in preventing TASS and endophthalmitis.

2.4.3 Protease Inhibitor

Proteases are produced by cells in response to LPS that are activators of the immune and consequent inflammatory response [112–116]. This suggests that a protease inhibitor may be an effective method to reduce inflammation following cataract surgery in CEC. A protease with a specific role in the cornea is thrombin. Thrombin is a serine protease known to break down the gap junctions and destabilizes tight junctions reducing the barrier function of CEC [89]. Aprotinin, a general protease inhibitor, reduces the inflammatory response *in vitro* on HUVECs stimulated with LPS or TNF-α [54], and the production of antibodies in mice [116]. Despite protease's known ability to induce inflammation in endothelial cells, and their abilities to reduce the barrier function in CEC, surprisingly little research exists exploring the ability of protease inhibitors, such as aprotinin, in reducing damage to the corneal endothelium.

2.5 Drug Delivering Methods

The two most common methods for delivering drugs to the eye are topical application and intracameral injections, both of which have limitations. A drug delivery system implanted in the eye allows an efficient and sustained release of drug into the anterior segment, which may help to combat post cataract surgery infection.

2.5.1 Topical and intracameral injections

Despite topical steroid or antibiotic application inefficiency in reaching the target tissues, including CEC, it is routinely performed following cataract surgery [5,117,118]. Due to the high turnover rate of tear fluid, less than 5% to 10% of topical drug dosage applied reaches the corneal endothelium and anterior segment [46,47,103,119]. Also, the cornea's structure of a hydrophobic epithelium followed by a hydrophilic stroma limits both water soluble and insoluble drugs access to the corneal endothelium [103,120]. Due to the chronic symptoms of uveitis, a symptom of TASS and endophthalmitis, it is necessary to maintain a therapeutic level of corticosteroid in the anterior chamber over time [104].

Intracameral injection is a highly popular drug delivery method to ensure patient compliance and that the drug reaches the endothelium; however, it is invasive and can increase the risk of infection, and the drug may still have a short half life in the anterior segment [48,104,119]. Intracameral injection may also lead to the incidence of endophthalmitis, or TASS [104]. The lack of efficiency in the case of topical applications, and challenges or risks faced with intracameral applications could be avoided with a drug delivering device in the eye.

2.5.2 Drug delivering devices

Drug delivering devices allow a preventative method of administering drug following surgery to decrease the inflammatory response that the body is required to handle; therefore, reducing the appearance of the symptoms and complications of disease [121]. This is

important in an acute complication, such as TASS, due to its fast time of presentation. Drug delivering devices help increase the efficiency of the drug and improve safety and comfort over topical [48] or intracameral injections [103]. Subconjunctival implants allow for higher drug concentrations sustained over a longer time period compared to subconjunctival injections [103]. These benefits of drug delivering devices allow for prolonged therapeutic effects and automatic patient compliance to ensure the maximal benefit with the lowest cost.

2.5.3 Current drug delivering devices – non IOLs

Drug delivering devices are either biodegradable or non-biodegradable polymers [47,101,103,122]. Biodegradable polymer implants that have been investigated for intravitreal drug delivery consist primarily of a variety of polyesters [103]. These devices are implanted into a variety of locations within the eye depending on the targeted tissue for drug release. The ideal drug delivering device should offer a high level of efficacy against pathogens and the inflammatory response, minimize cell and protein adhesion, provide a sustained drug delivery over weeks or months, and produce minimal side effects [103].

Recently, drug-delivering polymer inserts have been developed for use intraocularly to increase the benefits of the corticosteroids. Two types of devices are currently used clinically to deliver dexamethasone [47,103]. One polymer device may be injected into sub-Tenon's capsule to prevent vitreous humour inflammation and complications following eye surgery, including cataracts [103]. While this may be effective for many other ocular diseases, this injection location may not provide the necessary drug delivery to the anterior segment and corneal endothelium following cataract surgery.

The second type of device is not fixed in a given place, and is free to move around within the vitreous of the eye. Ozurdex^{TM} (Allergan, Inc, Irvine, California) [103] and SurodexR (Oculex Pharmaceuticals Inc., Sunnyvale, California) [47,123] are current FDA approved intraocular pellets that deliver dexamethasone. These implanted drug delivering devices allow a more controlled release than a single intracameral injection, by allowing for a sustained release of drug. When implanted at the end of a cataract surgery, they eliminate the

need for topical corticosteroids [47,103,123]. However, these devices are not fixed within the vitreous and may lead to migration of the implant to the interface between the posterior convexity of the IOL and the posterior capsule or lead to peripheral anterior synechiae [47]. This may lead to difficulties removing the implant and interference with the IOL and vision. Creating an IOL that is also a drug delivering device would remove the risks of a free floating drug delivery system, and reduce the need for a separate implant in the eye that may have to be removed at a later date, leading to further surgery and possible complications.

2.5.4 Drug delivering devices - IOLs

Despite an IOL always being placed during cataract surgery, few research groups have evaluated using the IOL itself as a drug delivery system for prevention of complications of endophthalmitis following cataract surgery. No drug delivery system has yet been created with the focus of preventing TASS. The inflammatory response seen with the physical trauma of cataract surgery is another focus of drug delivering IOLs. This may be achieved by loading the IOL with dexamethasone, NSAIDs, or matrix meatalloprotienase inhibitors (MMPi). Matrix metalloproteinases (MMP) are activated following the mechanical stress of IOL implantation, which leads to degradation of the extra cellular matrix [101]. Incorporating a drug into the IOL itself eliminates the need for either a separate device to be injected into the eye, or multiple intracameral injections.

In attempts to reduce endophthalmitis, hydrophilic acrylic IOLs are often soaked by surgeons in fluoroquinolones, including norfloxacin, gatifloxacin, levofloxacin and moxifloxacin [122,124–127]. However, few studies have evaluated the effectiveness of this practice. Acrylic IOLs are able to release antibiotic at suitable levels *in vitro* to kill endophthalmitis-causing organisms [124–126]. The release of norfloxacin was maintained at a clinically relevant dose *in situ* over 114 days [122], which is long enough to combat late presenting endophthalmitis. An *in vivo* study in rabbits that compared intracameral injection versus an antibiotic delivering IOL determined the same efficacy against reducing infection [127]. This suggests that an IOL is a suitable method for delivering drug to the anterior

segment of the eye and preventing endopthalmitis. These effects were not studied in relation to endothelial toxicity and consequent possibility of TASS.

Other IOLs are modified with NSAIDs, corticosteroids, or MMPi in an attempt to combat the inflammatory response occurring from trauma during cataract surgery and placement of the IOL [47,101,128]. The NSAID and dexamethasone loaded IOLs demonstrate an ability *in vitro* and *in vivo* rabbit models to reduce inflammation [47,128], which may prove beneficial in the treatment of TASS and reducing endophthalmitis symptoms. The NSAID loaded IOLs maintained a constant release for three months [128], which helps to treat longer term inflammation that is sometimes seen in endophthalmitis. MMPi loaded IOLs decrease *in vitro* cell viability in corneal and retinal epithelial cells, as well as stromal fibroblasts [101]. However, reduced cell viability suggests a toxicity that may affect other surrounding tissues, such as the corneal endothelium. Dexamethasone or NSAIDs appear better options than MMPi at reducing an inflammatory response following cataract surgery. With regards to reducing TASS, dexamethasone is already a recognized topical treatment and merits further investigation on its effects on CEC as a drug delivery system.

Evaluation needs to be performed on drug delivering IOLs to establish the efficacy and toxicity of drugs in relation to the corneal endothelium. The current focus in the literature does not include testing of CEC either *in vivo* or *in vitro*, despite the risks to vision if polymers or drugs reduce their viability. The ability of these drugs to counteract cytotoxin and endotoxin inflammatory response should be evaluated to determine their effects at reducing TASS, not just general inflammation following cataract surgery. The ability of these compounds, especially dexamethasone, to be delivered via IOL indicates that this may be a successful route to explore in reducing the incidence of TASS.

2.6 Role of *in vitro* models

To understand the mechanism of the inflammation response prior to human trials, as well as for ethical, safety, and cost reasons, both *in vivo* and *in vitro* models are necessary [129–133]. Due to the low occurrence of TASS, most studies are prospective, consequently dealing

with the clinical response as seen *in vivo* [9,13,22,90,134–137]. Research in endophthalmitis is more varied, with both *in vivo* prospective clinical responses [2,5,11,17,20,49,94,138,139,139–141], *in vivo* animal studies with drugs and various organisms [142,143], and *in vitro* studies investigating the effects of drugs on certain organisms [144–147]. *In vivo* clinical studies also exist for treatment of general inflammation following cataract surgery [45,105].

There are few instances in the literature where an *in vivo* study is created to determine the effects of antibiotics or preservatives used in cataract surgery on the health of the eye and preventing surgical complications. These studies primarily focus on the viability, density, and morphology of the CEC following exposure to drugs, whether in rabbit or human eyes [129,148–153]. However, observations on the corneal endothelium in patients are limited to mostly qualitative factors; limiting the conclusions that can be made to why or how a substance is influencing the CEC.

Despite the necessity of *in vivo* animal models, there are a number of limitations to these studies. One of the main concerns is the ability of these models to accurately and consistently predict human response [98,130,133,152–155]. *In vivo* studies are limited in their ability to understand the underlying mechanisms involved with treatment responses [130]. With a better understanding of the mechanisms involved, drug efficacy may be better predicted, and more effective treatments can be developed to reduce surgical complications. *In vivo* models are much more expensive to run than *in vitro* studies, and as a consequence most are short term studies [156]. For this reason, *in vitro* models are used in an attempt to reduce, replace, or refine the number of *in vivo* models needed, which reduces the number of animals needed, and cost of the *in vivo* study [27,133].

There is a significant lack of the literature evaluating the specific effects of drugs *in vitro* on endothelial cells with an aim of reducing TASS and endophthalmitis. Some *in vitro* studies only determine release profile from materials based on reported therapeutic efficacy and not their toxicity or efficacy on CEC [124]. There is no pre-existing or standard model

currently used to help pre-screen drugs and materials based on CEC response *in vitro* prior to implantation in the cornea *in vivo.*

In vitro models may allow formation of a better hypothesis related to the appropriate dosing schedule for a drug that would create a safe and effective method of drug treatment. An *in vitro* model allows screening of drugs and compounds quickly under a variety of conditions and with complex biological fluids [132]. While *in vitro* models also have some limitations due to over simplification, *in vitro* assays are necessary to reduce costs [27,133,157], and allow a quick screening of different drugs [27,133,157].

Models for *in vitro* analysis with human CEC and their toxicity to drugs are rarely reported in the literature. There is one cell line from Bednarz (Germany) that is recurrent in the literature [145,146,158], and has been used by one group to evaluate the efficacy and toxicity of an antifungal and an antibiotic on various eye tissues in an effort to reduce infectious keratitis and endophthalmitis [145,146]. A primary human CEC tested the toxicity of various antibiotics and inflammatory inhibitors reported in the literature for application following cataract surgery [159]; however, dexamethasone was not among these, and further testing is required to determine their efficacy on these cells. The human umbilical vein endothelial cell (HUVEC) cell line is much more sensitive to inflammatory cytokines, especially TNF-α than corneal keratocytes *in vitro* [160]. Despite this, HUVECs are often used *in vitro* to study inflammatory responses as they show a clear response to endotoxin and cytokine stimulus [51,64,69,75,161,162]. The cytokines activate the NF-κB pathway for CEC and vascular endothelial cells in the same manner [56,163]. Dexamethasone can downregulate inflammatory markers following LPS stimulus on HUVECs [164], as it also appears to do in a prospective analysis of TASS treatment [137].

2.6.1 Interspecies variation in the corneal endothelium

Variability in CEC exists between species in cell density, response to injury, and their ability to replicate. These are all factors that need to be considered during *in vitro* and *in vivo* testing to create an appropriate model for drug and material testing. The animal chosen for the *in*

vivo and *in vitro* assays should be chosen based on the similarities to the human system we are attempting to understand [133].

Human CEC do not replicate *in vivo*. Cats and other primates' endothelial cells also have minimal ability to replicate *in vivo* [29,31,33,40,42,165]. This is in contrast to rabbit and bovine CEC that replicate *in vivo* allowing them to repair and replenish after injury [41,42,166]. This allows the CEC to return to their normal shape and size several weeks after injury [42]. Human CEC only repair their function by cell migration and enlargement [41,42,166]. In cat and monkey CEC, proliferation of CEC does occur, but at a much lower rate than rabbit, and their cells do not fully return to the same shape and size [42]. The ability of proliferation of CEC seen *in vivo* is the largest inter-species variance in CEC, and represents one of the biggest challenges faced when determining the suitability of an *in vitro* animal model. This ability to reproduce may show exaggerated improvement in response to drugs for treatment of inflammation after cataract surgery to that seen in humans. Further investigation into the effects of drugs and drug delivering devices needs to be evaluated in endophthalmitis and TASS prevention in animals with non replicating CEC to more accurately mimic human CEC. Despite important differences in proliferation as discussed above, due to their easier availability and well known phenotype, rabbit CEC are also commonly used in *in vivo* and *in vitro* models to evaluate CEC [26,27,30,85,108,142–147,167–169].

2.7 Thesis research questions

TASS is a dangerous complication of cataract surgery on which very little research has been conducted outside of a clinical setting. This research project aimed to develop an *in vitro* model to help with the prevention of TASS by measuring the endothelial cell response to drug delivering IOLs. This research modeled TASS in a controlled laboratory setting and determined the effects of various treatments of drug, and drug delivering materials on endothelial cell viability and phenotype.

Specifically, this research focused on testing a novel interpenetrating network (IPN) biomaterial for use as an IOL. The IPN consisted of a copolymer of poly (dimethyl siloxane) (PDMS) and poly(N-isopropyl acrylamide) (pNIPAAm) (copolymer) that was compared against a control PDMS only material (polymer) for drug delivery to prevent TASS and endophthalmitis. The efficacy of this system was tested *in vitro* to allow for efficient screening of material and drugs to prevent TASS following cataract surgery.

The hypothesis of this research paper was to use a novel NF-kB inhibitor, PPM-18, in conjunction with a drug delivering PDMS/pNIPAAm interpenetrating polymer networks as an intraocular lens (IOL) to successfully reduce the effects TASS and consequent vision loss. To determine the efficacy of PPM-18, it was compared to the cytokine inhibitor dexamethasone, a potent anti-inflammatory steroid already used during cataract surgery, along with trpitolide, another cytokine inhibitor [7,105,106,164]. An *in vitro* methodology was developed to determine changes in the viability of HUVECs via MTT assay and cell phenotype changes via characterization of known endothelial activation markers: ICAM-1, PECAM-1, VCAM-1 β_1-integrin, and E-selectin, with flow cytometry. Due to the acute nature of TASS, cell activation was measured between 24 h and 4 days.

Chapter 3
Methodology

3.1 Cell Culture

Primary HUVECs were obtained from Sciencell and grown to confluence in T-75 tissue culture flasks. They were grown in Endothelial Cell Media (Sciencell, Carlsbad, USA) containing 1% endothelial cell growth factor, 5% fetal bovine serum, and 1% penicillin-streptomycin (ECM). All assays were performed between passages two and six. Following the sixth passage cell morphology visibly changed, becoming more elongated and similar in appearance to fibroblasts and therefore cells were discarded [52,160,162,170–174].

3.2 Interpenetrating Network (IPN) Preparation

Two different interpenetrating polymer networks were tested. A vinyl terminated poly(dimethylsiloxane) (PDMS) polymer (polymer) was prepared as previously described, with minor adjustments [175]. The material was synthesized in collaboration with Lina Liu in Heather Sheardown's Lab at McMaster University.

Briefly, the PDMS monomer was mixed with the Sylgard184 curing agent (Dow Corning Corp., Midland, USA), and allowed to cure for 24 h at 20^{o}C. The resulting polymer films were rinsed in tetrahydrofruan (THF) to remove unreacted monomer and crosslinker.

The second material was a novel hydroxyl terminated PDMS (PDMS-OH) crosslinked with poly(*N*-isopropyl acrylamide) (pNIPAAm) as previously described [175]. The PDMS-OH was prepared using a methacryloxypropyltriethoxysilane (MATO) crosslinker and tin(II)-2-ethylhexanote catalyst. This mixture was added drop-wise onto a water layer to form a thin film and cured for 5 days at room temperature. The PDMS-OH film was purified by a rinse in THF, then dried in a fumehood for 48 h, and followed by vacuum for 24 h. The PDMS-OH was then crosslinked with pNIPAAm. The pNIPAAm monomer (Sigma-Aldrich Co., Oakville, Canada) was mixed with the N,N'-methylenehis acrylamide crosslinker (Sigma-Aldrich Co.) and the ultraviolet (UV) sensitive initiator Xanthane (Sigma-Aldrich

Co). The PDMS-OH was then immersed in the mixture and allowed to equilibrate over 24 h at room temperature. These equilibrated polymers placed under UV for 2 h to allow the pNIPAAm to copolymerize with the PDMS-OH (copolymer), followed by curing for 24 h at room temperature. The resulting copolymer was separated from the bulk PNIMAAm and purified by extraction with THF for 48 h to remove unreacted monomer and crosslinker. THF was then removed from the material for 48 h in the fumehood followed by vacuum for 24 h.

Both copolymer and polymer materials formed films approximately 0.6 – 0.8 mm thick. Disks 5 mm in diameter were then punched out for use in experiments. These disks were used either in their unloaded state, or loaded with drug for experimentation. Prior to use in assays, the material was sterilized by exposure to UV for 20 min.

Both materials are loaded with drugs in the same way as previously described [176]. Breifly, drugs were dissolved in DMSO and dry material were placed in the solution for 48 h at room temperature, and then dried in a fumehood and 37^{o}C vacuum. Dexamethasone and PPM-18 samples of both polymer and copolymer were loaded. Dexamethasone samples were loaded to provide a cumulative release of 10 nM or 100 nM over a 4 day period. PPM-18 samples were loaded to provide a cumulative release of 10 µM over a 4 day period.

3.3 *In vitro* HUVECs activation and drug toxicity

Initial toxicity testing was completed on HUVECs using known cell stimulatory mediators LPS (Sigma-Aldrich Co), phorbol myristate acetate (PMA) (Sigma-Aldrich Co), and TNF-α (R&D Systems Inc., Minneapolis, USA) to determine appropriate levels for further specialized testing. HUVECs were grown in either 48 well plates. 6 x 10^4 cells were seeded into each well on a 48 well plate. In cases where the volume of cells and media applied to the plate was less than 100 µL then an approximately additional 200 µL of media were added to each well to ensure adequate dispersion and nutrition. The plates were then incubated for 24 h at 37^{o}C and 5% CO_2 to allow cells to adhere and reach confluence. LPS (2 pg/mL to 200 ng/mL), PMA (10, 50, 100 nM) and TNF-α (1 pg/mL – 1 mg/mL) were added the next day and incubated for up to four days. Medium was not replenished.

HUVECs response to the drugs in medium was also carried out following the protocol as described above with dexamethasone (10 nM) (Calbiochem, Darmstat, Germany), triptolide (Calbiochem), PPM-18 (10 µM) (VWR International, Mississauga, Canada; Cayman Chemical, Ann Arbor, USA), and aprotinin (Calbiochem). Dexamethasone concentrations were initially tested from 0.1 – 100 nM [7] and final comparison tests between drugs were done at 10 nM. Triptolide concentrations were initially tested at 1-30 nM [7] and final runs were completed at 3 nM. HUVECs were incubated first with only these concentrations. PPM-18 concentrations were initially tested from 0.1 – 30 µM [111], with final comparison tests done at 10 µM.

3.4 HUVECs interaction with biomaterials

HUVECs were grown in either 48 or 24 well plates, depending on the cell count following detachment from the culture flask. 6 x 10^4 cells were seeded into each well on a 48 well plate and 12 x 10^4 cells per well in a 24 well plate. The plates were incubated for 24 hr at 37^{o}C and 5% CO_2 to allow cells to adhere and reach confluence. Small discs of IPNs materials were either placed gently on the cell monolayer (in a 48 well plate containing 250 µL of fresh ECM), or in a 24 well plate within a hanging well insert and 1 mL of ECM. These are illustrated in Figure 6.

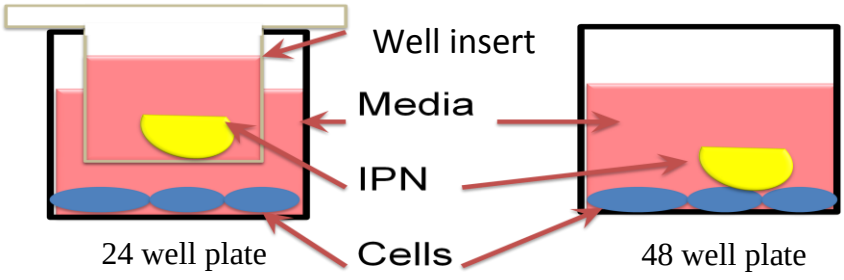

Figure 6: Drug delivery *in vitro* model in either a 24 or 48 well plate

The number of discs was adjusted to ensure appropriate drug release. The release for dexamethasone IPN was 10 nM or 100 nM over 4 days, and for PPM-18 loaded IPN was 10 µm or 30 µM over 4 days.

3.5 Viability assay

Drug toxicity and material biocompatibility were assessed by measuring viability using the MTT assay. MTT (3-(4,5-dimethylthiazol-2yl)-2,5diphenyl tetrazolium bromide) is a tetrazolium salt that measures the activity of dehydrogenase enzymes, only found in living cells, through a rapid colorimetric assay that was initially developed by Mosmann in 1983 [177].

The protocol followed for MTT testing on HUVECs was modified from one previously described [178]. MTT was dissolved in ECM at a ratio of 0.5 mg/mL. The solution was vortexed and warmed to 37^{o}C to help facilitate complete dissolving of the MTT, and was then sterile filtered.

Before adding the MTT solution to the cell monolayer in a 48 well place, supernatant in each well was aspirated, and rinsed with PBS. 100 µL of MTT solution was added to each well. If too much MTT solution was added, the cells would not remain adherent to the bottom of the plate. The plates were incubated for 12-24 h at 37^{o}C and 5% CO_2. During incubation, a dark blue formazan product was produced by the mitochondria of living cells cleaving the MTT [177]. After the incubation period, solution was aspirated off the plates and 200 µL of DMSO was added to each well (dissolving the formazan crystals). The dissolved solution was transferred to a 96-well plate and read on an absorbance reader at 595 nm wavelength, ensuring no final measurement was above 2.0. Plates were read within 1 h of adding the DMSO. The absorbance was directly proportional to the number of living cells, with more absorbance indicating a greater number of living cells [177]. The final measurements were recorded and analyzed on the computer as a percentage change from control.

3.6 Flow Cytometry

Flow cytometry is a common technique to assess cell population, determine cell size, and characterize cell phenotype. A laser of a specific wavelength is aimed at a stream of

hydrodynamic focused fluid, so only a single cell is passed through the beam at a time. This is crucial to allow for accurate collection of data. The cells may pass through the beam at thousands per second (Figure 7).

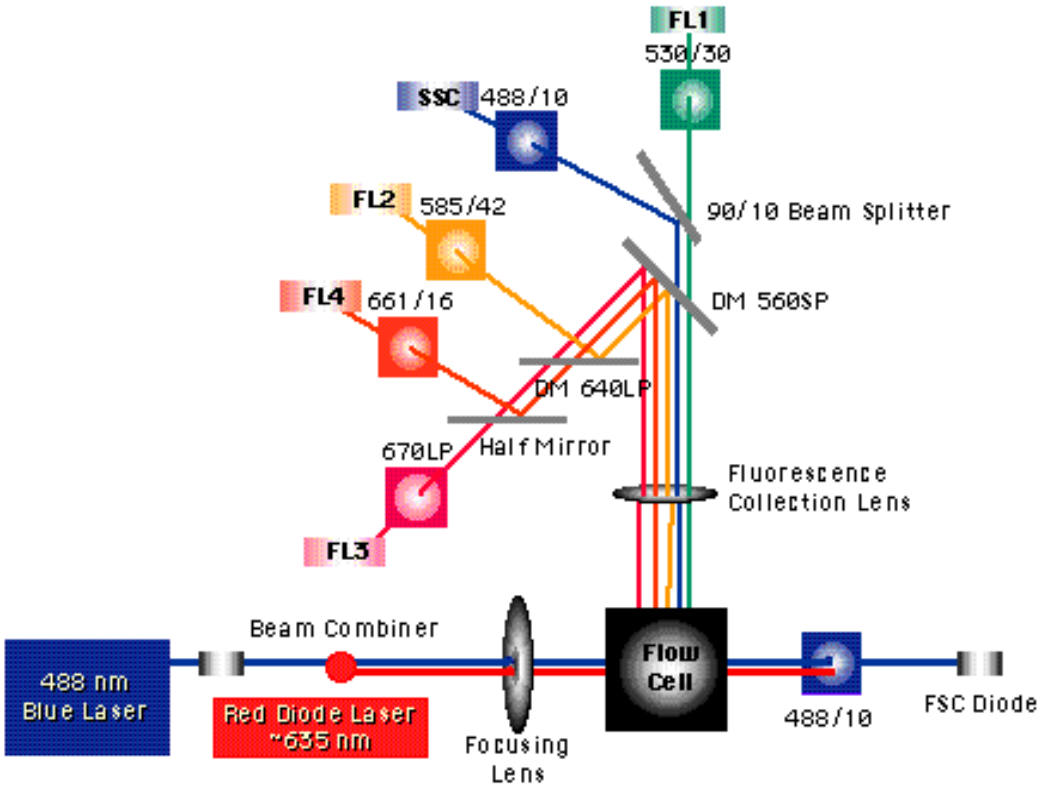

Figure 7: BD FACSCalibur optical path configuration. Figure taken from BD FACSCalibur brochure which demonstrates its basic set up, and is the same flow cytometer used in this research.

As the cell passes through the laser there is both forward and side scatter. Forward scatter determines cell and particulate size. Side scatter is caused by granularity and complexity within the cell, which when combined with the forward scatter data can isolate different cell types from within a larger population (Figure 8).

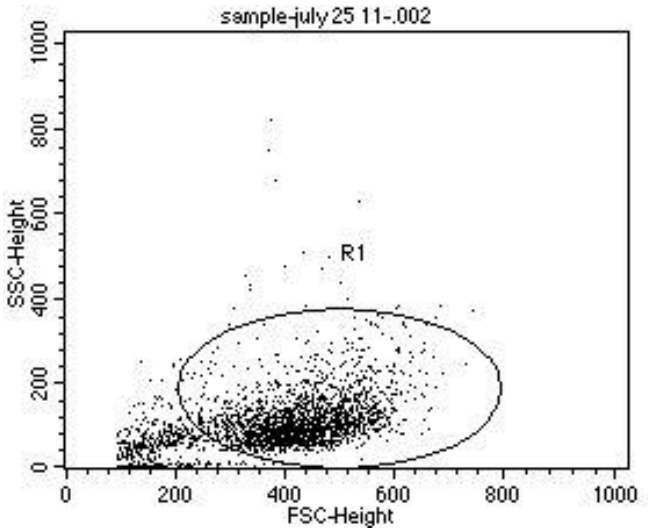

Figure 8: Flow cytometry plot for forward scatter (FSC) vs. side scatter (SSC). The forward scatter indicates particle size, and side indicates granularity. This plot is gated on the HUVEC population.

As these cells were incubated with fluorescent marker, the fluorescence of these cells is emitted in proportion to the amount of marker attached to cell, which are read on separate channels. There were three fluorescence markers used in our assays. Fluorescein isothiocyanate (FITC) is the green fluorescence marker most commonly used. It is the major derivative of fluorescein. FITC has an excitation of 495 nm and an emission at 521 nm. Phycoerythrin (PE; orange fluorescence marker) can be excited at 495 nm, but also at around 545/566 nm. The emission peak of 575 nm allows it to be used simultaneously with FITC as a marker on cells. Phycoerytrin-cyanine dye conjugate (PE-Cy5; red fluorescence marker) has an excitation of 488 nm and an emission at 667 nm, allowing it to be compatible with both FITC and PE conjugated antibodies. These create further population graphs of the comparison of the channels over time, such as FITC vs. PE (Figure 9A), as well as a histogram of the intensity of each fluorescent cell, such as PE only (Figure 9B).

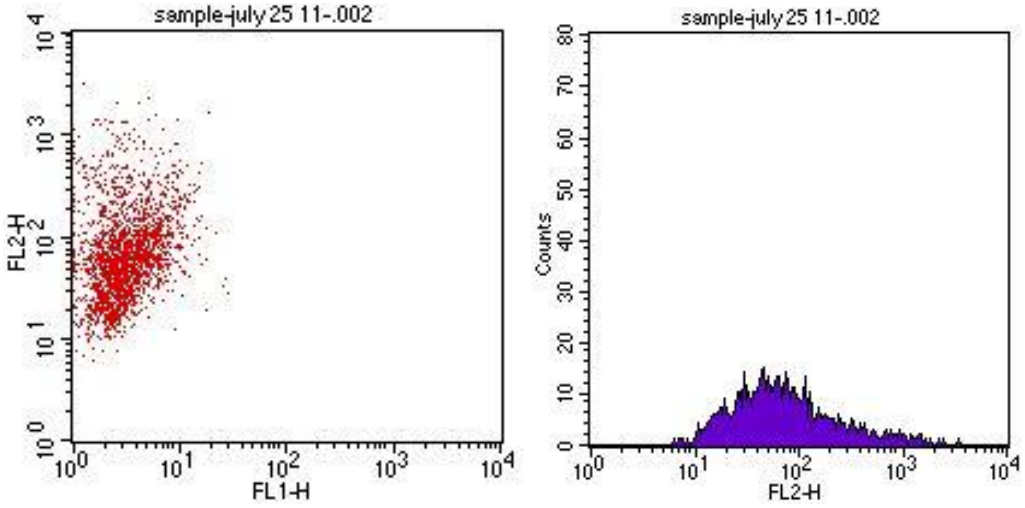

Figure 9: Example of typical fluorescent data plots in flow cytometry. (A) Fluorescent intensity of FITC markers (FL1) vs. intensity of PE markers (FL2) on untreated HUVECs positive for the PE marker and negative for FITC marker. (B) Fluorescent intensity histogram for PE channel indicating presence of PE marker on cells.

3.6.1 Flow Cytometry Protocol

To ensure an adequate number of cells for flow cytometry, samples ran in 48-well plates were run in duplicate and pooled.

Following interactions with materials or drugs, cell samples were processed for flow cytometry. HUVECs were removed from the wells with TrypLExpress (55 min at 37^{o}C, Invitrogen, Burlington, Ontario, Canada). Cells were washed and resuspended in DMEM/FBS. Small aliquots (30uL) of HUVECs, diluted in DMEM-FBS, were incubated for 1 h at 4^{o}C with saturating concentration of fluorescently-labeled antibodies against ICAM-1, Integrin-β1, E-selectin, CD44, and VCAM-1. Samples were then diluted in Hepes Tyrode Buffer, fixed in 1% paraformaldehyde (final concentration) and analysed by flow cytometry within 5 days.

To determine if exposure to drug or biomaterial led to cell apoptosis or necrosis, caspase activation and propidium iodide (PI) uptake on adherent cells was studied. HUVECs were

removed from the wells as described above. Small aliquots of HUVECs, diluted in DMEM/FBS, were incubated with a fluorescently-labelled pan caspase inhibitor (FITC-VAD-FMK, Calbiochem, San Diego, California) for 1 h at 37^{o}C. Samples were washed and resuspended in wash buffer, 1 mL of PI was added to each tube and samples were analyzed immediately by flow cytometry. Table 5 below summarizes the assays performed on HUVECs following incubations with material/drug. All antibodies were purchased from BD Diagnostics, Canada. The samples were stored at 4°C and analyzed within 5 days with the Becton Dickinson FACSCalibur flow cytometer (BD Diagnostics, Mountain View, USA).

Table 5: Selected CEC membrane receptors or intracellular stains and their measured response.

Membrane receptor or intracellular stain	Functions
ICAM-1	endothelial cell adhesion molecule [64–69]
β_1-Integrin	cell adhesion molecule present in all human cells [72]
PECAM-1	endothelial cell adhesion and signaling receptor [75,76]
CD44	transmembrane endothelium glycoprotein adhesion molecule [78,79]
E-selectin	endothelial cell adhesion molecule [67,69]
VCAM-1	endothelial cell adhesion molecule [64,68]
PI	evaluates cell necrotic response [179]
VAD-FMK	measures caspase activation

3.6.2 Flow cytometry acquisition/analysis

All membrane receptors and caspase samples were acquired on a BD FACSCalibur flow cytometer using CELLQuest Software. Appropriate isotype controls were used with each experiment. Analysis was also performed using FACSExpress post data acquisition.

3.7 Statistical analysis

All results are reported as means ± standard deviation (SD). To evaluate the significance of the differences in cell viability and cell activation, an ANOVA was carried out followed by a multiple pair-wise comparisons using the Tukey HSD test using Statistica V10 (StatSoft, Tulsa, OK, USA). Samples were compared to cells grown without material or drug. A p value of less than 0.05 was required for statistical significance.

Chapter 4

Results

4.1 HUVECs response to soluble drug

4.1.1 Cell Viability following exposure to soluble drug

4.1.1.1 MTT response to soluble drugs at varying concentrations

Testing of the viability of soluble drugs through MTT was the first test performed. This test provided a reliable initial screening for the toxicity of drugs to allow us to choose appropriate concentrations to continue with further analysis on HUVECs response.

Dexamethasone showed no significant differences for viability between control and treatments following a 24 h application of drug in media. These results are summarized in Table 6.

Table 6: HUVECs' viability after 24 h to dexamethasone. HUVECs were exposed to dexamethasone (0.01-1000 nm) for 24 h and viability was assessed by MTT and compared to HUVECs in ECM. n=4.

Treatment (nM)	**% Viability** (mean ± SD)
0	99±2
0.1	106±13
1	96±3
10	100±10
100	100±7
1000	100±2

PPM18 showed no significant differences in cell viability between control and drug treatments after 24 h exposure (Table 7). The PPM-18 used in these tests was purchased from VWR International.

Table 7: HUVECs' viability after 24 h exposure to PPM-18. HUVECs were exposed to PPM-18 (0.1 - 30 µm) for 24 h and viability was assessed by MTT and compared to HUVECs in ECM. n=4.

Treatment (µM)	**% Viability** (mean ± SD)
0	101±5
0.1	105±6
0.3	105±6
1	103±4
3	101±7
10	104±6
30	101±5

As shown in Figure 10, triptolide showed a significant decrease ($p<0.01$) in viability for 100 nM and 300 nM compared to all lower concentrations and control.

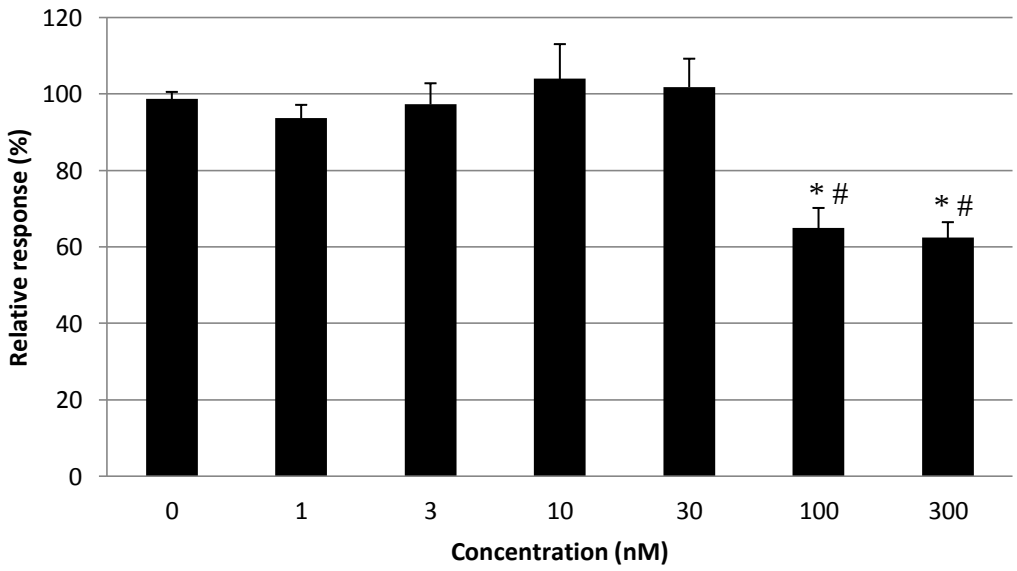

Figure 10: Response of HUVECs after 24 h exposure to triptolide. HUVECs were exposed to triptolide (0 - 300 nM) for 24 h and viability was assessed by MTT and compared to HUVECs in ECM. n=4.

*statistically significant from control ($p<0.05$)

#statistically significant from concentrations 30 nM and below ($p<0.05$)

These viability results from the MTT assays indicated that dexamethasone (0.01-1000 nM) and PPM-18 (0.01-1000 nM) were non toxic at the levels tested, while triptolide was non-toxic at levels of 30 nM and lower. Based on these results, further testing was performed to characterize the response of HUVECs in the presence of LPS and/or drug using flow cytometry.

4.1.2 Change in cellular phenotype in response to soluble drug

Drug concentrations determined to be non-toxic were identified, and the changes in HUVEC's cellular phenotype in response to soluble drug was assessed. Exposure to dexamethasone (10 nM), triptolide (3 nM), aprotinin (20 μM), and PPM-18 (10 μM) showed no significant up or down regulation of the membrane receptors tested. The cellular responses observed for ICAM-1, E-Selectin, CD44, β_1-integrin and PECAM-1 are shown in Table 8.

Table 8: Phenotype changes to soluble drugs after 24 h. HUVECs were exposed to dexamethasone (10 nM), triptolide (3 nM), aprotinin (20 μM), and PPM-18 (10 μM) for 24 h and analyzed by flow cytometry. For cell activation markers ICAM-1, E-selectin, CD44, β_1-integrin, and PECAM-1, activation is expressed relative to control cells, HUVECs in ECM. n=3.

Treatment	**ICAM-1 (%)** (mean±SD)	**E-selectin (%)** (mean±SD)	**CD44 (%)** (mean±SD)	**β_1-integrin (%)** (mean±SD)	**PECAM-1 (%)** (mean±SD)
Dexamethasone (10 nM)	117±21	103±3	104±11	103±5	99±9
Triptolide (3 nM)	141±19	105±2	104±2	105±4	99±4
Aprotinin (20 μM)	128±32	100±19	99±15	90±11	
PPM-18 (10 μM)	129±36	113±9	105±2	109±4	99±13

As none of the drugs induce a significant difference in expression for any of the activation markers, we were able to continue to test these drugs against their ability to regulate LPS response and investigate their loading into polymer and copolymer materials.

4.2 HUVECs response to LPS

To develop an *in vitro* model of inflammation of TASS, the ability of LPS to activate HUVECs was assessed. Through activation of HUVECs to LPS, we aimed to measure a given drugs' ability to reduce the inflammatory response of LPS on HUVECs.

4.2.1 Cell Viability following exposure to LPS

MTT viability testing was completed with LPS at concentrations ranging from 2 pg/mL to 200 ng/mL. There were no significant differences between any of the tested levels for LPS. The values are shown below in Table 9.

Table 9: HUVECs' viability following 24 h exposure to LPS. HUVECs were exposed to LPS (2 pg/mL to 200 ng/mL) for 24 h; viability was assessed by MTT and compared to control cells, HUVECs in ECM. n=3.

LPS Treatment (ng/mL)	**MTT (%)** (mean±SD)
Control (0.0)	102 ±3
200.0	92±9
20.0	99 ±18
2.0	101±17
0.2	101±13
2.0×10^{-2}	99 ±24
2.0×10^{-3}	108 ±18
2.0×10^{-4}	105 ±12
2.0×10^{-5}	105 ±7
2.0×10^{-6}	103±13

Using flow cytometry, PI was used to label necrotic cells in a given treatment sample. The results for HUVECs with and without LPS stimulation (100 ng/mL) are reported in Table 10. No significant difference was observed between unstimulated HUVECs and LPS stimulated cells, suggesting that LPS did not induce a necrotic or apoptotic response in cells.

Table 10: Necrosis in HUVECs following 4 day exposure to LPS. HUVECs were exposed to LPS (100 ng/mL) for 4 days and analyzed by flow cytrometry. Control cells are HUVEC grown in ECM alone. n=7.

Treatment	**Live Cells (%)** (mean±SD)	**Necrotic Cells (%)** (mean±SD)
Control	82±9	14±7
LPS	83±10	13±7

4.2.2 Change in cellular phenotype in response to LPS

Cellular phenotype changes were evaluated in response to LPS (0.2 and 2.0 µg/mL) prior to testing drug and material response to determine LPS suitability as an inflammatory stimulus on HUVECs. Tests were performed at 48 h to provide insight into the response over a relevant TASS time point. ICAM-1, E-selectin, β_1-integrin, CD44, and PECAM-1 were all evaluated. The only significant differences found were between LPS (2 µg/mL) and control for ICAM-1 and E-selectin ($p<0.05$). All values are shown in Table 11. The upregulation seen in ICAM-1 and E-selectin suggests that LPS is a suitable marker for inflammation in HUVECs.

Table 11: Relative response of HUVECs to 48 h exposure to LPS. HUVEC were exposed to LPS (0.2 µg/mL and 2.0 µg/mL) for 48 h and analyzed by flow cytometry. For cell activation markers, ICAM-1, E-selectin, CD44, β_1-integrin, and PECAM-1, activation is expressed relative to control cells, HUVECs in ECM. n=3.

Treatment	**ICAM-1 (%)** (mean±SD)	**E-selectin (%)** (mean±SD)	**CD44 (%)** (mean±SD)	**β_1-integrin (%)** (mean±SD)	**PECAM-1 (%)** (mean±SD)
Control	100±0	100±0	100±0	100±0	100±0
LPS (0.2 µg/mL)	426±56	105±2	115±23	134±21	97±8
LPS (2.0 µg/mL)	*710±357	*134±23	126±33	134±26	92±6

*significant difference from control ($p<0.05$)

Since the literature indicated that a peak in E-selectin expression on cells may occur at shorter times, a small investigative experiment was performed at various time points. As seen in Figure 11, there appears to be a peak expression of E-selectin at 6 h that is then reduced by 48 h.

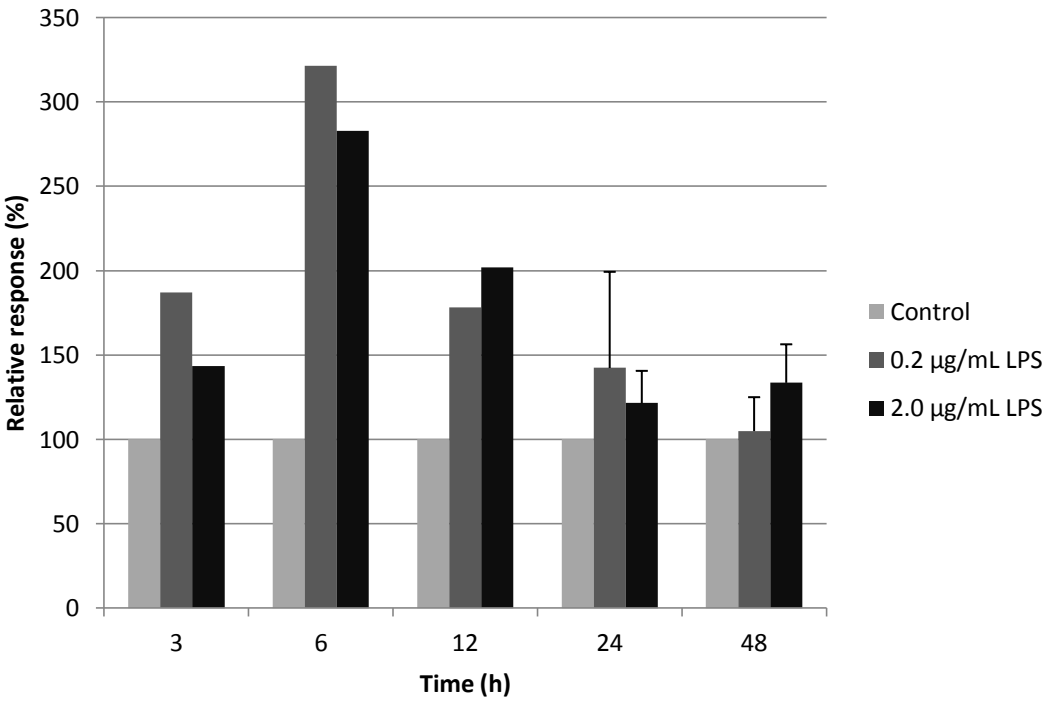

Figure 11: Response of HUVECs to LPS between 3 h and 48 h. HUVECs were exposed to LPS (0.2 µg/mL and 2.0 µg/mL) for 48 h and evaluated at 3 h, 6 h, 12 h, 24 h, and 48 h for E-selectin expression by flow cytometry. E-selectin expression is reported relative to control cells, HUVECs in ECM. n=1 for 3 h-12 h; n=3 for 24 h-48 h.

4.3 HUVECs response to LPS and soluble drugs

The ability of soluble drugs to reduce cytokine activation of cells was measured based on non toxic levels of drugs, as discussed in 4.1 and those found in the literature. All tests were carried out with LPS stimulation at 100 ng/mL. Although this level was not tested for upregulation of markers, further review of the literature indicated this was an appropriate level to see both cellular response and changes in cell phenotype.

The effects of drugs on LPS stimulated HUVECs were first measured after a 24 h time point. As shown in Figure 12, LPS with or without drugs upregulated ICAM-1 expression. LPS alone and LPS with aprotinin (20 µM), dexamethasone (10 nM), triptolide (3 nM) or

PPM-18 (10 µM) were all significantly different ($p<0.01$) from unstimulated HUVECs. There were no significant differences between any of the stimulated cell treatments, suggesting that the presence of drugs had no effect on ICAM-1 upregulation induced by LPS.

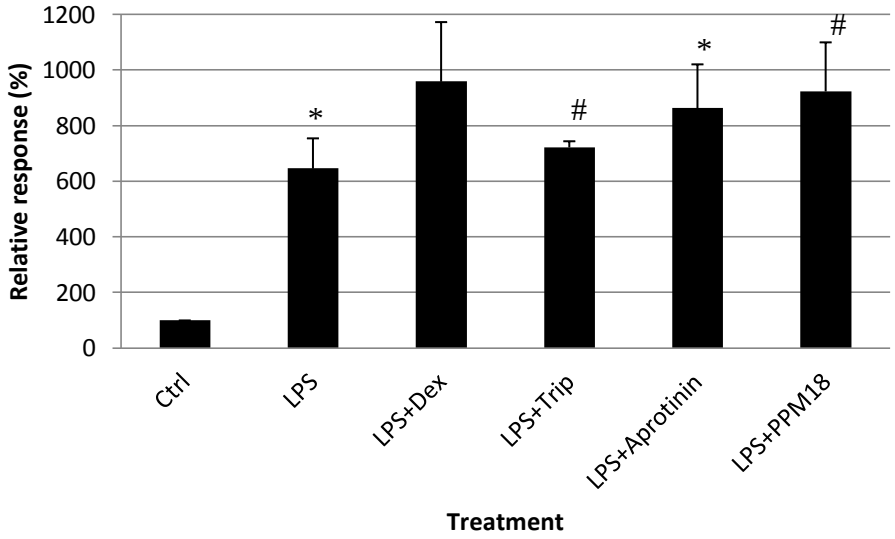

Figure 12: ICAM-1 upregulation in HUVEC after 24 h exposure to LPS and LPS with dexamethasone, triptolide, aprotinin, and PPM-18. HUVECs were exposed to LPS, LPS and dexamethasone (10 nM), LPS and triptolide (3 nM), LPS and aprotinin (20 µM), or LPS and PPM-18 (10 µM) for 24 h and analysed by flow cytometry. ICAM-1 expression is reported relative to control cells, HUVECs in ECM. n=3 except for LPS n=4.

*statistically significant from control ($p<0.01$)
statistically significant from control ($p<0.001$).

Dexamethasone was then tested at higher concentrations to ensure that its inability to down regulate LPS stimulus was not due to an inappropriate drug concentration. After 24 h, there was a significant difference in ICAM-1 upregulation ($p<0.001$) between the unstimulated HUVECs and all LPS stimulated cells with or without drug (Figure 13). This suggested that

these levels of dexamethasone, while non-toxic to cells were not able to reduce the upregulation in ICAM-1 caused by LPS.

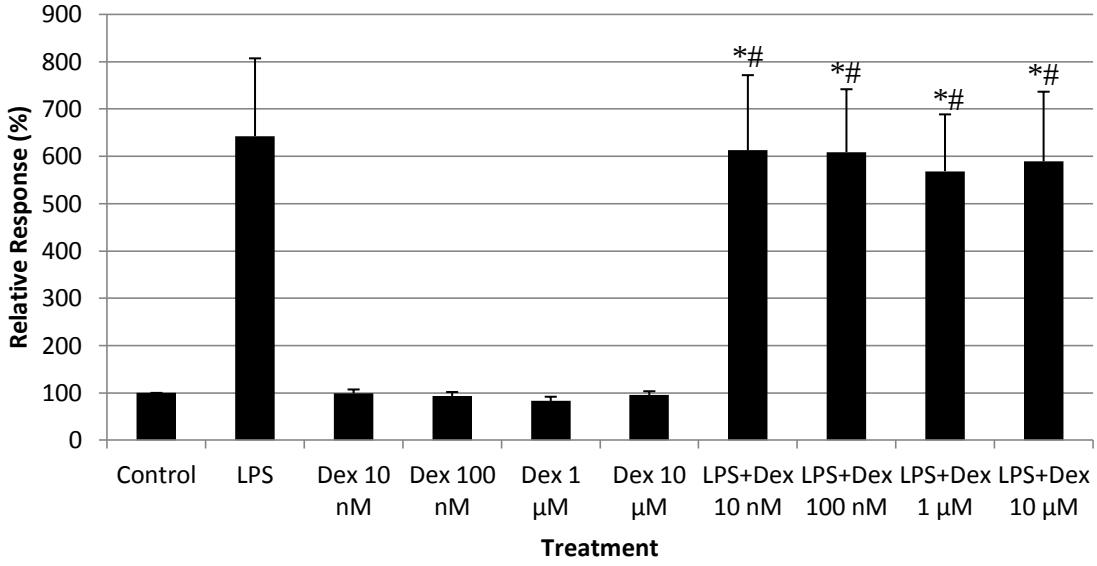

Figure 13: ICAM-1 upregulation in HUVECs following exposure to dexamethasone with and without LPS for 24 h. HUVECs were exposed to varying concentrations of dexamethasone (10 nm - 10 µm) with and without LPS (100 ng/mL) for 24 h and analysed with flow cytometry. ICAM-1 expression is reported relative to control cells, HUVECs in ECM. n=3; LPS n=2.

*statistically significant from control ($p<0.001$)

statistically significant from cells exposed to drug only ($p<0.001$)

To determine if dexamethasone required a longer time to exert its effects on LPS-stimulated cells, a 4 day time point was assessed. After 4 days, the significant difference in ICAM-1 expression ($p<0.001$) between unstimulated cells and all LPS stimulated cells, with or without drug, was still present. There was also a significant difference between all LPS stimulated with drugs cells and cells exposed to drug only, further confirming our results that dexamethasone did not reduce LPS-induced ICAM-1 expression ($p<0.001$) (Figure 14).

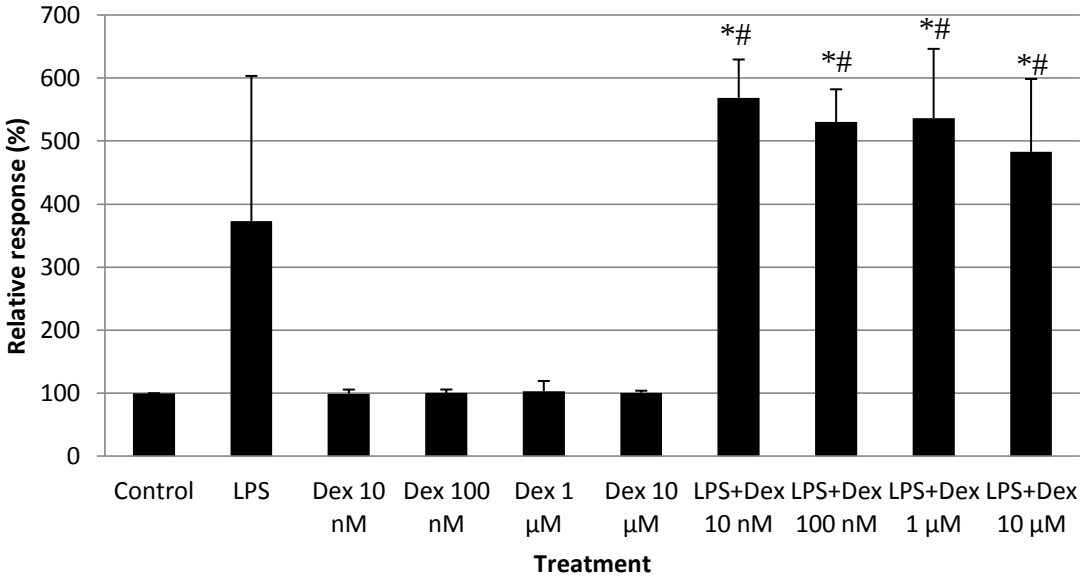

Figure 14: Response of HUVECs to varying concentrations of dexamethasone with and without LPS for ICAM-1 at 4 days. HUVECs were exposed to varying concentrations of dexamethasone (10 nm - 10 µm) with and without LPS (100 ng/mL) for 4 days and analysed with flow cytometry. ICAM-1 expression is reported relative to control cells, HUVECs in ECM. n=3; LPS n=2.

*statistically significant from control ($p<0.001$)

statistically significant from cells exposed to drug only ($p<0.001$)

As seen in Table 12, the ability of varying concentrations of dexamethasone to affect and reduce LPS-stimulated expression of VCAM-1, β_1-integrin, E-selectin and CD44 on HUVECs was not significant at 24 h,.

Table 12: Response of HUVECs to varying concentrations of dexamethasone with and without LPS at 24 h and 4 days.

HUVECs were exposed to varying concentrations of dexamethasone (10 nM - 10 µM) with and without LPS (100 ng/mL) for 24 h and 4 days and analysed with flow cytometry relative to control. For cell activation markers, VCAM-1, CD44, E-selectin, and β_1-integrin, activation is expressed relative to control cells, HUVECs in ECM. n=3.

Treatment	VCAM-1 (%) (mean±SD)		CD44 (%) (mean±SD)		E-selectin (%) (mean±SD)		β_1-integrin (%) (mean±SD)	
	24 h	4 days	24 h	4 days	24 h	4 days	24 h	4 days
Control (no dex)	100±0	100±0	100±0	100±0	100±0	100±0.1	100±0	100±0
LPS	91±32	111±26	110±1	121±9	93±8	99±8	105±9	96±5
Dex 10nM	130±68	90±2	122±14	104±4	105±26	88±6	110±8	93±3
Dex 100nM	89±24	101±7	110±2	101±3	89±12	93±8	101±5	93±5
Dex 1µM	115±24	92±2	99±9	102±78	97±20	91±10	102±7	97±5
Dex 10µM	104±45	97.5±5	107±5	104±16	97±17	98±17	102±5	99±6
LPS + Dex 10nM	115±55	*137±28	104±11	136±39	102.±7	100±15	99±9	112±20
LPS + Dex 100nM	170±54	*138±21	102±14	137±33	99±9	103±9	99±11	106±14
LPS + Dex 1µM	108±19	*136±16	98±15	123±28	101±15	93±9	143±72	103±9
LPS + Dex 10µM	173±87	119±6	95±18	132±22	106±20	107±8	89±11	108±14

[#] significantly different from dexamethasone 10 nM and 1µM ($p<0.05$)

As mentioned previously, PPM-18 had sourcing challenges after receiving the initial supply from VWR, with which the preliminary viability tests had been carried out. An alternative supplier of PPM-18 was found (Cayman Chemical, Ann Arbor, USA), and this PPM-18 was used for the remainder of the tests. PPM-18 applied to HUVECs appeared to cause changes in the cellular phenotype as measured with ICAM-1, VCAM-1 E-selectin, CD44, and β_1-integrin. However, after statistical analysis, the presence PPM-18 in cell medium did not significantly upregulate or downregulate ICAM-1 response (Table 13). VCAM-1 results are also shown in Table 13, and despite an upregulation by both PPM-18 alone and with LPS, the only significant differences are between PPM-18 at 30 µM with LPS and the unstimulated HUVECs ($p<0.01$).

Table 13: Response of HUVECs after 4 day exposure to PPM-18 stimulated cells with or without LPS. HUVECs were exposed to PPM-18 (10 µM and 30 µM) with or without LPS (100 ng/mL) for 4 days and analysed with flow cytometry. ICAM-1 and VCAM-1 expression are reported relative to control cells, HUVECs in ECM. n=3.

Treatment	**ICAM-1 (%)** (mean±SD)	**VCAM-1 (%)** (mean±SD)
Control	100 ±0	100±0
LPS	166 ±47	96±17
PPM-18 (10 µM)	90 ±7	273±28
PPM-18 (30 µM)	104 ±27	265±47
LPS + PPM-18 (10 µM)	111 ±27	302±48
LPS + PPM-18 (30 µM)	101 ±21	*381±168

* significant difference from control and LPS ($p<0.01$)

For E-selectin, there were significant differences in the response from unstimulated HUVECs and LPS only cells compared to PPM-18 (10 µM) exposed HUVECs (Figure 15). The response to LPS with PPM-18 (10 µM and 30 µM) was also significantly upregulated

compared to unstimulated HUVECs and LPS only cells ($p<0.05$). This response suggested that PPM-18 stimulated the expression in E-selectin in cells independently of LPS.

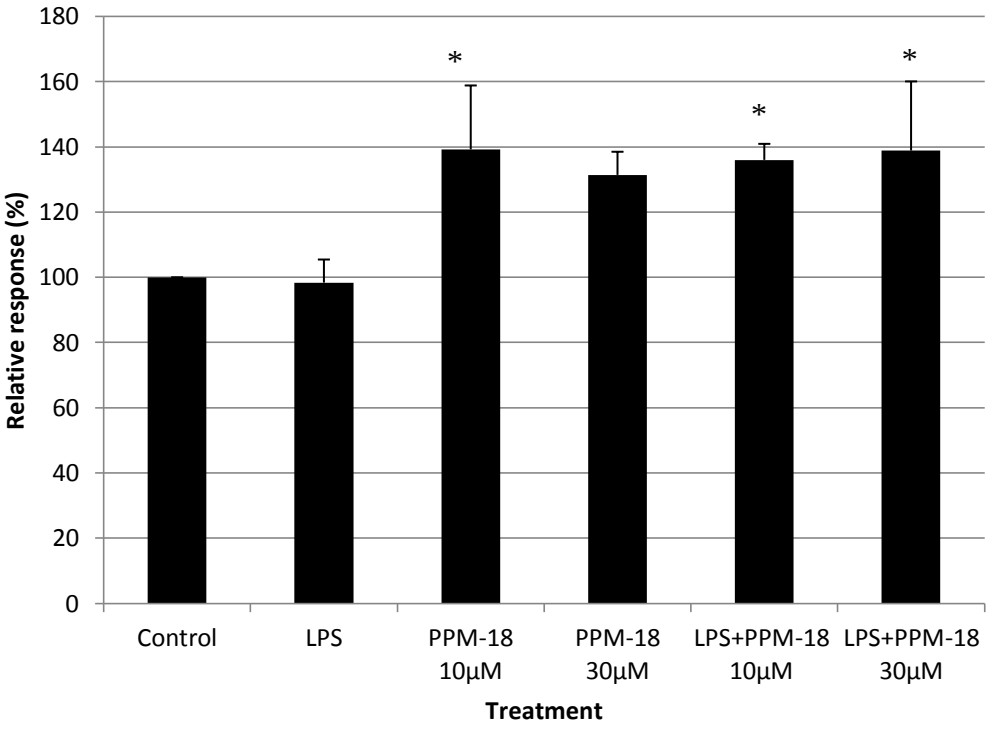

Figure 15: E-selectin expression on HUVECs after 4 day exposure to PPM-18 stimulated cells with or without LPS. HUVECs were exposed to PPM-18 (10 µM and 30 µM) with or without LPS (100 ng/mL) for 4 days and analysed with flow cytometry. E-selectin expression is reported relative to control cells, HUVECs in ECM. n=3.

* significant difference from control and LPS ($p<0.05$)

When compared to HUVECs and LPS stimulated cells, CD44 was significantly upregulated ($p<0.05$) in response to PPM-18 (10 µM and 30 µM) both with and without LPS (Figure 16).

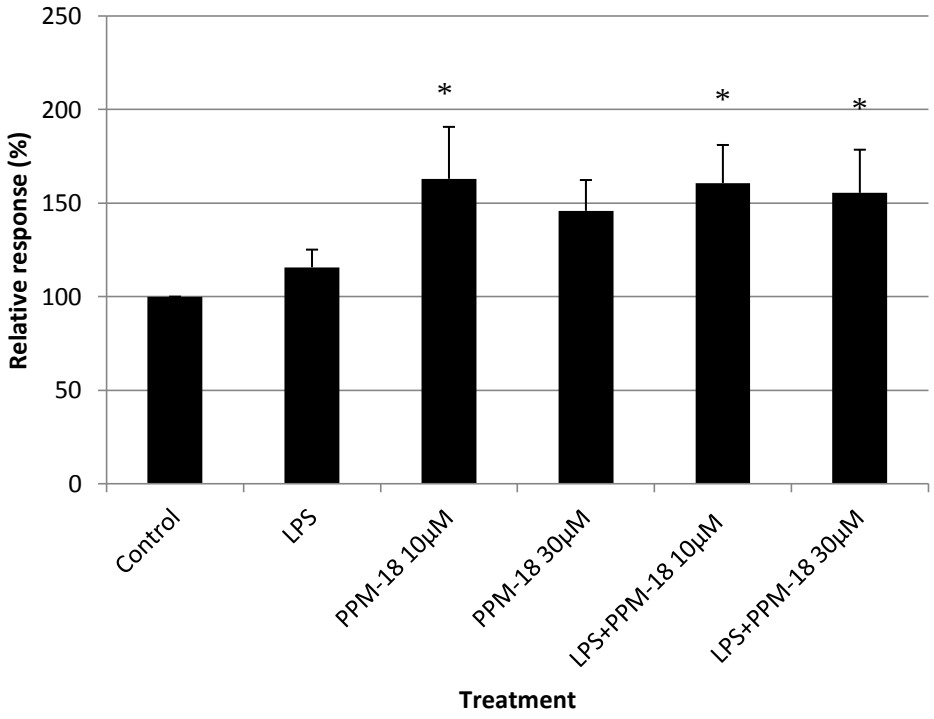

Figure 16: CD44 expression in HUVECs after 4 day exposure to PPM-18 stimulated cells with or without LPS. HUVECs were exposed to PPM-18 (10 µM and 30 µM) with or without LPS (100 ng/mL) for 4 days and analysed with flow cytometry. CD44 expression is reported relative to control cells, HUVECs in ECM. n=3.

* significant difference from control and LPS ($p < 0.05$)

As illustrated in Figure 17, in the presence of PPM-18 with or without LPS, β_1-integrin was significantly downregulated when compared to unstimulated HUVECs or LPS stimulated cells ($p<0.05$). This downregulation was an unexpected response and further indicated that PPM-18 was significantly compromising HUVEC's phenotype.

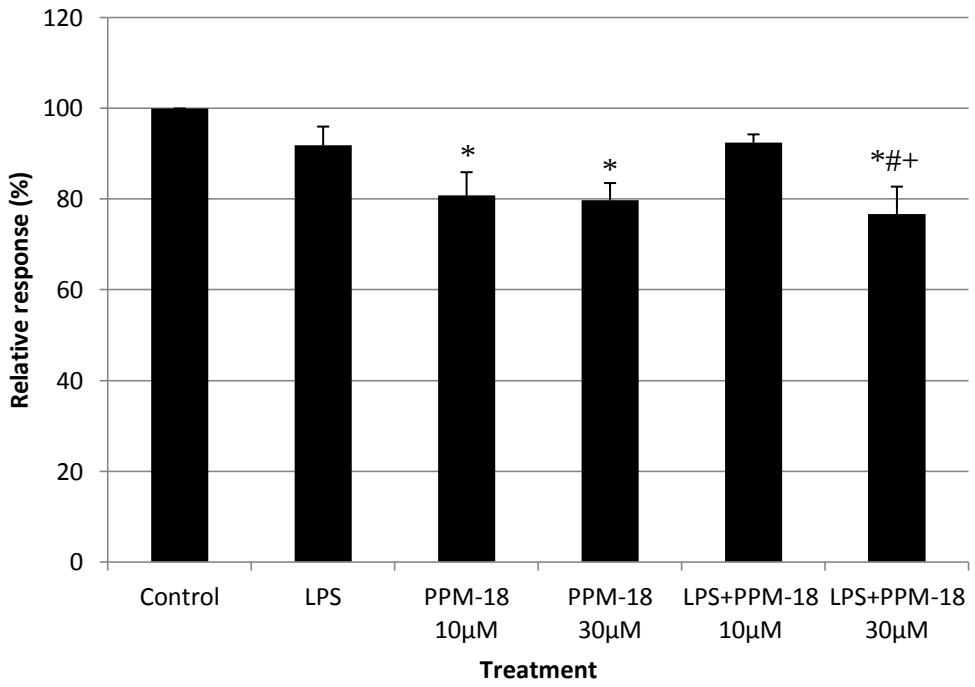

Figure 17: β_1-integrin expression on HUVECs after 4 day exposure to PPM-18 stimulated cells with or without LPS. HUVECs were exposed to PPM-18 (10 µM and 30 µM) with or without LPS (100 ng/mL) for 4 days and analysed with flow cytometry. β_1 integrin expression is reported relative to control cells, HUVECs in ECM. n=2.

* significant difference from control ($p < 0.01$)

significant difference from LPS ($p<0.05$)

+ significant difference from LPS+PMM-18 (10 µM)

4.4 Biocompatibility of polymer and copolymer with and without drug loading

The effects of the polymer and copolymer were evaluated primarily through changes in cellular phenotype. The cell scatter plots, which report the size and granularity of the particles passing through the flow cytometer, showed significant changes in cell scatter following interaction with drug loaded material. Some materials underwent the drug loading procedure, but without drugs in the loading solutions. These are referred to as “mock loaded

polymers." Figure 18 illustrates some of the commonly observed changes in the scatter plots. Most samples could be considered as having scatter plots similar to untreated cells as shown in Figure 18.A. Samples containing PPM-18 loaded material showed different cell scatter characteristics (Figure 18.B), where both cell size and granularity were reduced. Consequently, the gating region was moved slightly to include the analysis of a larger population of events. Typically, the change in scatter characteristics did not reduce the number of events. However, increasing the levels of dexamethasone in order to see a greater cellular response resulted in lower event number as well as a greatly reduced scatter as shown in plot Figure 18.C. When LPS was added to the 100 ng/mL samples of dexamethasone copolymer, an increase in event size was observed (see Figure 18.D). Due to the odd shapes and low event counts obtained with dexamethasone at 100 ng/mL, results were considered not reliable and this concentration was not tested further.

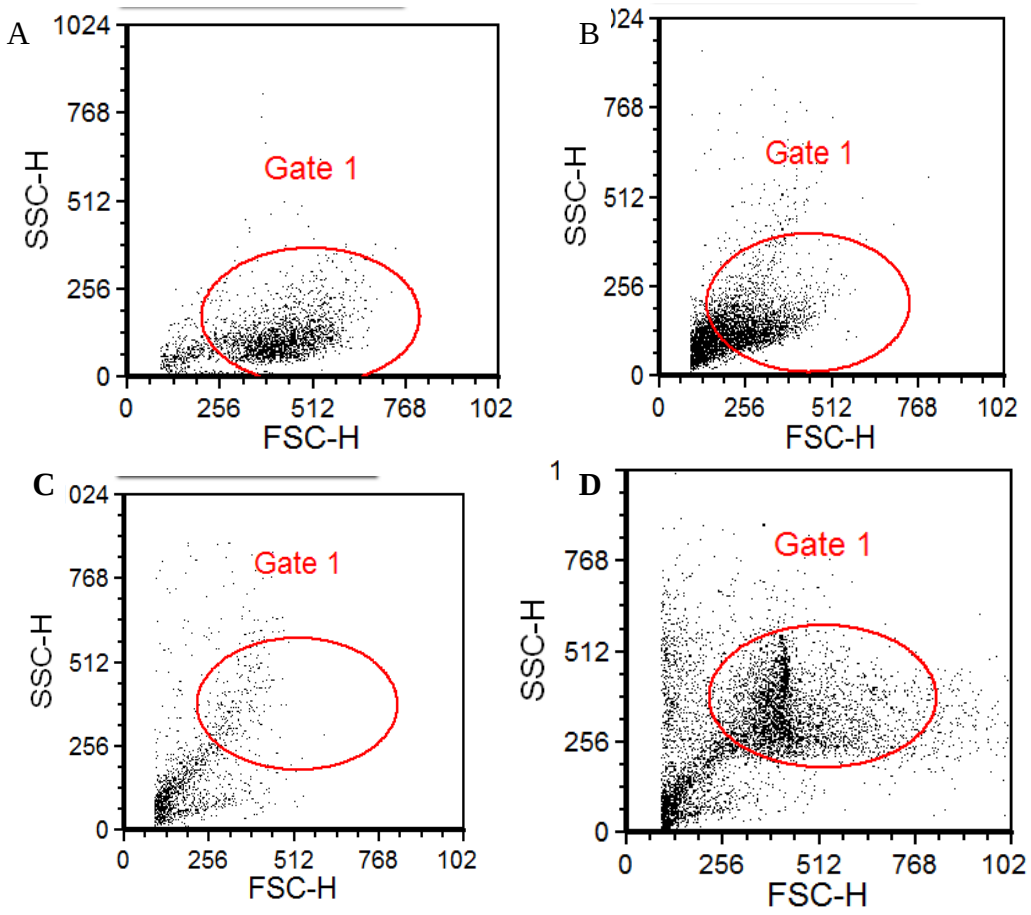

Figure 18: Scatter plots showing cell shape response to various polymer and copolymer treatments after 4 days exposure to HUVECs. (A) Typical cell size distribution and region used to gate on HUVECs. These are untreated control cells. (B) Cell scatter in response to 10µM PPM-18 polymer. This is a typical cell scatter change seen in response to PPM-18 loaded into a material or on its own. Region was moved to include more cells. (C) 100 nM Dexamethasone loaded copolymer. (D) 100 nM Dexamethasone copolymer with LPS at 100ng/mL.

Viability of HUVECs in response to the polymer and copolymer, both unloaded and mock loaded, were evaluated using the percentage of necrotic cells stained with PI. There was no difference seen between treatment types as shown in Table 14, suggesting that the materials were not toxic on their own.

Table 14: HUVECs' necrosis following 4 days exposure to polymer and copolymer, unloaded or mock loaded. HUVECs were exposed to material treatment and analysed by flow cytometry. Necrotic cells were identified by PI uptake. n=4.

Treatment	**Live Cells (%)** (mean±SD)	**Necrotic Cells (%)** (mean±SD)
Control	82±9	15±8
Polymer	83±9	15±8
Copolymer	83±10	14±8
Polymer mock loaded	85±8	13±5
Copolymer mock loaded	82±9	14±5

Initial evaluation of HUVECs' response to both materials for any of the measured markers (ICAM-1, VCAM-1, or CD44) showed that there was no significant difference between HUVECs with no material or those that were exposed to the material in media over 4 days. No significant difference was seen in HUVECs exposed to materials that had undergone the drug loading process, but had no drug added to the drug loading solvent. The values are summarized below in Table 15.

Table 15: Response of HUVEC after 4 day exposure to polymer and copolymer, unloaded or mock loaded. HUVECs were incubated with materials for 4 days and analysed with flow cytometry. ICAM-1, VCAM-1 and CD44 expression are reported relative to expression on control cells, HUVECs in ECM. n=4, polymer mock loaded n=3, copolymer mock loaded n=2.

Treatment	**ICAM-1 (%)** (mean±SD)	**VCAM-1 (%)** (mean±SD)	**CD44 (%)** (mean±SD)
Control - No Material	100 ±0	100 ±0	100 ±0
Polymer	122 ±10	127±43	104±10
Copolymer	111±17	111±22	97 ±7
Polymer mock loaded	145±42	114±28	101±11
Copolymer mock loaded	125±13	141±50	102 ±10

The drug loaded materials were compared against each other and the non drug delivering materials in Table 16. Large variability in the ICAM-1 expression in HUVECs was seen in response to the PPM-18 copolymer samples. Two batches of polymer sample were tested with improvements made to the polymerization process to reduce contamination between batch 1 and batch 2. This lead to a reduction in ICAM-1 expression as seen by batch 2 response.

Table 16: ICAM-1 response in HUVECs after 4 day exposure to polymer and copolymer materials, unloaded, mock loaded or loaded with either dexamethasone or PPM-18. HUVECs were exposed to soluble dexamethasone (10 nM), soluble PPM-18 (10 µM), and polymer or copolymer, either unloaded, mock loaded or loaded with either dexamethasone (10 nM) or PPM-18 (10 µM) for 4 days, and analysed by flow cytometry. ICAM-1 expression is reported relative to expression on control cells, HUVECs in ECM. n=4; PPM-18 polymer, copolymer batch 1 n=3, PPM-18 copolymer batch 2 n=2.

Treatment	**ICAM-1 (%)** (mean±SD)
Control	100±0
Dexamethasone	99±8
PPM-18	90±7
Polymer	122±10
Copolymer	111±17
Polymer mock loaded	229±172
Copolymer mock loaded	195±218
Dex polymer	109±13
Dex copolymer	108±6
PPM18 polymer	131±43
PPM18 copolymer, batch 1	1639±930
PPM18 copolymer, batch 2	104±8

With respect to VCAM-1, there was a significant difference between PPM18 loaded polymer and copolymer and all other samples as seen in Figure 19. A similar observation could be made for CD44 whereby PPM-18 loaded polymer and copolymer was significantly different from all other samples as indicated in Figure 20 ($p<0.01$). The observed upregulation by PPM-18 suggested that PPM-18 induced an inflammatory response that was

independent of the material or the loading process. Both VCAM-1 and CD44 were not influenced by the batch of the polymer, so results were pooled.

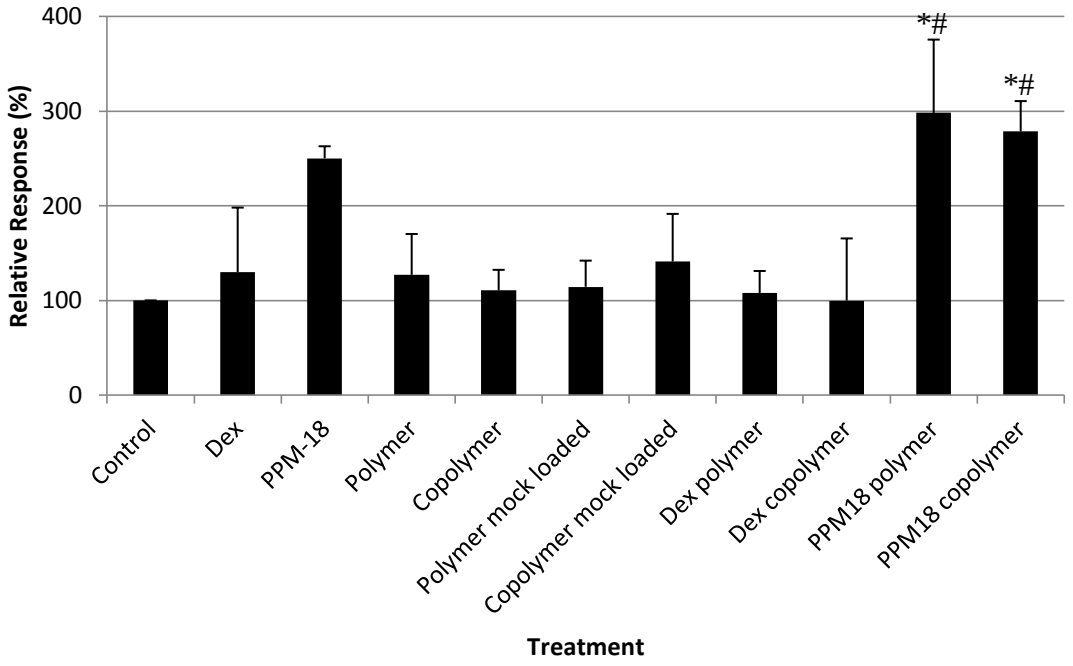

Figure 19: VCAM-1 expression on HUVECs after 4 day exposure to polymer and copolymer materials with various treatments and dexamethasone (10 nM) or PPM-18 (10 µM). HUVECs were exposed to soluble dexamethasone (10 nM), soluble PPM-18 (10 µM), and polymer or copolymer either unloaded, mock loaded, or loaded with either dexamethasone (10 nM) or PPM-18 (10 µM) for 4 days, and analysed by flow cytometry. VCAM-1 expression is reported relative to its expression on control cells, HUVECs in ECM. n=4; soluble drug, Dex copolymer and PPM-18 polymer n=3.

* significant difference from control, polymer unloaded and loaded, polymer loaded, and dexamethasone loaded and unloaded polymer and copolymer ($p<0.001$)

significant difference copolymer loaded ($p<0.01$)

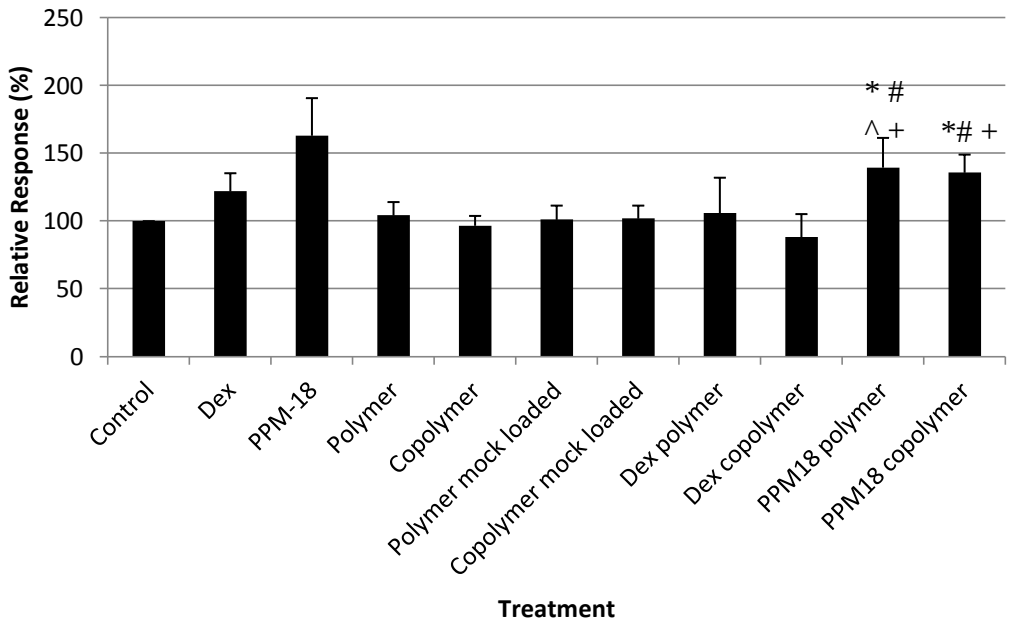

Figure 20: CD44 expression on HUVECs after 4 day exposure to polymer and copolymer materials with various treatments and dexamethasone (10 nM) or PPM-18 (10 µM). HUVECs were exposed to polymer and copolymer, unloaded, mock loaded or loaded with either dexamethasone (10 nM) or PPM-18 (10 µM) for 4 days, and analysed by flow cytometry. VCAM-1 expression is reported relative to its expression on control cells, HUVECs in ECM. n=4; soluble drugs, and PPM-18 polymer n=3.

* significant difference from control ($p<0.05$)

significant difference from unloaded copolymer ($p<0.05$)

^ significant difference from mock loaded polymer and copolymer ($p<0.05$)

+ significant difference from dexamethasone copolymer ($p<0.01$)

4.4.1 HUVECs viability response to materials

The cellular viability response of HUVECs to materials was characterized both with MTT and PI. Due to lack of materials and time constraints, the MTT testing was only performed once. In that experiment, there appeared to be a large reduction in viability of HUVECs in

response to exposure to either PPM-18 loaded materials, both after 24 h and 4 days (Figure 21). These materials were all from the second batch of polymer synthesis. This was expected given the previously observed upregulation of activation markers VCAM-1 and CD44. Soluble drug values were taken from the same assays as used to determine material viability. PPM-18 was from a different source than used for the initial viability assays. Due to limited number of cells, soluble dexamethasone was unable to be tested at 4 days, along with the loaded materials and soluble PPM-18.

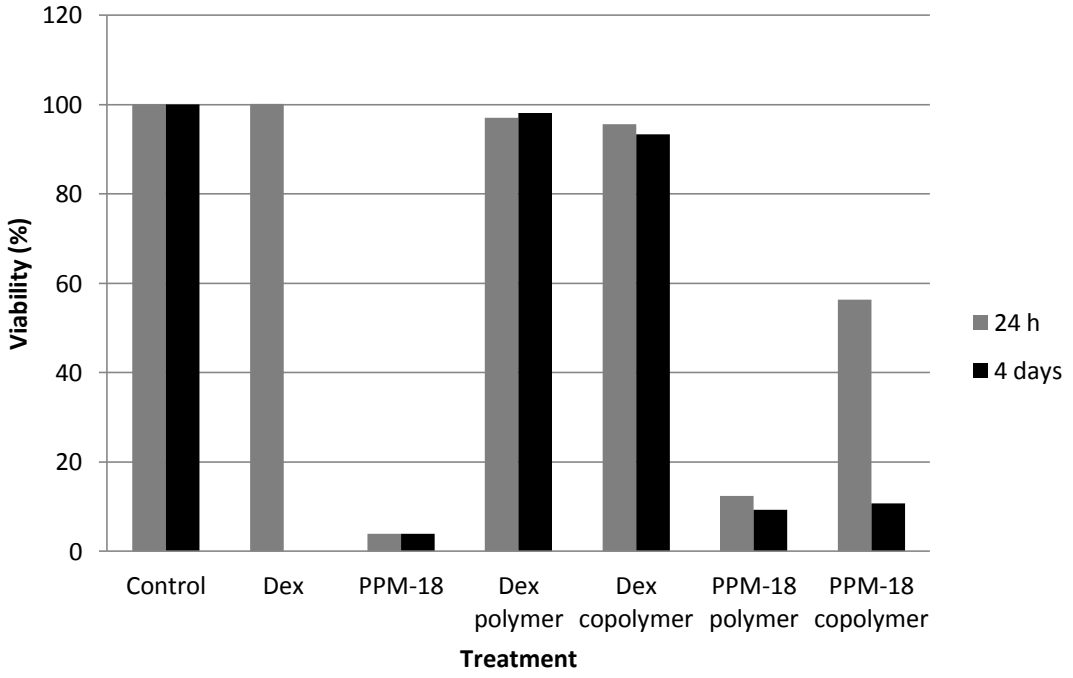

Figure 21: HUVECs' viability after 24 h exposure to dexamethasone and PPM-18: soluble, and loaded polymer or copolymer. HUVECs were exposed to dexamethasone (10 μM) and PPM-18 loaded into polymer and copolymer materials for 24 h and 4 days. Viability was assessed by MTT and compared to control, HUVECs only in ECM. Due to limited materials, n=1.

As an alternate method to assess viability, PI was used to test for the effects of materials on cellular viability after 4 days. Table 17 shows an almost complete necrotic response to PPM-18 loaded polymers. Only PPM-18 loaded polymer and copolymer showed significant differences between their level of necrotic cells and that of all other treatments' ($p<0.001$). These observations support the results seen in the MTT assay showing PPM-18 loaded material leading to a decrease in HUVECs' viability. The material response is compared to the soluble drug response from 0, which also explained the large variability in the PPM-18 necrotic response.

Table 17**: Population of HUVEC necrotic cells after 4 day exposure to soluble dexamethasone or PPM-18, and polymer and copolymer, unloaded or mock loaded, as well as dexamethasone or PPM-18 loaded polymer and copolymer.** HUVECs were exposed to soluble dexamethasone (10 nM), soluble PPM-18 (10 μM), and polymer and copolymer, unloaded or mock loaded, as well as dexamethasone (10 nM) or PPM-18 (10 μM) loaded polymer or copolymer for 4 days and analyzed by flow cytometry. Soluble dexamethasone and dexamethasone loaded polymer n = 1; PPM-18 polymer n=3; Soluble PPM-18 and PPM-18 copolymer n=2; all others n=4.

Treatment	**Live Cells (%)** (mean±SD)	**Necrotic Cells (%)** (mean±SD)
Control	81±8	11±5
Dexamethasone	83[1]	13[1]
PPM-18	29±40[1]	69±40[1]
Polymer	83±9	15±8
Copolymer	83±10	14±8
Polymer mock loaded	84±8	13±5
Copolymer mock loaded	82±9	14±5
Dexamethasone polymer	85	10
Dexamethasone copolymer	85±5	12±4
PPM-18 polymer	1±1	*100±1
PPM-18 copolymer	2±2	* 80±312

* significant difference from control, unloaded polymer, loaded polymer and copolymer, and dexamethasone polymer and copolymer ($p<0.001$)

[1] See next page for detailed results on toxicity of soluble drug

4.4.1.1 Cellular phenotype viability response

Exploratory experiments were performed following material testing, to further understand cell response to dexamethasone and PPM-18. Cell death and programmed cell death was assessed by flow cytometry with dexamethasone and PPM-18. To illustrate the toxicity of PPM-18, as compared to dexamethasone and control, scatter plots from all flow cytometry analysis are provided in Figure 22 and Figure 23. The plots indicate cellular activity by quadrant based on the uptake of PI or caspase activation (FITC-VAD-FMK).

These flow cytometry tests with caspase and PI were performed on cells that had been exposed to PPM-18 purchased from Cayman Chemical, a different supplier than the one used in the preliminary MTT viability testing where no decrease in cellular viability had been observed. With these later tests, there is clear indication that PPM-18 induced a severe necrotic response in HUVECs.

The first trial is shown in Figure 22. In Figure 22.A, showing unstimulated HUVECs after a 4 day culture, the majority of cells are live; however, in Figure 22.B and C, following treatment with PPM-18 (10 µM and 30 µM, respectively) the entire population of cells has undergone necrosis. Dexamethasone does not indicate a drastic increase from unstimulated HUVECs in necrotic or apoptotic cells. Upon repeating the experiment with PPM-18 (10 µM and 30 µM, Figure 23.B and C respectively), there is very little or no increase in necrosis or necrosis and apoptosis from unstimulated HUVECs (Figure 23.A). PI and caspase activation are very time dependent in measurement. The variations in the necrosis levels from those in the first experiment may be due to slightly different time-point readings after 4 days of incubation.

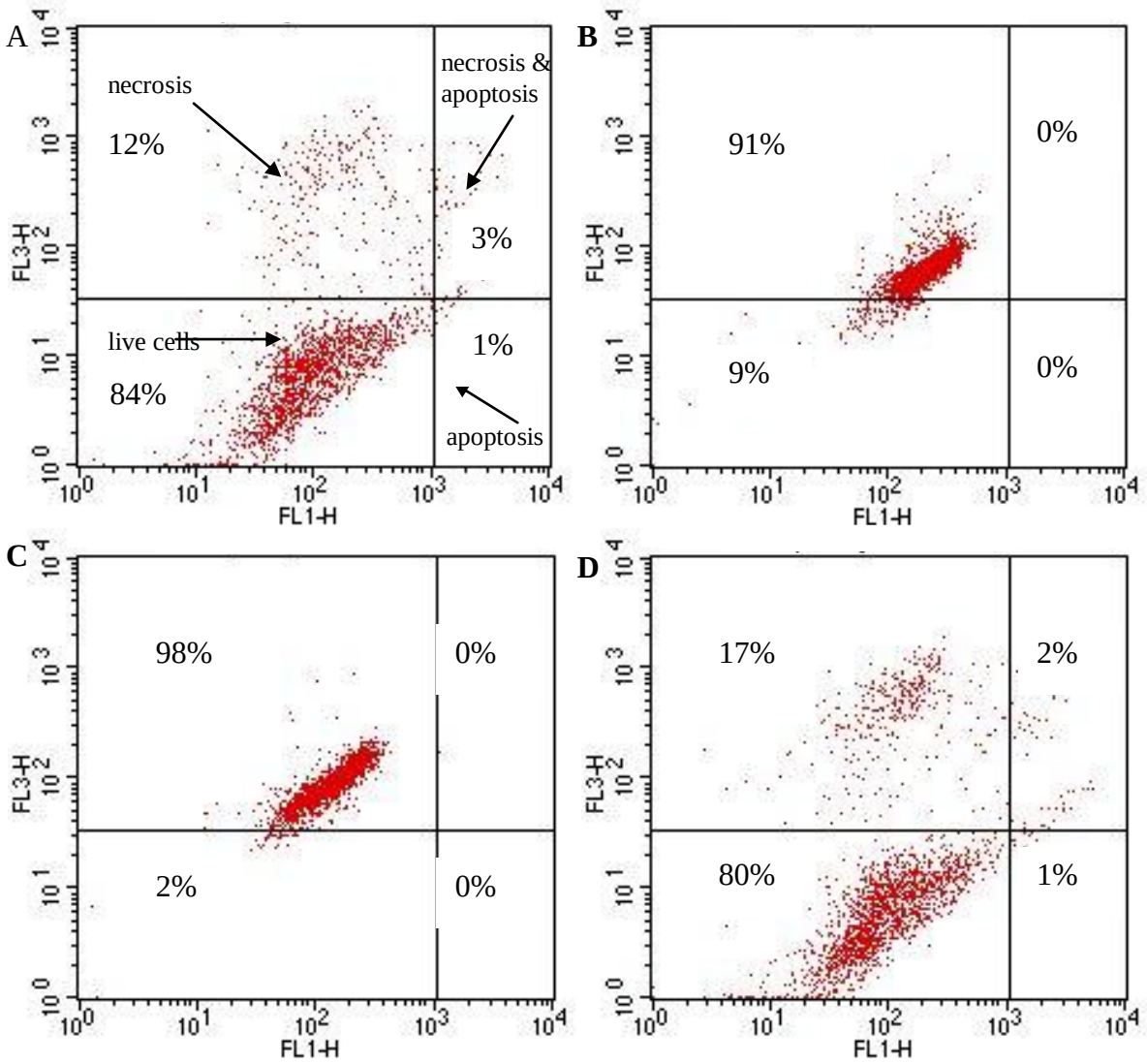

Figure 22: Plots illustrating necrosis and apoptosis levels in HUVECs following 4 day treatment for first assay performed with PPM-18 (10 µM and 30 µM) and dexamethasone (10 nM). The plots indicate percentage cellular activity by quadrant. The upper left indicates cells are necrotic, lower left is live cells, upper right shows necrotic and apoptotic cells, while lower left indicates apoptosis. Live cells were identified based on their exclusion of PI and FITC-VAD-FMK. Necrotic cells were identified by their uptake of PI. (A) Control, untreated HUVECs. (B) PPM-18 (10 µM) treated HUVECs. (C) PPM-18 (30 µM) treated HUVECs. (D) Dexamethasone (10 nM) treated HUVECs. HUVECs were exposed to drug for 4 days and analyzed by flow cytometry.

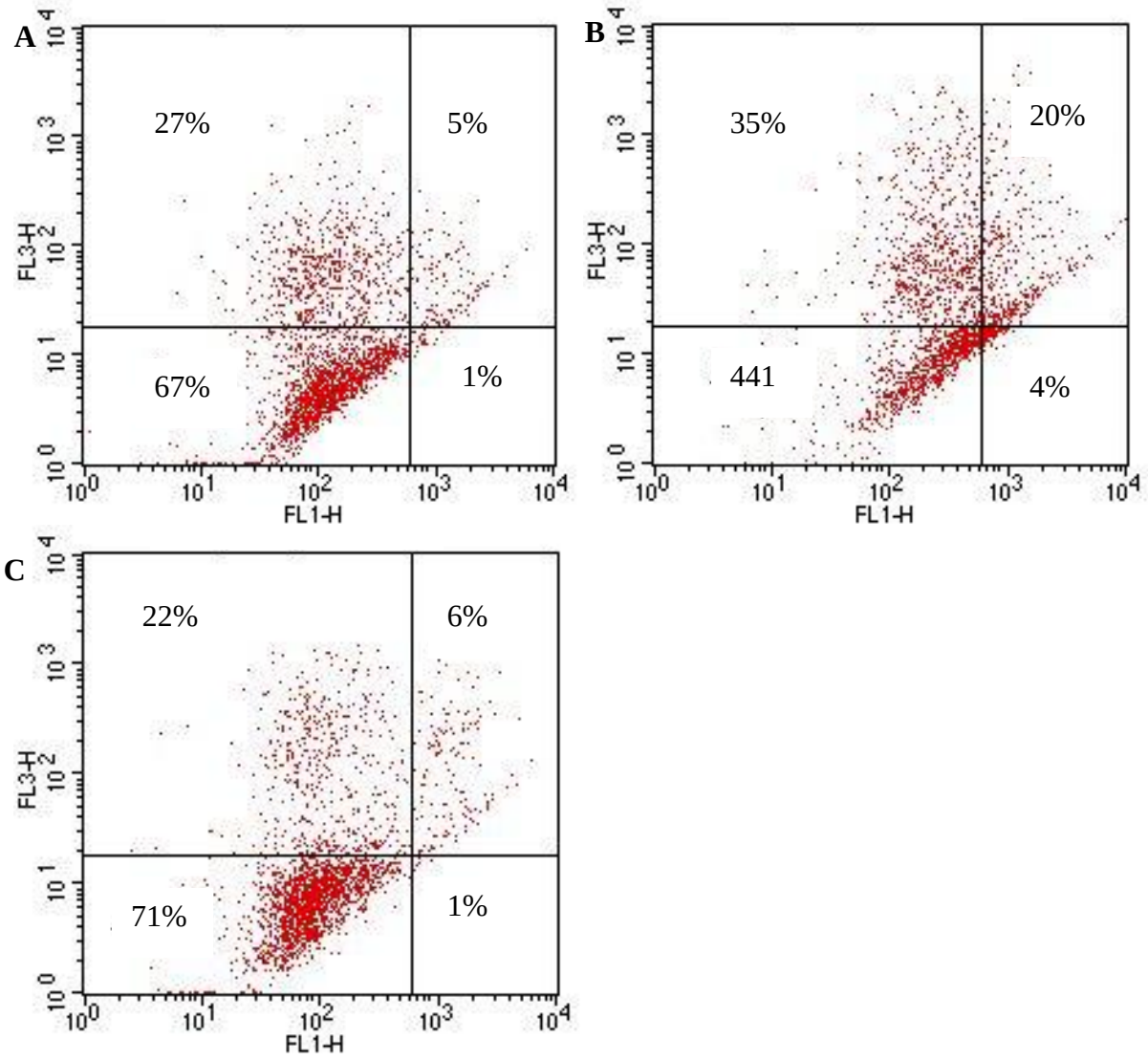

Figure 23: Plots illustrating necrosis and apoptosis levels in HUVECs following second 4 day treatment assays performed with PPM-18 (10 µM and 30 µM). The plots indicate percentage cellular activity by quadrant. The upper left indicates cells are necrotic, lower left is live cells, upper right shows necrotic and apoptotic cells, while lower left indicates apoptosis. Live cells were identified based on their exclusion of PI and FITC-VAD-FMK. Necrotic cells were identified by their uptake of PI. (A) Control, untreated HUVECs. (B) PPM-18 (10 µM) treated HUVECs. (C) PPM-18 (30 µM) treated HUVECs. HUVECs were exposed to drug for 4 days and analyzed by flow cytometry.

4.4.2 HUVECs' response to DMSO

Both dexamethasone and PPM-18 were dissolved in the organic solvent DMSO. Although residual levels of DMSO should remain low in media solution, the effects of low level DMSO exposure to HUVECs was characterized to understand the possible cellular response observed when drug, or drug loaded material was incubated with HUVECs. The relative concentrations of DMSO in ECM when incubated with HUVECs are shown in Table 18 for dexamethasone (10 nM, 100 nM, and 10 µM) and PPM (10 µM and 30 µM).

Table 18: DMSO concentrations present in ECM during incubation of HUVECs with soluble dexamethasone and PPM-18. Drugs were dissolved in organic solvent prior to dilution in PBS and then ECM. Values are given for DMSO content for dexamethasone (10 nM, 100 nM, and 10 µM) and PPM-18 (10 µM and 30 µM).

Treatment	DMSO concentration (%)
Dexamethasone (10 nM)	$3.29x10^{-7}$
Dexamethasone (100 nM)	$3.29x10^{-5}$
Dexamethasone (10 µM)	$3.29x10^{-3}$
PPM-18 (10 µM)	0.27
PPM-18 (30 µM)	0.83

Cellular phenotype response was measured to determine what changes were seen in HUVEC exposed to DMSO over time, and if this could cause some of the inflammatory response seen by PPM-18 on HUVECs. After 24h, ICAM-1 showed a slight, but not significant, upregulation in the presence of 1% DMSO in media. At 4 days, 2% DMSO showed a significant upregulation ($p<0.05$) when compared to all other time and concentrations (Figure 24).

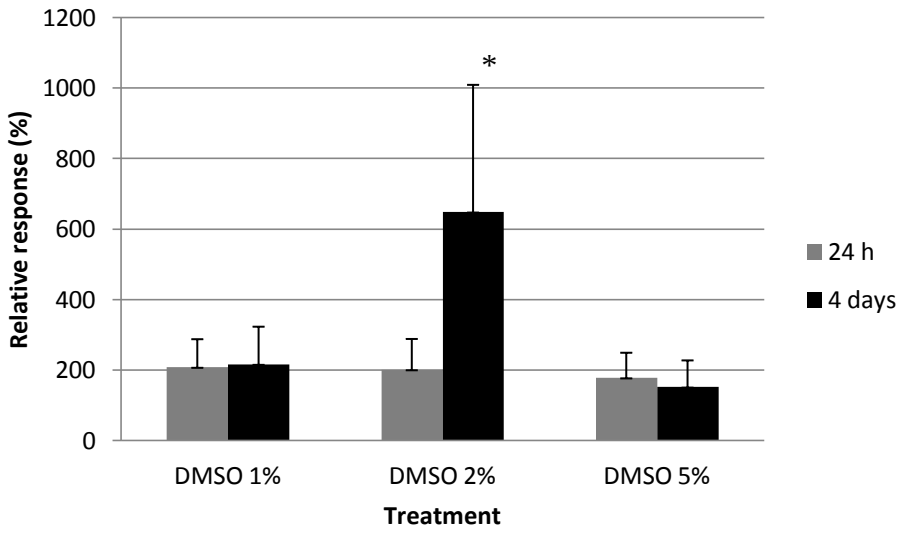

Figure 24: ICAM-1 upregulation on HUVEC after 24 h or 4 day exposure to various concentrations of DMSO. HUVECs were exposed to DMSO (1%, 2%, and 5%) for 24 h or 4 days, and analysed by flow cytometry. ICAM-1 expression is reported relative to its expression on control cells, HUVECs in ECM. n=3.

* significantly different from control and all other data points ($p<0.05$)

HUVECs also showed a response to DMSO as measured in β_1-integrin expression (Figure 25). Again, 4 day application of 2% DMSO showed the only significant upregulation from control ($p < 0.001$). It also significantly increased from 24 h to 4 days ($p<0.05$). The 24 h and 4 day time points for both 1% DMSO and 2% DMSO were significantly different from 5% DMSO. The 5% DMSO concentrations, although not significantly different from the controls showed to slightly downregulate β_1-integrin. There were also fewer events for DMSO 5% than the lower two concentrations, which suggests there was cell death occurring. The changes seen in ICAM-1 and β_1-integrin suggest that the presence of PPM-18 dissolved in DMSO in cells may be cause for some of the inflammatory and necrotic response seen following cell exposure to PPM-18.

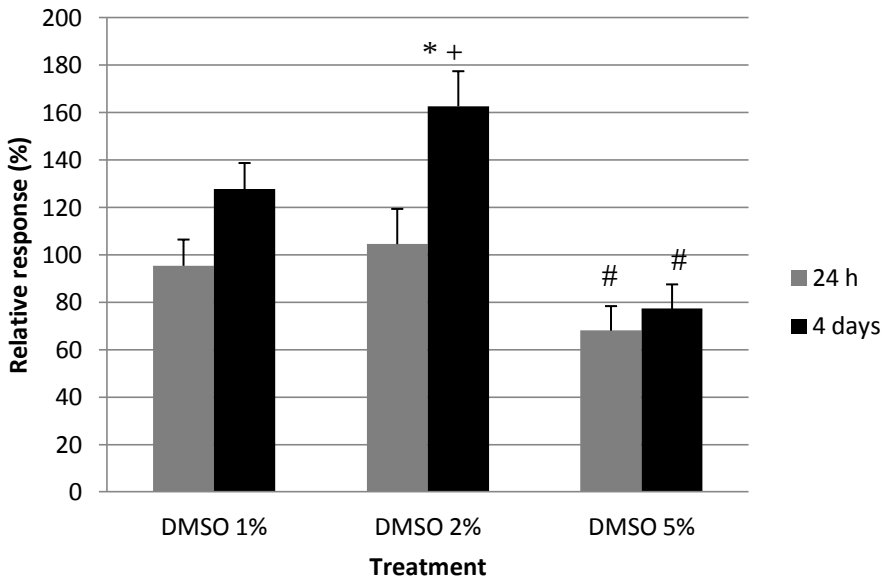

Figure 25: β_1-integrin expression on HUVEC after 24 h or 4 day exposure to various concentrations of DMSO. HUVECs were exposed to DMSO (1%, 2%, and 5%) for 24 h or 4 days, and analysed by flow cytometry. β_1-integrin expression is reported relative to its expression on control cells, HUVECs in ECM. n=3.

* significant difference from control ($p<0.001$)

significant difference from all lower concentrations at both time points ($p<0.05$)

+ significant difference from same treatment different at different time ($p<0.05$)

Chapter 5
Discussion

5.1 Response to soluble drug and LPS

5.1.1 Viability response

The *in vitro* model using LPS was developed to induce an inflammatory response, but not a toxic response, in endothelial cells. Therefore, LPS concentration was chosen based on increase in cell activation with no reduction in cell viability. Our LPS activation results are in accordance with previous studies showing that LPS stimulation for 24 h does not reduce corneal endothelial cell viability [145,180]. LPS has been reported to activate the apoptotic pathways, with caspase activation peaking at 6 h following stimulation in HUVECs, but then decreased by 24 h [51]. This suggests that while LPS does not cause reduced viability, it activates a small apoptotic response in HUVEC, and under normal conditions, this response can be overcome within 24 hours, leading to no significant effect in cell viability.

Dexamethasone was first chosen as a control treatment due to its reported ability to reduce the apoptotic responses in endothelial cells [51,181,182]. Our results indicate that soluble dexamethasone is non-toxic over a range of concentrations considered therapeutic (100 nM-12 μM) [47]. Kerachian et al indicated that a high dose of dexamethasone (1 mM) slightly reduced primary HUVECs' viability to 92% after 48 h [164], which agrees with our findings that soluble dexamethasone at the concentrations used herein were non toxic to endothelial cells.

There is currently little research on PPM-18 activation of cells. No study has investigated the potential changes in cellular phenotype following PPM-18 exposure *in vitro*. Rather, focus has been on finding a compound that reduces inflammation in general. The potent anti-inflammatory properties of PPM-18, a member of the family of 1,4-naphthoquinones, occurs mostly through preventing neutrophil degranulation as discovered by Lien et al [183] and his study suggested that it was safe to use. This was confirmed in our initial tests with PPM-18 showing low toxicity and a potential to reduce HUVEC activation, further suggesting the

ability of PPM-18 to be a broader anti-inflammatory compound (i.e with target cells other than leukocytes). However, as described in the result section, later results with PPM-18 showed high level of necrosis. Due to PPM-18 being on backorder for 12 months, a new supplier was identified and it is possible that the purity and molecular structure may have differed between the two suppliers. PPM-18 has been reported to be of similar structure to 1,4-naphthoquinone, and 2-methyl-1,4-naphthoquinone [184]. Toxicity tests after 24 h have shown a lethal concentration in half of the cells (LC50) when exposed to 6 µM of 1,4-naphthoquinone and 15 µM of 2-methyl-1,4-naphthoquinone [184]. Thus while these compounds possess anti-inflammatory properties [52,160,162,170–174], they also appear to have the potential to be highly toxic. This may somewhat explain the increase in necrosis observed when HUVEC were exposed to PPM-18. PPM-18 exposure may have activated the apoptotic pathways, leaving cells still viable when the MTT tests were first performed at 24 h.

5.1.2 Endothelial cell phenotype changes following LPS stimulation

Despite the literature suggesting changes in endothelial cell phenotype with regards to ICAM-1 [64,67–71], β_1-integrin [73,74], PECAM-1 [75,77], CD44 [78], E-selectin [64,67–70], and VCAM-1 [57,59,62,64,68,70] expression, our results tend to suggest otherwise. While ICAM-1 appeared to consistently respond to stimulation, inconsistent responses were obtained with the other markers. These markers were also expected to show dexamethasone reducing the stimulatory effect of LPS, which would have allowed for dexamethasone to behave as a control to the effects of the novel drug PPM-18.

ICAM-1 is a popular cell adhesion marker to measure for HUVEC and endothelial cell activation in response to LPS. In all endothelial cell studies, except one co-culture study [65], ICAM-1 was shown to be upregulated on HUVECs after LPS stimulation for up to 48 h [64,67–69,82]. In primary aortic endothelial cells, this upregulation was seen by 4 h and maintained levels across 72 h [81]. These studies agree with the significant upregulation seen in our HUVEC model in response to LPS, indicating that LPS led to cell activation.

Activation of HUVECs and human saphenous vein endothelial cells with LPS also leads to VCAM-1 upregulation for treatments between 3-48 h [65,68,164,185]. This is in contradiction to the response seen following LPS stimulation of our *in vitro* model. The sensitivity of saphenous vein endothelial cells to LPS may be greater than HUVEC, or these studies may have used a more sensitive assay to detect VCAM-1 expression (such as the ELISA method), which allowed them to observe a response to LPS, where we did not.

In our experiments, no upregulation of E-selectin following LPS stimulation was observed. The time at which E-selectin up regulation is measured on endothelial cells following LPS stimulation appears to influence the ability to measure its expression. E-selectin upregulation on HUVECs following stimulation with LPS has been measured at times up to 16 h following stimulant application [67,69,82,164]. Maximal expression of LPS induced E-selectin expression has been reported to be around 6 h for primary HUVECs [64], and 4 h in primary aortic endothelial cells [81]. In aortic endothelial cells, E-selectin was reduced to basal levels by 24 h and remained at that level up to 72 h after stimulation [81]. This downregulation mechanism in E-selectin expression after a short time is further supported by a study reporting that primary HUVECs did not expressed increased E-selectin levels following a 48 h stimulation with LPS [65]. All together, these observations support our exploratory results showing an upregulation of E-selectin at earlier time points (3 and 6 h), and further explains the lack of upregulation at 24 h and 4 day time points for LPS stimulation.

No difference in PECAM-1 expression was observed at 18 h in LPS stimulated HUVECs [65], possibly due to the immediate return to basal levels past 60 min as seen by Shen et al [75]. Shen et al showed a peak expression of PECAM-1 in response to LPS on HUVECs at 30 min, that was reduced back to control levels of untreated cells by 60 min [75]. Again, HUVECs did not express PECAM-1 following activation [77]. These HUVECs were stimulated with the same amount of LPS as this study used, but they were able to show the PECAM-1 expression appeared only very briefly after stimulus. This infers that at the time points of 24 h and 4 days in our study, HUVECs had already reversed most, if not all, of their PECAM-1 upregulation.

Since TASS and endophthalmitis are rarely presented immediately following cataract surgery, the time chosen to identify cell activation and upregulation of cell receptors are 24 h to 4 days. As E-selectin and PECAM-1 appeared to be upregulated immediately after stimulus and then downregulated within 24 h, these markers of activation are not relevant for this *in vitro* model.

CD44 was chosen as an additional marker from the more commonly investigated endothelial cell adhesion molecules, as it has shown to play a role in macrophage adhesion to endothelial cells following LPS stimulation [78]. However, there is currently little known about CD44 expression on endothelial cells following LPS stimulation. CD44 has been shown to mediate neutrophil adhesion on endothelial cells in liver sinusoids, but not in postsinusoidal venules [73]. Microvascular endothelial cells also did not show a change in CD44 expression following stimulation with LPS [186]. However, the same study also demonstrated that differences existed in levels of ICAM-1 expression both in baseline expression and LPS stimulated cells within HUVECs and microvascular endothelial cells [186]. This further emphasizes differences between endothelial cell types. These studies indicate that CD44 may only be expressed and stimulated on specific endothelial cell types, which may explain the lack of response seen in HUVECs in our studies.

5.1.3 Phenotype changes following exposure to drug

The use of the corticosteroid dexamethasone has been reported extensively in the literature, showing its effect on the expression of ICAM-1 [64,65,67–71,81,82,164], E-selectin [64,64,67–70,81,82,164] and VCAM-1 [57,59,62,64,65,68,68,70,82,164,185]. Dexamethasone does not affect baseline expression of these markers in HUVECs [164] or in endothelial cells from other sources such as human coronary artery endothelial cells [187] or microvascular endothelial cells [186]. However, high concentrations of dexamethasone (1 mM) has shown to induce significant upregulation of three adhesion molecules, ICAM-1, VCAM-1, and E-selectin on endothelial cells [164]; this is probably due to dexamethasone reaching toxic levels [188,170]. These observations support our findings, whereby

dexamethasone in the micromolar range did not upregulate or downregulate any of the markers of activation tested.

Similarly to our results, Lu et al found that LPS stimulation increased ICAM-1 expression and that neither triptolide (30 nM) nor dexamethasone alone raised the basal ICAM-1 expression [7]. However, in their study, both triptolide (1 - 30 nM) and dexamethasone (100 nM) reduced the effect of LPS on ICAM-1 expression by 35% and 27% respectively. These discrepancies with our results may be explained by the fact that corneal fibroblasts were used and that LPS activation in fibroblasts may be more easily inhibited by triptolide and dexamethasome when compared to endothelial cells. Lu et al also measured ICAM-1 expression using a whole cell ELISA and it is possible that it is more sensitive than flow cytometry in identifying changes in ICAM-1 expression [189,190].

5.1.4 Soluble drug with LPS phenotype changes

Dexamethasone has been used previously in an effort to reduce the inflammatory response and upregulation of cellular adhesion molecules in endothelial cells [164,186,170]. However, in primary HUVECs and microvasacular endothelial cells stimulated with LPS, dexamethasone at 10 µM did not significantly reduce ICAM-1 expression [186,170]. Additionally, an increase of ICAM-1 expression levels on microvascular endothelial cells and HUVECs was also observed when dexamethasone was added to LPS treated cells [164,186]. These results agree with our findings that dexamethasone was unable to reduce LPS activation in endothelial cells.

On the other hand, other studies showing a decrease in LPS stimulation with dexamethasone at similar levels than the ones used in this study, contradict our findings. Zouki et al found treatment with dexamethasone (100 nM) inhibited approximately 60% of the LPS expression of E-selectin and ICAM-1 caused by LPS stimulation on human coronary artery endothelial cells after 4 h [187]. This observation may be due to the short time of LPS stimulation and/or that dexamethasone only has a limited time efficacy following treatment. LPS was also reported to increase VCAM-1 expression on human saphenous vein endothelial

cells, which dexamethasone was able to significantly reduce at levels of 10 nM and above [185]. These cells were pretreated with dexamethasone for 48 h before LPS stimulation [185], which may increase dexamethasone's effectiveness. While Meβmer et al previously demonstrated that low concentration of dexamethasome was able to significantly reduce apoptosis induced by LPS in endothelial cells [181,182], bovine glomerular endothelial cells were used. It is possible that glomerular, saphenous vein, and aortic endothelial cells are more sensitive to stimulus. However, the inhibitory effect of dexamethasone on LPS-induced apoptosis also appears to be time-dependent whereby the effectiveness of dexamethasone is lost by 18 h [182]. This suggests that there may be a time limit on the effects of dexamethasone on cells.

Some of the trends observed in upregulation were not significant, most likely due to the high variability of the results. Often, large differences in receptor expression existed between the various days of experiments. The reason for greater upregulation from control on one day of data collection over another is unclear, but this may be due to the passage of the HUVECs used in each experiment. HUVECs were observed to change morphology after five or six passages. When this change was observed, the cells were no longer used for assays; however, changes within the cell may have occurred before being visible morphologically and this may have influenced cell response, and caused consequent variability in the data collected.

5.2 Biocompatibility of polymer and copolymer materials

In order to understand the effects of the polymer and copolymer drug delivery system, we evaluated both their response as a material alone, as well as loaded with drugs. PDMS, the polymer used in this study is commonly used as a biomaterial [191–195]. Depending on the copolymerization and the surface modifications, the biocompatible properties of PDMS can be further controlled Two studies suggested that unmodified PDMS materials do not allow cellular proliferation. PDMS alone appears to restrict the migration of human corneal epithelial cells and mouse fibroblasts onto the polymer surface [191,192]. In the application of an IOL, this is an ideal property for the material to maintain clarity and vision. However,

when dealing with PDMS and cell adhesion, caution should be exercised as a study also reported that smooth PDMS surface allowed human fibroblasts to adhere to the material and grow to confluence by 7 days [193]. The ability of different copolymers to modify the migration of cells, including HUVECs [194], highlights how chemical/surface modification of these materials may influence cellular behaviour.

PNIPAAm is typically used as a copolymer in combination with surface treatments to modify the biological response. Except for one study showing pNIPAAm reducing 3T3 fibroblast viability [196], pNIPAAm as part of various copolymer systems appears to be biocompatible. No decrease in cell viability on ECV304 human endothelial cells [197] or mouse 3T3 fibroblasts [198] were observed. pNIPAAm also increased the affinity of hydroxyapatite to marrow stromal cells [199], and allowed *in vivo* rabbit corneal epithelial regrowth [200]. This confirms our observations that PDMS and pNIPAAm themselves are non toxic to a variety of cell types, including HUVECs.

5.2.1 Drug delivering materials

In this study, PPM-18 loaded materials showed a significant increase in expression of cell adhesion markers ICAM-1, VCAM-1, and CD44. *In vitro* biocompatibility studies with drug delivering materials often focuses on cellular viability without further analysis of cellular response. This presents challenges when comparing our polymer and copolymer cellular responses to others reviewed in the literature.

Dexamethasone loaded polymers have been shown to be biocompatible. In the dexamethasone posterior segment drug delivery system by Allergan Inc, the device showed a significant improvement in visual acuity in the treatment of macular edema compared to a non-treated group [105]. Another dexamethasone implant by Siqueira et al also reduced inflammation seen in an *in vivo* rabbit model following cataract surgery [47]. However, the reduction in inflammation was not seen until 6 or 9 days following implantation [47], which may explain why after 4 days no changes were observed in our *in vitro* studies. On the other hand, a PDMS copolymer dexamethasone drug delivery system has led to a significant

decrease in viability when applied to Murine L929 fibroblasts [201]. Their lowest dexamethasone loading corresponded to the highest we measured, which suggests that at higher concentrations, dexamethasone may be toxic or that some toxic interactions between drug and polymer may occur at these levels. Another study also found 100 nM of soluble dexamethasone significantly inhibited cell growth [201]. This may explain our observations of 100 nM dexamethasone copolymer inducing an initial change in morphology along with a dramatic necrotic response.

The polymers used as well as the drug and the drug loading protocol all play a role in the biocompatibility of a drug delivery device. The ability to effectively remove all of the solvents and unreacted monomer present in the polymer also will impact biocompatibility. This is clearly shown with respect to ICAM-1 in Table 16, and the variation between different batches of polymers. This may explain the increase necrosis seen with PPM-18 polymer copolymer compared to the soluble PPM-18 results. Despite a stringent purification procedure, there is a possibility that during polymerization of our polymer and copolymer, or loading with PPM-18 solvent residues remain within the material. These may then leach out during incubation with cells, leading to upregulation of activation markers on cells. Briganti et al investigated this possibility with PDMS extracts through application to HUVECs to determine their possible toxicity from THF used in synthesis, but they saw no significant toxicity [195]. There is a possibility that in this study some of the toxicity seen was due to the interaction of PPM-18 loading and the copolymer material or polymerization process. This sensitivity to the materials seemed to be dependent on activation marker used. ICAM-1 appears to be highly sensitive to chemical presence; whereas VCAM-1 appears to be less sensitive to chemical interaction, and primarily responded to interaction with foreign material.

5.2.2 DMSO and drug loading response on materials

Dexamethasone and PPM-18 were dissolved in organic solvents prior to direct incubation with cells or loading into the biomaterials. The possibility that this may induce a toxic

response to cells without LPS stimulation was investigated, and indicated a reduction in viability even at 1%. The lower cell activation seen at 5% was probably due to cell death, from the low event count observed during flow cytometry due to DMSO causing necrosis of cells. At levels of DMSO application less than that used for our soluble PPM-18 drug delivery, apoptotic markers have been expressed on HUVECs [202] and retinal pigment epithelial cells [203]. DMSO at 2% was also reported to cause damage after 10 min *in vitro* on human CEC [204], further indicating the sensitivity of endothelial cells to DMSO *in vitro*. The ability of DMSO to activate HUVECs at low levels suggests that this may explain the toxicity seen by PPM-18 when applied to cells, and possibly during drug delivery from the material. The concentration of DMSO applied with PPM-18 treatments could not be reduced further due to the PPM-18 solubilized in DMSO precipitating at lower dilutions.

Chapter 6
Conclusions and Future Work

6.1 Conclusions

From this study, we have effectively created an *in vitro* model for analyzing the activation of HUVECs to LPS stimulus over 4 days for ICAM-1. PECAM-1 and E-selectin are only acutely expressed on HUVECs following LPS stimulus, and are downregulated within 24 h, which makes them unsuitable markers for further testing within this model. Dexamethasone (10 nM-10 μM) was ineffective in reducing LPS upregulation in HUVECs, which means further work is needed to identify a more effective drug to inhibit HUVEC response to LPS stimulus. Significant necrosis was seen in soluble PPM-18 as well as in PPM-18 loaded polymer and copolymer materials, which may be due to DMSO as a solubilising agent, as well as PPM-18 itself. A similar response was seen in the higher level (100 nM) of drug delivering dexamethasone polymer and copolymer materials that lead to severe necrosis of cells. Neither drug nor drug delivering system proved successful in reducing LPS stimulation on cells. Further work is required to determine the possible mechanisms for this response, along with the refinement of our *in vitro* TASS model.

6.2 Future work

Following the analysis of the tests and results with soluble drugs and materials, there are a number of assays suggested to further improve and validate our model.

Due to the differences seen between our initial toxicity testing with PPM-18 and later phenotype and drug delivery, evaluation of the sources of our drugs may be necessary. Testing different sources, and achieving consistent results would assist with replication and strengthen our results. While general cytokine inhibitors, such as triptolide, can be used, specifically blocking TNF-α may be another strategy to explore to prevent endothelial cell damage.

It is also possible that our materials support cell growth; cell proliferation on the surface is not desired as a property of a material to be used as an IOL and it is thus recommended that the potential for endothelial cell growth on these materials be examined. HUVEC adhesion on the materials would have a significant impact on the results but also on the way the drug delivery materials are tested (well insert versus direct contact incubation).

Tight junctions play an integral part of the function and mechanism of the corneal endothelium. The presence of these junctions in HUVECs should be evaluated to further confirm their usefulness as a cell line for CEC. This can be done with antibody staining against ZO-1, claudins, and JAM-A for fluorescence microscopy. As there may be specific conditions, such as surface coating or time requirements for these tight junctions to form, our *in vitro* model would have to be modified accordingly to allow for their evaluation.

It would also be beneficial to have the drug delivery *in vitro* model occur in a physiological environment closer to the anterior segment of the eye. BSSplus (Alcon Laboratories Inc, Fort Worth, USA) is an irrigating solution used during cataract surgery. It has a composition very similar to that found in the anterior segment. Evaluation of this solution may be performed to compare cellular responses between ECM and BSSplus.

Co-culturing various cell types may lead to better *in vitro* models [27]. Future work may explore co-culture of macrophages with HUVECs under stimulus conditions in order to further investigate and model the inflammatory response observed with TASS and endophthalmitis.

Finally, our model should be validated through comparison to primary CEC response. Due to the ease of sourcing and low cost, a bovine model of CEC may be used.

References

1. Parsons C, Jones DS, Gorman SP. The intraocular lens: challenges in the prevention and therapy of infectious endophthalmitis and posterior capsular opacification. Expert Rev Med Devices. 2005 Mar;2(2):161–73.

2. Pijl BJ, Theelen T, Tilanus MAD, Rentenaar R, Crama N. Acute endophthalmitis after cataract surgery: 250 consecutive cases treated at a tertiary referral center in the Netherlands. Am. J. Ophthalmol. 2010 Mar;149(3):482–7.e1–2.

3. Brightbill FS, McDonnell PJ, McGhee CNJ. Corneal surgery: theory, technique and tissue. Elsevier Health Sciences; 2009.

4. Kohnen T, Baumeister M, Kook D, Klaproth OK, Ohrloff C. Cataract surgery with implantation of an artificial lens. Dtsch Arztebl Int. 2009 Oct;106(43):695–702.

5. Rosha DS, Ng JQ, Morlet N, Boekelaar M, Wilson S, Hendrie D, et al. Cataract surgery practice and endophthalmitis prevention by Australian and New Zealand ophthalmologists. Clin. Experiment. Ophthalmol. 2006 Aug;34(6):535–44.

6. Pavesio CE, DeCory HH. Treatment of ocular inflammatory conditions with loteprednol etabonate. British Journal of Ophthalmology. 2008 Apr 1;92(4):455–9.

7. Lu Y, Liu Y, Fukuda K, Nakamura Y, Kumagai N, Nishida T. Inhibition by triptolide of chemokine, rroinflammatory cytokine, and adhesion molecule expression induced by lipopolysaccharide in corneal fibroblasts. Invest. Ophthalmol. Vis. Sci. 2006 Sep 1;47(9):3796–800.

8. Joyce NC, Zhu CC, Harris DL. Relationship among oxidative stress, DNA damage, and proliferative capacity in human corneal endothelium. Invest. Ophthalmol. Vis. Sci. 2009 May;50(5):2116–22.

9. Mamalis N. Anatomy of a TASS outbreak. Journal of Cataract & Refractive Surgery. 2007 Mar;33(3):357–8.

10. Jun EJ, Chung SK. Toxic anterior segment syndrome after cataract surgery. Journal of Cataract & Refractive Surgery. 2010 Feb;36(2):344–6.

11. Raizman MB. Determining the role for antibiotics in the prevention of endophthalmitis after cataract surgery. Arch Ophthalmol. 2011 Apr 1;129(4):501–2.

12. Fintelmann RE, Naseri A. Prophylaxis of postoperative endophthalmitis following cataract surgery: current status and future directions. Drugs. 2010 Jul 30;70(11):1395–409.

13. Mamalis N, Edelhauser HF, Dawson DG, Chew J, LeBoyer RM, Werner L. Toxic anterior segment syndrome. J Cataract Refract Surg. 2006 Feb;32(2):324–33.

14. Gribomont AC. Post-cataract surgery endophthalmitis: an update. Bull Soc Belge Ophtalmol. 2009;(311):43–9.

15. Ozcelik ND, Eltutar K, Bilgin B. Toxic anterior segment syndrome after uncomplicated cataract surgery. Eur J Ophthalmol. 2010 Feb;20(1):106–14.

16. DeCroos FC, Afshari NA. Perioperative antibiotics and anti-inflammatory agents in cataract surgery. Curr Opin Ophthalmol. 2008 Jan;19(1):22–6.

17. Wejde G, Montan P, Lundström M, Stenevi U, Thorburn W. Endophthalmitis following cataract surgery in Sweden: national prospective survey 1999-2001. Acta Ophthalmologica Scandinavica. 2005 Jan;83(1):7–10.

18. Lemley CA, Han DP. Endophthalmitis: a review of current evaluation and management. Retina (Philadelphia, Pa.). 2007 Aug;27(6):662–80.

19. Lauschke JL, Singh R, Wei M, Bhardwaj G, Figueira E, Montfort J, et al. Factors influencing the incidence of postoperative endophthalmitis. Am. J. Ophthalmol. 2011 Apr;151(4):732; author reply 733.

20. Ng JQ, Morlet N, Bulsara MK, Semmens JB. Reducing the risk for endophthalmitis after cataract surgery: population-based nested case-control study: endophthalmitis population study of Western Australia sixth report. J Cataract Refract Surg. 2007 Feb;33(2):269–80.

21. Hatch WV. Risk factors for acute endophthalmitis after cataract surgery: a population-based study. Ophthalmology. 2009 Mar 1;116(3):425–30.

22. Maier P, Birnbaum F, Bohringer D, Reinhard T. Toxic anterior segment syndrome following penetrating keratoplasty. Arch Ophthalmol. 2008 Dec 1;126(12):1677–81.

23. Bausz M, Fodor E, Resch MD, Kristóf K. Bacterial contamination in the anterior chamber after povidone-iodine application and the effect of the lens implantation device. J Cataract Refract Surg. 2006 Oct;32(10):1691–5.

24. Sharifi E, Porco TC, Naseri A. Cost-effectiveness analysis of intracameral cefuroxime use for prophylaxis of endophthalmitis after cataract surgery. Ophthalmology. 2009 Oct;116(10):1887–96.

25. Krachmer JH, Mannis MJ, Holland EJ. Cornea. Gulf Professional Publishing; 2005.

26. Cook SD, Aitken DA, Brown SM. Growth and characterization of rabbit corneal cells in vitro. Graefe's Arch Clin Exp Ophthalmol. 1987 Sep;225(5):351–6.

27. Dey S. Corneal cell culture models: a tool to study corneal drug absorption. Expert Opin Drug Metab Toxicol. 2011 Apr, in print; 18.

28. DelMonte DW, Kim T. Anatomy and physiology of the cornea. J Cataract Refract Surg. 2011 Mar;37(3):588–98.

29. Joyce NC. Cell cycle status in human corneal endothelium. Exp. Eye Res. 2005 Dec;81(6):629–38.

30. Joyce NC, Harris DL, Mc Alister JC, Ali RR, Larkin DFP. Effect of overexpressing the transcription factor E2F2 on cell cycle progression in rabbit corneal endothelial cells. Invest. Ophthalmol. Vis. Sci. 2004 May;45(5):1340–8.

31. Joyce NC. Proliferative capacity of the corneal endothelium. Progress in Retinal and Eye Research. 2003 May;22(3):359–89.

32. Senoo T, Joyce NC. Cell cycle kinetics in corneal endothelium from old and young donors. Invest. Ophthalmol. Vis. Sci. 2000 Mar;41(3):660–7.

33. Senoo T, Obara Y, Joyce NC. EDTA: a promoter of proliferation in human corneal endothelium. Invest. Ophthalmol. Vis. Sci. 2000 Sep;41(10):2930–5.

34. Doughty MJ, Fonn D, Trang Nguyen K. Assessment of the reliability of calculations of the coefficient of variation for normal and polymegethous human corneal endothelium. Optom Vis Sci. 1993;70(9):759–70.

35. Hull DS, Green K, Thomas L, Alderman N. Hydrogen peroxide-mediated corneal endothelial damage. Induction by oxygen free radical. Invest. Ophthalmol. Vis. Sci. 1984 Nov;25(11):1246–53.

36. Doughty MJ. Concerning the symmetry of the “hexagonal” cells of the corneal endothelium. Exp. Eye Res. 1992 Jul;55(1):145–54.

37. Doughty MJ. The cornea and corneal endothelium in the aged rabbit. Optom Vis Sci. 1994 Dec;71(12):809–18.

38. Doughty MJ, Fonn D. Pleomorphism and endothelial cell size in normal and polymegethous human corneal endothelium. International Contact Lens Clinic. 1993;20(5-6):116–23.

39. Carlson KH, Bourne WM, McLaren JW, Brubaker RF. Variations in human corneal endothelial cell morphology and permeability to fluorescein with age. Exp. Eye Res. 1988 Jul;47(1):27–41.

40. Nucci P, Brancato R, Mets MB, Shevell SK. Normal endothelial cell density range in childhood. Arch. Ophthalmol. 1990 Feb;108(2):247–8.

41. Amano S, Kaji Y, Mimura T. Biology of corneal endothelial cells in vivo and in vitro. Jpn. J. Ophthalmol. 2010 May;54(3):211–4.

42. Mishima S. Clinical investigations on the corneal endothelium-XXXVIII Edward Jackson Memorial Lecture. Am. J. Ophthalmol. 1982 Jan;93(1):1–29.

43. Srinivas SP. Dynamic regulation of barrier integrity of the corneal endothelium. Optom Vis Sci. 2010 Apr;87(4):E239–54.

44. Mergler S, Pleyer U. The human corneal endothelium: new insights into electrophysiology and ion channels. Prog Retin Eye Res. 2007 Jul;26(4):359–78.

45. Paganelli F, Cardillo JA, Melo LAS Jr, Oliveira AG, Skaf M, Costa RA. A single intraoperative sub-Tenon's capsule triamcinolone acetonide injection for the treatment of post-cataract surgery inflammation. Ophthalmology. 2004 Nov;111(11):2102–8.

46. Davies NM. Biopharmaceutical considerations in topical ocular drug delivery. Clinical and Experimental Pharmacology and Physiology. 2000 Jul 17;27(7):558–62.

47. Siqueira RC, Filho ER, Fialho SL, Lucena LR, Filho AM, Haddad A, et al. Pharmacokinetic and toxicity investigations of a new intraocular lens with a dexamethasone drug delivery system: a pilot study. Ophthalmologica. 2006;220(5):338–42.

48. Zeimer R, Goldberg MF. Novel ophthalmic therapeutic modalities based on noninvasive light-targeted drug delivery to the posterior pole of the eye. Adv. Drug Deliv. Rev. 2001 Oct 31;52(1):49–61.

49. Li J, Morlet N, Ng JQ, Semmens JB, Knuiman MW. Significant nonsurgical risk factors for endophthalmitis after cataract surgery: EPSWA fourth report. Invest. Ophthalmol. Vis. Sci. 2004 May;45(5):1321–8.

50. Hassell JR, Birk DE. The molecular basis of corneal transparency. Exp. Eye Res. 2010 Sep;91(3):326–35.

51. Liberto MC, Matera G, Lamberti AG, Barreca GS, Quirino A, Focà A. In vitro Bartonella quintana infection modulates the programmed cell death and inflammatory reaction of endothelial cells. Diagn. Microbiol. Infect. Dis. 2003 Feb;45(2):107–15.

52. Shioiri T, Muroi M, Hatao F, Nishida M, Ogawa T, Mimura Y, et al. Caspase-3 is activated and rapidly released from human umbilical vein endothelial cells in response to lipopolysaccharide. Biochim. Biophys. Acta. 2009 Oct;1792(10):1011–8.

53. Saikumar P, Dong Z, Mikhailov V, Denton M, Weinberg JM, Venkatachalam MA. Apoptosis: definition, mechanisms, and relevance to disease. Am. J. Med. 1999 Nov;107(5):489–506.

54. Wang JH, Redmond HP, Watson RW, Duggan S, McCarthy J, Barry M, et al. Mechanisms involved in the induction of human endothelial cell necrosis. Cell. Immunol. 1996 Feb 25;168(1):91–9.

55. Rieck P, Oliver L, Engelmann K, Fuhrmann G, Hartmann C, Courtois Y. The role of exogenous/endogenous basic fibroblast growth factor (FGF2) and transforming growth factor beta (TGF beta-1) on human corneal endothelial cells proliferation in vitro. Exp. Cell Res. 1995 Sep;220(1):36–46.

56. Sagoo P, Chan G, Larkin DFP, George AJT. Inflammatory cytokines induce apoptosis of corneal endothelium through nitric oxide. Invest. Ophthalmol. Vis. Sci. 2004 Nov 1;45(11):3964–73.

57. Brasier AR. The nuclear factor-kappaB-interleukin-6 signalling pathway mediating vascular inflammation. Cardiovasc. Res. 2010 May 1;86(2):211–8.

58. Sethi G, Tergaonkar V. Potential pharmacological control of the NF-κB pathway. Trends Pharmacol. Sci. 2009 Jun;30(6):313–21.

59. González-Ramos R, Van Langendonckt A, Defrère S, Lousse J-C, Colette S, Devoto L, et al. Involvement of the nuclear factor-[kappa]B pathway in the pathogenesis of endometriosis. Fertility and Sterility. 2010 Nov;94(6):1985–94.

60. Gupta SC, Sundaram C, Reuter S, Aggarwal BB. Inhibiting NF-κB activation by small molecules as a therapeutic strategy. Biochim. Biophys. Acta. 2010 Dec;1799(10-12):775–87.

61. Miyamoto S. Nuclear initiated NF-κB signaling: NEMO and ATM take center stage. Cell Res. 2011 Jan;21(1):116–30.

62. Crisostomo PR, Wang Y, Markel TA, Wang M, Lahm T, Meldrum DR. Human mesenchymal stem cells stimulated by TNF-alpha, LPS, or hypoxia produce growth factors by an NF kappa B- but not JNK-dependent mechanism. Am. J. Physiol., Cell Physiol. 2008 Mar;294(3):C675–82.

63. Rowland FN, Donovan MJ, Lindsay M, Weiss WI, O'Rourke J, Kreutzer DL. Demonstration of inflammatory mediator-induced inflammation and endothelial cell damage in the anterior segment of the eye. Am. J. Pathol. 1983 Jan;110(1):1–12.

64. Makó V, Czúcz J, Weiszhár Z, Herczenik E, Matkó J, Prohászka Z, et al. Proinflammatory activation pattern of human umbilical vein endothelial cells induced by IL-1β, TNF-α, and LPS. Cytometry A. 2010 Oct;77(10):962–70.

65. Dunky A, Neumüller J, Menzel J. Interactions of lymphocytes from patients with psoriatic arthritis or healthy controls and cultured endothelial cells. Clin. Immunol. Immunopathol. 1997 Dec;85(3):297–314.

66. Martinesi M, Treves C, d' Albasio G, Bagnoli S, Bonanomi AG, Stio M. Vitamin D derivatives induce apoptosis and downregulate ICAM-1 levels in peripheral blood mononuclear cells of inflammatory bowel disease patients. Inflamm. Bowel Dis. 2008 May;14(5):597–604.

67. Schildberger A, Rossmanith E, Weber V, Falkenhagen D. Monitoring of endothelial cell activation in experimental sepsis with a two-step cell culture model. Innate Immun. 2010;16(5):278–87.

68. Takahashi T, Ohno O, Ikeda Y, Sawa R, Homma Y, Igarashi M, et al. Inhibition of lipopolysaccharide activity by a bacterial cyclic lipopeptide surfactin. J. Antibiot. 2006 Jan;59(1):35–43.

69. Tomczok J, Sliwa-Tomczok W, Klein CL, Bittinger F, Kirkpatrick CJ. Application of X-ray microanalysis to study of the expression of endothelial adhesion molecules on human umbilical vein endothelial cells in vitro. Histochemistry. 1994 Nov;102(5):337–43.

70. Waldow T, Witt W, Weber E, Matschke K. Nitric oxide donor-induced persistent inhibition of cell adhesion protein expression and NFkappaB activation in endothelial cells. Nitric Oxide. 2006 Sep;15(2):103–13.

71. Yin W, Ghebrehiwet B, Weksler B, Peerschke EIB. Regulated complement deposition on the surface of human endothelial cells: effect of tobacco smoke and shear stress. Thromb. Res. 2008;122(2):221–8.

72. Shang T, Yednock T, Issekutz AC. alpha9beta1 integrin is expressed on human neutrophils and contributes to neutrophil migration through human lung and synovial fibroblast barriers. J. Leukoc. Biol. 1999 Nov;66(5):809–16.

73. McDonald B, McAvoy EF, Lam F, Gill V, de la Motte C, Savani RC, et al. Interaction of CD44 and hyaluronan is the dominant mechanism for neutrophil sequestration in inflamed liver sinusoids. J. Exp. Med. 2008 Apr 14;205(4):915–27.

74. Andrews EJ, Wang JH, Winter DC, Laug WE, Redmond HP. Tumor cell adhesion to endothelial cells is increased by endotoxin via an upregulation of beta-1 integrin expression. J. Surg. Res. 2001 May 1;97(1):14–9.

75. Shen Y, Sultana C, Arditi M, Kim KS, Kalra VK. Endotoxin-induced migration of monocytes and PECAM-1 phosphorylation are abrogated by PAF receptor antagonists. Am J Physiol Endocrinol Metab. 1998 Sep 1;275(3):E479–86.

76. Paik JH, Chae Ss, Lee MJ, Thangada S, Hla T. Sphingosine 1-phosphate-induced endothelial cell migration requires the expression of EDG-1 and EDG-3 receptors and Rho-dependent activation of alpha vbeta3- and beta1-containing integrins. J. Biol. Chem. 2001 Apr 13;276(15):11830–7.

77. Peng Y, Li J, Geng M. The glycan profile of endothelial cells in the present of tumor-conditioned medium and potential roles of beta-1,6-GlcNAc branching on HUVEC conformation. Mol. Cell. Biochem. 2010 Jul;340(1-2):143–52.

78. Hollingsworth JW, Li Z, Brass DM, Garantziotis S, Timberlake SH, Kim A, et al. CD44 regulates macrophage recruitment to the lung in lipopolysaccharide-induced airway disease. Am. J. Respir. Cell Mol. Biol. 2007 Aug;37(2):248–53.

79. Xue L, Liang H, Jiang X. Up-regulation of CD44 expression by interleukin-13 in a murine model of asthma. Mol Med Report. 2011 Dec;4(6):1233–7.

80. Kam Leung. AlexaFluor 488-conjugated antibody against lymphatic vessel endothelial hyaluronan receptor-1 (LYVE-1). 2011 Mar 24, in print.

81. Giese MJ, Shum DC, Rayner SA, Mondino BJ, Berliner JA. Adhesion molecule expression in a rat model of Staphylococcus aureus endophthalmitis. Invest. Ophthalmol. Vis. Sci. 2000 Jan;41(1):145–53.

82. Noratto GD, Angel-Morales G, Talcott ST, Mertens-Talcott SU. Polyphenolics from açaí (Euterpe oleracea mart.) and red muscadine grape (Vitis rotundifolia) protect human umbilical vascular endothelial cells (HUVEC) from glucose- and lipopolysaccharide (LPS)-induced inflammation and target microRNA-126. J. Agric. Food Chem. 2011 Jul 27;59(14):7999–8012.

83. Maurice DM. The structure and transparency of the cornea. J. Physiol. (Lond.). 1957 Apr 30;136(2):263–86.

84. Maurice DM. The location of the fluid pump in the cornea. J. Physiol. (Lond.). 1972 Feb;221(1):43–54.

85. Watsky MA, McDermott ML, Edelhauser HF. In vitro corneal endothelial permeability in rabbit and human: the effects of age, cataract surgery and diabetes. Exp. Eye Res. 1989 Nov;49(5):751–67.

86. Ramachandran C, Srinivas SP. Formation and disassembly of adherens and tight junctions in the corneal endothelium: regulation by actomyosin contraction. Invest. Ophthalmol. Vis. Sci. 2010 Apr;51(4):2139–48.

87. Ma L, Kuang K, Smith RW, Rittenband D, Iserovich P, Diecke FPJ, et al. Modulation of tight junction properties relevant to fluid transport across rabbit corneal endothelium. Exp. Eye Res. 2007 Apr;84(4):790–8.

88. Watsky MA, McCartney MD, McLaughlin BJ, Edelhauser HF. Corneal endothelial junctions and the effect of ouabain. Invest. Ophthalmol. Vis. Sci. 1990 May;31(5):933–41.

89. D'hondt C, Ponsaerts R, Srinivas SP, Vereecke J, Himpens B. Thrombin inhibits intercellular calcium wave propagation in corneal endothelial cells by modulation of hemichannels and gap junctions. Invest. Ophthalmol. Vis. Sci. 2007 Jan;48(1):120–33.

90. Moshirfar M, Whitehead G, Beutler BC, Mamalis N. Toxic anterior segment syndrome after Verisyse iris-supported phakic intraocular lens implantation. J Cataract Refract Surg. 2006 Jul;32(7):1233–7.

91. Hellinger WC, Hasan SA, Bacalis LP, Thornblom DM, Beckmann SC, Blackmore C, et al. Outbreak of toxic anterior segment syndrome following cataract surgery associated with impurities in autoclave steam moisture. Infect Control Hosp Epidemiol. 2006 Mar;27(3):294–8.

92. Monson MC, Mamalis N, Olson RJ. Toxic anterior segment inflammation following cataract surgery. J Cataract Refract Surg. 1992 Mar;18(2):184–9.

93. Avisar R, Weinberger D. Corneal endothelial morphologic features in toxic anterior segment syndrome. Cornea. 2010 Mar;29(3):251–3.

94. Sampat KM, Garg SJ. Complications of intravitreal injections. Curr Opin Ophthalmol. 2010 May;21(3):178–83.

95. Clark A. Quality of life after postoperative endophthalmitis. Clinical & Experimental Ophthalmology. 2008 Aug 1;36(6):526–31.

96. Das D, Das S, Bandyopadhyay S, Mondal KK, Ray B, Das A, et al. A prospective evaluation of anterior chamber contamination following cataract surgery. J Indian Med Assoc. 2009 Jan;107(1):30, 32–3.

97. Holland SP, Morck DW, Lee TL. Update on toxic anterior segment syndrome. Current Opinion in Ophthalmology. 2007 Feb;18(1):4–8.

98. Campochiaro PA, Lim JI. Aminoglycoside toxicity in the treatment of endophthalmitis. The Aminoglycoside Toxicity Study Group. Arch. Ophthalmol. 1994 Jan;112(1):48–53.

99. Axer-Siegel R, Stiebel-Kalish H, Rosenblatt I, Strassmann E, Yassur Y, Weinberger D. Cystoid macular edema after cataract surgery with intraocular vancomycin. Ophthalmology. 1999 Sep;106(9):1660–4.

100. Tehrani M, Dick HB, Wolters B, Pakula T, Wolf E. Material properties of various intraocular lenses in an experimental study. Ophthalmologica. 2004 Feb;218(1):57–63.

101. Morarescu D, West-Mays JA, Sheardown HD. Effect of delivery of MMP inhibitors from PDMS as a model IOL material on PCO markers. Biomaterials. 2010 Mar;31(8):2399–407.

102. Kodjikian L, Beby F, Rabilloud M, Bruslea D, Halphen I, Fleury J, et al. Influence of intraocular lens material on the development of acute endophthalmitis after cataract surgery? Eye (Lond). 2008 Feb;22(2):184–93.

103. Paganelli F, Cardillo JA, Dare ARJ, Melo LAS Jr, Lucena DR, Silva AA Jr, et al. Controlled transscleral drug delivery formulations to the eye: establishing new concepts and paradigms in ocular anti-inflammatory therapeutics and antibacterial prophylaxis. Expert Opin Drug Deliv. 2010 Aug;7(8):955–65.

104. Cunningham MA, Edelman JL, Kaushal S. Intravitreal Steroids for Macular Edema: The Past, the Present, and the Future. Survey of Ophthalmology. March;53(2):139–49.

105. Williams GA, Haller JA, Kuppermann BD, Blumenkranz MS, Weinberg DV, Chou C, et al. Dexamethasone posterior-segment drug delivery system in the treatment of

macular edema resulting from uveitis or Irvine-Gass syndrome. Am. J. Ophthalmol. 2009 Jun;147(6):1048–54, 1054.

106. Kim J, Peng C-C, Chauhan A. Extended release of dexamethasone from silicone-hydrogel contact lenses containing vitamin E. Journal of Controlled Release. 2010 Nov 20;148(1):110–6.

107. Lu Y, Fukuda K, Nakamura Y, Kimura K, Kumagai N, Nishida T. Inhibitory effect of triptolide on chemokine expression induced by proinflammatory cytokines in human corneal gibroblasts. Invest. Ophthalmol. Vis. Sci. 2005 Jul 1;46(7):2346–52.

108. Cheng CK, Berger AS, Pearson PA, Ashton P, Jaffe GJ. Intravitreal sustained-release dexamethasone device in the treatment of experimental uveitis. Invest. Ophthalmol. Vis. Sci. 1995 Feb;36(2):442–53.

109. Beer PM, Bakri SJ, Singh RJ, Liu W, Peters GB, Miller M. Intraocular concentration and pharmacokinetics of triamcinolone acetonide after a single intravitreal injection. Ophthalmology. 2003 Apr;110(4):681–6.

110. Esposito E, Cuzzocrea S. TNF-alpha as a therapeutic target in inflammatory diseases, ischemia-reperfusion injury and trauma. Curr. Med. Chem. 2009;16(24):3152–67.

111. Yu SM, Wu JF, Lin TL, Kuo SC. Inhibition of nitric oxide synthase expression by PPM-18, a novel anti-inflammatory agent, in vitro and in vivo. Biochem J. 1997 Dec 1;328(Pt 2):363–9.

112. Kawabata A, Kuroda R, Morimoto N, Kawao N, Masuko T, Kakehi K, et al. Lipopolysaccharide-induced subsensitivity of protease-activated receptor-2 in the mouse salivary glands in vivo. Naunyn Schmiedebergs Arch. Pharmacol. 2001 Sep;364(3):281–4.

113. Cicala C, Pinto A, Bucci M, Sorrentino R, Walker B, Harriot P, et al. Protease-activated receptor-2 involvement in hypotension in normal and endotoxemic rats in vivo. Circulation. 1999 May 18;99(19):2590–7.

114. Kawabata A, Kuroda R, Nakaya Y, Kawao N, Nishikawa H. Ex vivo evidence that the phosphodiesterase inhibitor IBMX attenuates the up-regulation of PAR-2 in the endotoxemic rat aorta. Thromb. Res. 2001 Mar 15;101(6):513–5.

115. Nystedt S, Ramakrishnan V, Sundelin J. The proteinase-activated receptor 2 is induced by inflammatory mediators in human endothelial cells. Comparison with the thrombin receptor. J. Biol. Chem. 1996 Jun 21;271(25):14910–5.

116. Descombes P, Olivier JP, Vischer TL. The effect of protease inhibitors on the immune response in mice. Agents Actions. 1982 Oct;12(4):499–502.

117. Gupta MS, McKee HDR, Stewart OG. Perioperative prophylaxis for cataract surgery: survey of ophthalmologists in the north of England. J Cataract Refract Surg. 2004 Sep;30(9):2021–2.

118. Sekimoto M, Imanaka Y, Evans E, Ishizaki T, Hirose M, Hayashida K, et al. Practice variation in perioperative antibiotic use in Japan. Int J Qual Health Care. 2004 Oct;16(5):367–73.

119. Gaudana R, Ananthula HK, Parenky A, Mitra AK. Ocular drug delivery. AAPS J. 2010 Sep;12(3):348–60.

120. Xu X, Yu N, Bai Z, Xun Y, Jin D, Li Z, et al. Effect of menthol on ocular drug delivery. Graefes Arch Clin Exp Ophthalmol. 2011 May 20, in print.

121. Ulualp K, Condon RE. Antibiotic prophylaxis for scheduled operative procedures. Infect. Dis. Clin. North Am. 1992 Sep;6(3):613–25.

122. Garty S, Shirakawa R, Warsen A, Anderson EM, Noble ML, Bryers JD, et al. Sustained antibiotic release from an intraocular lens-hydrogel assembly for cataract surgery. Invest Ophthalmol Vis Sci. 2011 Mar 29, in print.

123. Tan DT, Chee SP, Lim L, Theng J, Van Ede M. Randomized clinical trial of Surodex steroid drug delivery system for cataract surgery: anterior versus posterior placement of two Surodex in the eye. Ophthalmology. 2001 Dec;108(12):2172–81.

124. Shaw J, Smith EF, Desai RU, Enriquez B, Schrier A. Can intraocular lenses deliver antibiotics intracamerally? J Ocul Pharmacol Ther. 2010 Dec;26(6):587–9.

125. Kleinmann G, Apple DJ, Chew J, Hunter B, Stevens S, Larson S, et al. Hydrophilic acrylic intraocular lens as a drug-delivery system for fourth-generation fluoroquinolones. Journal of Cataract & Refractive Surgery. 2006 Oct;32(10):1717–21.

126. Kleinmann G, Apple DJ, Chew J, Stevens S, Hunter B, Larson S, et al. Hydrophilic acrylic intraocular lens as a drug-delivery system: Pilot study. J Cataract Refract Surg. 2006 Apr;32(4):652–4.

127. Tsuchiya Y, Kobayakawa S, Tsuji A, Tochikubo T. Preventive Effect Against Post-Cataract Endophthalmitis: Drug Delivery Intraocular Lens versus Intracameral Antibiotics. Curr Eye Res. 2008 Jan;33(10):868–75.

128. Duarte ARC, Simplicio AL, Vega-González A, Subra-Paternault P, Coimbra P, Gil MH, et al. Impregnation of an intraocular lens for ophthalmic drug delivery. Curr Drug Deliv. 2008 Apr;5(2):102–7.

129. Pan Q, Qiu WY, Huo YN, Yao YF, Lou MF. Low levels of hydrogen peroxide stimulate corneal epithelial cell adhesion, migration, and wound healing. Invest. Ophthalmol. Vis. Sci. 2011 Mar;52(3):1723–34.

130. Gesche J, Fehrenbach H, Koslowski R, Ohler FM, Pynn CJ, Griese M, et al. rhKGF stimulates lung surfactant production in neonatal rats in vivo. Pediatr Pulmonol. 2011 Apr 1, in print.

131. Smith C, Martinez M, Peet J, Khanna R. Differential outcome of IL-2/Anti-IL-2 complex therapy on effector and memory CD8+ T Cells following vaccination with an adenoviral vector encoding EBV epitopes. J. Immunol. 2011 May 15;186(10):5784–90.

132. Desbois AP, Coote PJ. Wax moth larva (Galleria mellonella): an in vivo model for assessing the efficacy of antistaphylococcal agents. J Antimicrob Chemother. 2011 May 28, in print.

133. Mortensen A, Sorensen IK, Wilde C, Dragoni S, Mullerová D, Toussaint O, et al. Biological models for phytochemical research: from cell to human organism. Br. J. Nutr. 2008 May;99 E Suppl 1:ES118–26.

134. Kelly M. Toxic anterior segment syndrome after cataract surgery--Maine, 2006. MMWR Morb. Mortal. Wkly. Rep. 2007 Jun 29;56(25):629–30.

135. Cutler Peck CM, Brubaker J, Clouser S, Danford C, Edelhauser HE, Mamalis N. Toxic anterior segment syndrome: Common causes. Journal of Cataract & Refractive Surgery. 2010 Jul;36(7):1073–80.

136. Buzard K, Zhang JR, Thumann G, Stripecke R, Sunalp M. Two cases of toxic anterior segment syndrome from generic trypan blue. J Cataract Refract Surg. 2010 Dec;36(12):2195–9.

137. Huang Y, Dai Y, Wu X, Lan J, Xie L. Toxic anterior segment syndrome after pediatric cataract surgery. J AAPOS. 2010 Oct;14(5):444–6.

138. ESCRS ESG. Prophylaxis of postoperative endophthalmitis following cataract surgery: Results of the ESCRS multicenter study and identification of risk factors. Journal of Cataract & Refractive Surgery. 33(6):978–88.

139. Payne JF, Keenum DG, Sternberg P Jr, Thliveris A, Kala A, Olsen TW. Concentrated intravitreal amphotericin B in fungal endophthalmitis. Arch. Ophthalmol. 2010 Dec;128(12):1546–50.

140. Pathengay A, Mathai A, Shah GY, Ambatipudi S. Intravitreal piperacillin/tazobactam in the management of multidrug-resistant Pseudomonas aeruginosa endophthalmitis. J Cataract Refract Surg. 2010 Dec;36(12):2210–1.

141. Al-Mezaine HS, Kangave D, Al-Assiri A, Al-Rajhi AA. Acute-onset nosocomial endophthalmitis after cataract surgery: incidence, clinical features, causative organisms, and visual outcomes. J Cataract Refract Surg. 2009 Apr;35(4):643–9.

142. Ozkiris A, Evereklioglu C, Esel D, Akgün H, Göktas S, Erkiliç K. The efficacy of piperacillin/tazobactam in experimental Pseudomonas aeruginosa endophthalmitis: a histopathological and microbiological evaluation. Curr. Eye Res. 2005 Jan;30(1):13–9.

143. Sakalar YB, Ozekinci S, Celen MK. Treatment of experimental Bacillus cereus endophthalmitis using intravitreal moxifloxacin with or without dexamethasone. Journal of Ocular Pharmacology and Therapeutics: The Official Journal of the Association for Ocular Pharmacology and Therapeutics. 2011 Aug 11, in print.

144. Kim SY, Yang J, Lee YC. Safety of moxifloxacin and voriconazole in corneal storage media on porcine corneal endothelial cells. J Ocul Pharmacol Ther. 2010 Aug;26(4):315–8.

145. Kernt M, Kampik A. Intracameral voriconazole: in vitro safety for human ocular cells. Toxicology. 2009 Apr 28;258(2-3):84–93.

146. Kernt M, Neubauer AS, Liegl RG, Lackerbauer CA, Eibl KH, Alge CS, et al. Intracameral moxifloxacin: in vitro safety on human ocular cells. Cornea. 2009 Jun;28(5):553–61.

147. Ritterband DC, Shah MK, Meskin SW, Seedor JA, Koplin RS, Perez W, et al. Efficacy and safety of voriconazole as an additive in Optisol GS: a preservation medium for corneal donor tissue. Cornea. 2007 Apr;26(3):343–7.

148. Chang YS, Tseng SY, Tseng SH, Wu CL, Chen MF. Triamcinolone acetonide suspension toxicity to corneal endothelial cells. J Cataract Refract Surg. 2006 Sep;32(9):1549–55.

149. Chang YS, Tseng SY, Tseng SH, Wu CL. Cytotoxicity of lidocaine or bupivacaine on corneal endothelial cells in a rabbit model. Cornea. 2006 Jun;25(5):590–6.

150. Price MO, Quillin C, Price FW Jr. Effect of gatifloxacin ophthalmic solution 0.3% on human corneal endothelial cell density and aqueous humor gatifloxacin concentration. Curr. Eye Res. 2005 Jul;30(7):563–7.

151. Maár N, Graebe A, Schild G, Stur M, Amon M. Influence of viscoelastic substances used in cataract surgery on corneal metabolism and endothelial morphology: comparison of Healon and Viscoat. J Cataract Refract Surg. 2001 Nov;27(11):1756–61.

152. Ben-Eliahu S, Tal K, Milstein A, Levin-Harrus T, Ezov N, Kleinmann G. Protective effect of different ophthalmic viscosurgical devices on corneal endothelium during severe phacoemulsification model in rabbits. Ophthalmic Surg Lasers Imaging. 2011 Apr;42(3):152–6.

153. Lichtinger A, Sandstedt CA, Padilla K, Schwartz DM, Chayet AS. Corneal endothelial safety after ultraviolet light treatment of the light-adjustable intraocular lens. J Cataract Refract Surg. 2011 Feb;37(2):324–7.

154. Lamb DJ, Zhang L. Challenges in prostate cancer research: animal models for nutritional studies of chemoprevention and disease progression. J. Nutr. 2005 Dec;135(12 Suppl):3009S-3015S.

155. Kernodle DS. Decrease in the effectiveness of Bacille Calmette-Guérin vaccine against pulmonary tuberculosis: a consequence of increased immune suppression by microbial antioxidants, not overattenuation. Clin. Infect. Dis. 2010 Jul 15;51(2):177–84.

156. Kleemann R, Verschuren L, Morrison M, Zadelaar S, van Erk MJ, Wielinga PY, et al. Anti-inflammatory, anti-proliferative and anti-atherosclerotic effects of quercetin in human in vitro and in vivo models. Atherosclerosis. 2011 May 5, in print.

157. Reichel A. Addressing central nervous system (CNS) penetration in drug discovery: basics and implications of the evolving new concept. Chem. Biodivers. 2009 Nov;6(11):2030–49.

158. Bednarz J, Teifel M, Friedl P, Engelmann K. Immortalization of human corneal endothelial cells using electroporation protocol optimized for human corneal endothelial and human retinal pigment epithelial cells. Acta Ophthalmol Scand. 2000 Apr;78(2):130–6.

159. Ayaki M, Taguchi Y, Soda M, Yaguchi S, Iwasawa A, Koide R. Cytotoxicity of topical medications used for infection and inflammation control after cataract surgery in cultured corneal endothelial cells. Biocontrol Sci. 2010 Sep;15(3):97–102.

160. Bian ZM, Elner VM, Lukacs NW, Strieter RM, Kunkel SL, Elner SG. Glycated human serum albumin induces IL-8 and MCP-1 gene expression in human corneal keratocytes. Curr. Eye Res. 1998 Jan;17(1):65–72.

161. Schaub M, Harwaldt P, Wilhelm J, Heidt MC, Grebe M, Tillmanns H, et al. FR167653 Ameliorates expression of proinflammatory mediators in human umbilical venous endothelial cells and human monocytes. Transplant. Proc. 2009 Aug;41(6):2616–20.

162. Sun B, Zou X, Chen Y, Zhang P, Shi G. Preconditioning of carbon monoxide releasing molecule-derived CO attenuates LPS-induced activation of HUVEC. Int. J. Biol. Sci. 2008;4(5):270–8.

163. Lam FW, Burns AR, Smith CW, Rumbaut RE. Platelets enhance neutrophil transendothelial migration via P-selectin glycoprotein ligand-1. Am. J. Physiol. Heart Circ. Physiol. 2011 Feb;300(2):H468–75.

164. Kerachian MA, Cournoyer D, Harvey EJ, Chow TY, Neagoe P-E, Sirois MG, et al. Effect of high-dose dexamethasone on endothelial haemostatic gene expression and neutrophil adhesion. J. Steroid Biochem. Mol. Biol. 2009 Sep;116(3-5):127–33.

165. Bahn CF, Glassman RM, MacCallum DK, Lillie JH, Meyer RF, Robinson BJ, et al. Postnatal development of corneal endothelium. Invest. Ophthalmol. Vis. Sci. 1986 Jan;27(1):44–51.

166. Waring GO 3rd, Bourne WM, Edelhauser HF, Kenyon KR. The corneal endothelium. Normal and pathologic structure and function. Ophthalmology. 1982 Jun;89(6):531–90.

167. Fan T, Wang D, Zhao J, Wang J, Fu Y, Guo R. Establishment and characterization of a novel untransfected corneal endothelial cell line from New Zealand white rabbits. Mol. Vis. 2009;15:1070–8.

168. Liu J, Saghizadeh M, Tuli SS, Kramerov AA, Lewin AS, Bloom DC, et al. Different tropism of adenoviruses and adeno-associated viruses to corneal cells: implications for corneal gene therapy. Mol. Vis. 2008;14:2087–96.

169. Mandell KJ, Holley GP, Parkos CA, Edelhauser HF. Antibody blockade of junctional adhesion molecule-A in rabbit corneal endothelial tight junctions produces corneal swelling. Invest. Ophthalmol. Vis. Sci. 2006 Jun;47(6):2408–16.

170. Rochelson B, Dowling O, Schwartz N, Metz CN. Magnesium sulfate suppresses inflammatory responses by human umbilical vein endothelial cells (HuVECs) through the NFkappaB pathway. J. Reprod. Immunol. 2007 Apr;73(2):101–7.

171. Kanayama S, Nishida K, Yamato M, Hayashi R, Maeda N, Okano T, et al. Analysis of soluble vascular endothelial growth factor receptor-1 secreted from cultured corneal and oral mucosal epithelial cell sheets in vitro. Br J Ophthalmol. 2009 Feb;93(2):263–7.

172. Hess DC, Thompson Y, Sprinkle A, Carroll J, Smith J. E-selectin expression on human brain microvascular endothelial cells,. Neuroscience Letters. 1996 Jul 26;213(1):37–40.

173. Mullins GE, Sunden-Cullberg J, Johansson A-S, Rouhiainen A, Erlandsson-Harris H, Yang H, et al. Activation of human umbilical vein endothelial cells leads to relocation and release of high-mobility group box chromosomal protein 1. Scand J Immunol. 2004 Dec;60(6):566–73.

174. Wenzel I, Roth J, Sorg C. Identification of a novel surface molecule, RM3/1, that contributes to the adhesion of glucocorticoid-induced human monocytes to endothelial cells. Eur. J. Immunol. 1996 Nov;26(11):2758–63.

175. Liu L, Sheardown H. Glucose permeable poly (dimethyl siloxane) poly (N-isopropyl acrylamide) interpenetrating networks as ophthalmic biomaterials. Biomaterials. 2005 Jan;26(3):233–44.

176. Wells LA, Furukawa S, Sheardown H. Photoresponsive PEG-anthracene grafted hyaluronan as a controlled-delivery biomaterial. Biomacromolecules. 2011 Apr 11;12(4):923–32.

177. Mosmann T. Rapid colorimetric assay for cellular growth and survival: Application to proliferation and cytotoxicity assays. Journal of Immunological Methods. 1983 Dec 16;65(1-2):55–63.

178. Gorbet MB, Tanti NC, Jones L, Sheardown H. Corneal epithelial cell biocompatibility to silicone hydrogel and conventional hydrogel contact lens packaging solutions. Mol. Vis. 2010;16:272–82.

179. Yeh CJ, Hsi BL, Faulk WP. Propidium iodide as a nuclear marker in immunofluorescence. II. Use with cellular identification and viability studies. J. Immunol. Methods. 1981;43(3):269–75.

180. Kernt M, Neubauer AS, Liegl RG, Lackerbauer CA, Eibl KH, Alge CS, et al. Intracameral moxifloxacin: in vitro safety on human ocular cells. Cornea. 2009 Jun;28(5):553–61.

181. Messmer UK, Winkel G, Briner VA, Pfeilschifter J. Glucocorticoids potently block tumour necrosis factor-alpha- and lipopolysaccharide-induced apoptotic cell death in bovine glomerular endothelial cells upstream of caspase 3 activation. Br. J. Pharmacol. 1999 Aug;127(7):1633–40.

182. Messmer UK, Winkel G, Briner VA, Pfeilschifter J. Suppression of apoptosis by glucocorticoids in glomerular endothelial cells: effects on proapoptotic pathways. Br. J. Pharmacol. 2000 Apr;129(8):1673–83.

183. Lien JC, Huang LJ, Wang JP, Teng CM, Lee KH, Kuo SC. Synthesis and antiplatelet, antiinflammatory and antiallergic activities of 2,3-disubstituted 1,4-naphthoquinones. Chem. Pharm. Bull. 1996 Jun;44(6):1181–7.

184. Klaus V, Hartmann T, Gambini J, Graf P, Stahl W, Hartwig A, et al. 1,4-Naphthoquinones as inducers of oxidative damage and stress signaling in HaCaT human keratinocytes. Arch. Biochem. Biophys. 2010 Apr 15;496(2):93–100.

185. Simoncini T, Maffei S, Basta G, Barsacchi G, Genazzani AR, Liao JK, et al. Estrogens and glucocorticoids inhibit endothelial vascular cell adhesion molecule-1 expression by different transcriptional mechanisms. Circ. Res. 2000 Jul 7;87(1):19–25.

186. Swerlick RA, Garcia-Gonzalez E, Kubota Y, Xu YL, Lawley TJ. Studies of the modulation of MHC antigen and cell adhesion molecule expression on human dermal microvascular endothelial cells. J. Invest. Dermatol. 1991 Aug;97(2):190–6.

187. Zouki C, Ouellet S, Filep JG. The anti-inflammatory peptides, antiflammins, regulate the expression of adhesion molecules on human leukocytes and prevent neutrophil adhesion to endothelial cells. FASEB J. 2000 Mar;14(3):572–80.

188. Li H, Yoneda M, Takeyama M, Sugita I, Tsunekawa H, Yamada H, et al. Effect of infliximab on tumor necrosis factor-alpha-induced alterations in retinal microvascular endothelial cells and retinal pigment epithelial cells. J Ocul Pharmacol Ther. 2010 Dec;26(6):549–56.

189. Methe H, Balcells M, Alegret M del C, Santacana M, Molins B, Hamik A, et al. Vascular bed origin dictates flow pattern regulation of endothelial adhesion molecule expression. Am. J. Physiol. Heart Circ. Physiol. 2007 May;292(5):H2167–75.

190. BD CBA Human Soluble CD54 (ICAM-1) Flex Set [Package Insert]. San Diego, USA: BD Biosciences; 2008.

191. Karkhaneh A, Mirzadeh H, Ghaffariyeh A, Ebrahimi A, Honarpisheh N, Hosseinzadeh M, et al. Novel materials to enhance corneal epithelial cell migration on keratoprosthesis. Br J Ophthalmol. 2011 Mar;95(3):405–9.

192. Alauzun JG, Young S, D'Souza R, Liu L, Brook MA, Sheardown HD. Biocompatible, hyaluronic acid modified silicone elastomers. Biomaterials. 2010 May;31(13):3471–8.

193. van Kooten TG, Whitesides JF, von Recum A. Influence of silicone (PDMS) surface texture on human skin fibroblast proliferation as determined by cell cycle analysis. J. Biomed. Mater. Res. 1998;43(1):1–14.

194. Hsu SH, Tseng HJ. In vitro biocompatibility of PTMO-based polyurethanes and those containing PDMS blocks. J Biomater Appl. 2004 Oct;19(2):135–46.

195. Briganti E, Losi P, Raffi A, Scoccianti M, Munaò A, Soldani G. Silicone based polyurethane materials: a promising biocompatible elastomeric formulation for cardiovascular applications. J Mater Sci Mater Med. 2006 Mar;17(3):259–66.

196. Cui Z, Lee BH, Pauken C, Vernon BL. Degradation, cytotoxicity, and biocompatibility of NIPAAm-based thermosensitive, injectable, and bioresorbable polymer hydrogels. J Biomed Mater Res A. 2011 Aug;98(2):159–66.

197. Wu DQ, Qiu F, Wang T, Jiang XJ, Zhang XZ, Zhuo RX. Toward the development of partially biodegradable and injectable thermoresponsive hydrogels for potential biomedical applications. ACS Appl Mater Interfaces. 2009 Feb;1(2):319–27.

198. Li YY, Zhang XZ, Kim GC, Cheng H, Cheng SX, Zhuo RX. Thermosensitive Y-shaped micelles of poly(oleic acid-Y-N-isopropylacrylamide) for drug delivery. Small. 2006 Jul;2(7):917–23.

199. Wei J, He P, Liu A, Chen X, Wang X, Jing X. Surface modification of hydroxyapatite nanoparticles with thermal-responsive PNIPAM by ATRP. Macromol Biosci. 2009 Dec 8;9(12):1237–46.

200. Shimmura S, Doillon CJ, Griffith M, Nakamura M, Gagnon E, Usui A, et al. Collagen-poly(N-isopropylacrylamide)-based membranes for corneal stroma scaffolds. Cornea. 2003 Oct;22(7 Suppl):S81–8.

201. Simmons A, Padsalgikar AD, Ferris LM, Poole-Warren LA. Biostability and biological performance of a PDMS-based polyurethane for controlled drug release. Biomaterials. 2008 Jul;29(20):2987–95.

202. Farin FM, Pohlman TH, Omiecinski CJ. Expression of cytochrome P450s and microsomal epoxide hydrolase in primary cultures of human umbilical vein endothelial cells. Toxicol. Appl. Pharmacol. 1994 Jan;124(1):1–9.

203. Song S-jeong, Chung H, Yu HG. Inhibitory effect of YC-1, 3-(5'-hydroxymethyl-2'-furyl)-1-benzylindazole, on experimental choroidal neovascularization in rat. Ophthalmic Res. 2008;40(1):35–40.

204. Sperling S, Larsen IG. Toxicity of dimethylsulfoxide (DMSO) to human corneal endothelium in vitro. Acta Ophthalmol (Copenh). 1979 Oct;57(5):891–8.

Appendix A

Copyright Permissions

Top of Form

ELSEVIER LICENSE

TERMS AND CONDITIONS

Aug 08, 2011

This is a License Agreement between Laura Doody ("You") and Elsevier ("Elsevier") provided by Copyright Clearance Center ("CCC"). The license consists of your order details, the terms and conditions provided by Elsevier, and the payment terms and conditions.

All payments must be made in full to CCC. For payment instructions, please see information listed at the bottom of this form.

Supplier	Elsevier Limited The Boulevard,Langford Lane Kidlington,Oxford,OX5 1GB,UK
Registered Company Number	1982084
Customer name	Laura Doody
Customer address	701-30 Blue Springs Drive Waterloo, ON N2V2A3
License number	2724340465237
License date	Aug 08, 2011
Licensed content publisher	Elsevier
Licensed content publication	Journal of Cataract & Refractive Surgery

Licensed content title	Toxic anterior segment syndrome
Licensed content author	Nick Mamalis,Henry F. Edelhauser,Daniel G. Dawson,Jesse Chew,Russell M. LeBoyer,Liliana Werner
Licensed content date	February 2006
Licensed content volume number	32
Licensed content issue number	2
Number of pages	10
Start Page	324
End Page	333
Type of Use	reuse in a thesis/dissertation
Intended publisher of new work	other
Portion	figures/tables/illustrations
Number of figures/tables/illustrations	1
Format	both print and electronic
Are you the author of this Elsevier article?	No
Will you be translating?	No
Order reference number	
Title of your thesis/dissertation	Evaluation of endothelial cell response to drug for intraocular lens delivery
Expected completion date	Oct 2011
Estimated size (number of pages)	100
Elsevier VAT number	GB 494 6272 12
Permissions price	0.00 USD

VAT/Local Sales Tax	0.0 USD / 0.0 GBP
Total	0.00 USD

ELSEVIER LICENSE

TERMS AND CONDITIONS

Aug 08, 2011

This is a License Agreement between Laura Doody ("You") and Elsevier ("Elsevier") provided by Copyright Clearance Center ("CCC"). The license consists of your order details, the terms and conditions provided by Elsevier, and the payment terms and conditions.

All payments must be made in full to CCC. For payment instructions, please see information listed at the bottom of this form.

Supplier	Elsevier Limited The Boulevard,Langford Lane Kidlington,Oxford,OX5 1GB,UK
Registered Company Number	1982084
Customer name	Laura Doody
Customer address	701-30 Blue Springs Drive Waterloo, ON N2V2A3
License number	2724331425451
License date	Aug 08, 2011
Licensed content publisher	Elsevier
Licensed content publication	Journal of Cataract & Refractive Surgery
Licensed content title	Toxic anterior segment syndrome after Verisyse iris-supported phakic intraocular lens implantation
Licensed content author	Majid Moshirfar,George Whitehead,Barry C. Beutler,Nick Mamalis

Licensed content date	July 2006
Licensed content volume number	32
Licensed content issue number	7
Number of pages	5
Start Page	1233
End Page	1237
Type of Use	reuse in a thesis/dissertation
Portion	figures/tables/illustrations
Number of figures/tables/illustrations	2
Format	both print and electronic
Are you the author of this Elsevier article?	No
Will you be translating?	No
Order reference number	
Title of your thesis/dissertation	Evaluation of endothelial cell response to drug for intraocular lens delivery
Expected completion date	Oct 2011
Estimated size (number of pages)	100
Elsevier VAT number	GB 494 6272 12
Permissions price	0.00 USD
VAT/Local Sales Tax	0.0 USD / 0.0 GBP
Total	0.00 USD

ELSEVIER LICENSE
TERMS AND CONDITIONS
Aug 09, 2011

This is a License Agreement between Laura Doody ("You") and Elsevier ("Elsevier") provided by Copyright Clearance Center ("CCC"). The license consists of your order details, the terms and conditions provided by Elsevier, and the payment terms and conditions.

All payments must be made in full to CCC. For payment instructions, please see information listed at the bottom of this form.

Supplier	Elsevier Limited The Boulevard,Langford Lane Kidlington,Oxford,OX5 1GB,UK
Registered Company Number	1982084
Customer name	Laura Doody
Customer address	701-30 Blue Springs Drive Waterloo, ON N2J4T2
License number	2724831502932
License date	Aug 09, 2011
Licensed content publisher	Elsevier
Licensed content publication	Trends in Pharmacological Sciences
Licensed content title	Potential pharmacological control of the NF-κB pathway
Licensed content author	Gautam Sethi,Vinay Tergaonkar

Licensed content date	June 2009
Licensed content volume number	30
Licensed content issue number	6
Number of pages	9
Start Page	313
End Page	321
Type of Use	reuse in a thesis/dissertation
Intended publisher of new work	other
Portion	figures/tables/illustrations
Number of figures/tables/illustrations	1
Format	both print and electronic
Are you the author of this Elsevier article?	No
Will you be translating?	No
Order reference number	
Title of your thesis/dissertation	Evaluation of endothelial cell response to drug for intraocular lens delivery
Expected completion date	Oct 2011
Estimated size (number of pages)	100
Elsevier VAT number	GB 494 6272 12
Permissions price	0.00 USD
VAT/Local Sales Tax	0.0 USD / 0.0 GBP
Total	0.00 USD

ELSEVIER LICENSE
TERMS AND CONDITIONS

Sep 12, 2011

This is a License Agreement between Laura Doody ("You") and Elsevier ("Elsevier") provided by Copyright Clearance Center ("CCC"). The license consists of your order details, the terms and conditions provided by Elsevier, and the payment terms and conditions.

All payments must be made in full to CCC. For payment instructions, please see information listed at the bottom of this form.

Supplier

Elsevier Limited
The Boulevard,Langford Lane
Kidlington,Oxford,OX5 1GB,UK

Registered Company Number
1982084
Customer name
Laura Doody
Customer address
701-30 Blue Springs Drive

Waterloo, ON N2J4T2
License number
2746660414557

License date

Sep 12, 2011

Licensed content publisher

Elsevier

Licensed content publication

Journal of Cataract & Refractive Surgery

Licensed content title

Anatomy and physiology of the cornea

Licensed content author

Derek W. DelMonte,Terry Kim

Licensed content date

March 2011

Licensed content volume number

37

Licensed content issue number

3

Number of pages

11

Start Page

588

End Page

598

Type of Use

reuse in a thesis/dissertation

Intended publisher of new work

other

Portion

figures/tables/illustrations

Number of figures/tables/illustrations

1

Format

both print and electronic

Are you the author of this Elsevier article?

No

Will you be translating?

No

Order reference number

Title of your thesis/dissertation

Evaluation of endothelial cell response to drug for intraocular lens delivery

Expected completion date

Oct 2011

Estimated size (number of pages)

100

Elsevier VAT number

GB 494 6272 12

Permissions price

0.00 USD

VAT/Local Sales Tax

0.0 USD / 0.0 GBP

Total

0.00 USD

Glossary

Cytokine	Cell signalling protein molecules to allow for intercellular communication.
Cytokine	Cell signalling protein molecules and are often toxic to cells. Example: TNF-α
Edema	An abnormal accumulation of fluid within the body leading to swelling.
Endotoxin	Toxins from Gram-negative bacteria. Example: LPS.
Glaucoma	An eye disease that relates to damage of the optic nerve that can lead to blindness if untreated.
in situ	Working with an entire organ or system outside of an organism.
in vitro	Biological experiments conducted with isolated components of an organism.
in vivo	Biological experiments conducted with living organisms in their natural state.
Intracameral	Pertaining to injection of drugs into the aqueous humour of the eye between the

	cornea and the iris.
Intraocular	Within the eye.
Intravitreal	In the vitreous of the eye.
Keratoplasty	Cornea transplantation surgery
Lipopolysaccharide	Large molecules consisting of a lipid and a polysaccharide that are present in the extracellular matrix of Gram negative material. It is an endotoxin that is not destroyed by sterilization.
Phacoemulsion	Procedure for breaking apart and removing the lens with ultrasound during cataract sugery.
Prophylactically	To protect or prevent disease.
Pyrogen	Fever inducing substance.
Synechiae	Eye condition where the iris adheres to the cornea or the lens.
Uveitis	Inflammation in the interior of the eye.
Vitritis	Accumulation of inflammatory cells in the vitreous humour or the aqueous humour.